AN ABSTRACT OF THE THESIS OF

Rajan B. Juniku for the degree of Master of Science in Chemistry presented on December 10, 2004.
Title: Designing Chiral Rhenium (VII) Trioxo Complexes.

Abstract
Approved: _____
Kevin P. Gable

The epoxide deoxygenation reaction is formally the reverse of the epoxidation reaction. Compared to epoxidation, which has reached its full maturity, epoxide deoxygenation has not been as intensively developed. Among the few deoxygenation reagents, a handful are catalytic in a metal complex, show high stereospecificity and operate under mild conditions. A common feature of all present deoxygenation reagents is that they do not perform asymmetric deoxygenation of racemic epoxides.

Rhenium (VII) trioxo complexes are emerging as pliable catalysts for epoxide deoxygenation. Designing a chiral rhenium (VII) trioxo complex was our goal. Guided by the mechanism of rhenium (VII) trioxo catalyzed

epoxide deoxygenation and the mechanism of the stereogenic information transfer, we have designed and prepared a chiral rhenium(VII) trioxo complex. This complex is void of stereogenic centers and the source of asymmetry is the restricted rotation around a carbon-carbon bond. Detailed conformational analysis of the new chiral complex was done by extensive NMR measurements and molecular modeling. The rotation barrier for the diolate was experimentally and computationally estimated to be 9.72 kcal/mol and 8.06 kcal/mol, respectively.

Unsuccessful attempts were made to prepare a camphor based scorpionate because of the extreme steric congestion. A menthone based scorpionate was successfully prepared. The related rhenium (VII) trioxo complex with this scorpionate revealed contradicting chemical and spectroscopic features.

Designing Chiral Rhenium (VII) Trioxo Complexes

by
Rajan B. Juniku

A THESIS

submitted to

Oregon State University

in partial fulfillment of
the requirements for the
degree of

Master of Science

Presented December 10, 2004
Commencement June 2005

Master of Science thesis of Rajan B. Juniku presented on December 10, 2004.

APPROVED:

Redacted for Privacy

Major Professor, representing Chemistry

Redacted for Privacy

Chair of The Department of Chemistry

Redacted for Privacy

Dean of Graduate School

I understand that my thesis will become part of the permanent collection of Oregon State University libraries. My signature below authorizes release of my thesis to any reader upon request.

Redacted for Privacy

Rajan B. Juniku, Author

ACKNOWLEDGMENTS

I would sincerely like to thank two individuals. First and foremost, I am deeply indebted to Dr. Gable for providing me with everything I needed for my research and for being available whenever I needed him. Working in Dr. Gable's lab was an exciting, memorable and very useful experience. In addition, I am grateful to Dr. Gable for helping me with writing thesis and for introducing me to the amazing world of Lunix/UNIX and Computational Chemistry. Last but not least, I would like to send many thanks to Mr. Kohnert, the NMR facility technician, whose help regarding the NMR spectrometer usage was indispensable.

I would like to thank Dr. Eric Brown for being my virtual lab mate all along. His lab notes and PhD thesis were the second most valuable guide in my work after Dr. Gable. Lastly, I would like to express gratitude to the OSU Chemistry Department for financial support through teaching assistantships.

TABLE OF CONTENTS

TABLE OF CONTENTS (Continued)

Page

LIST OF FIGURES

LIST OF FIGURES (Continued)

Figure Page

LIST OF FIGURES (Continued)

Figure Page

LIST OF TABLES

Table Page

For everything to Prof. Kevin Patrick Gable

Designing Chiral Rhenium Trioxo complexes

-Chapter 1-

Survey of Literature

1.1 Introduction

It is very common approach to convert olefins into epoxides as part of a more involved organic transformation. This is so for a good reason. Epoxides are a useful handle to synthetically elaborate a carbon-carbon chain.[1] This is further spurred with the advent of practical asymmetric catalytic epoxidation methods.[2]

Deoxygenation of epoxides has been known at least since 1955 as means to convert epoxides into olefins.[13] This was a useful transformation for it provided inverted olefins. With time other methodologies provided new ways to insure inversion or retention of epoxide stereochemistry, notably with introduction of transition organometallic complexes.

Rhenium oxo complexes have very adjustable chemistry as it is shown by prime examples such as MTO and Tp'ReO_3. The first one is very versatile catalyst, probable as one of the most efficient epoxidation catalyst, whereas the second one is a remarkable epoxide and vicinal diols oxygen atom transfer catalyst. Since their serendipitous discovery, they

have been for a long time a laboratory curiosity mainly in Herrmann's labs. However, they are becoming a very appealing and versatile catalytic system.

1.2 Epoxides

1.2.1 Epoxide Ring Opening Reactions

Epoxides are an important class of organic compounds for stereocontrolled synthesis. Their inherent strain in the three member ring and the polarity of the C-O bond imparts reactivity to the epoxide functional group toward different reactions. This and the ease of their synthesis make epoxides extremely useful synthons.

At the heart of epoxide chemistry lies epoxide ring opening reaction. There are three major epoxide ring opening reactions: 1) nucleophilic addition,[3] 2) deprotonation[4] and 3) reduction[5] (Scheme 1.1).

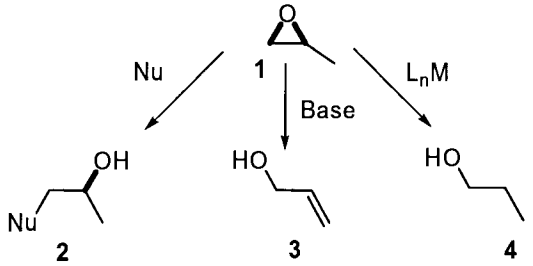

Scheme 1.1. Main Epoxide Ring Opening Reactions

Recently, increased attention has been devoted to the nucleophilic addition reactions.[8a]

Usually, epoxides are activated with a Lewis acid to facilitate the ring opening. The fact that an epoxide can be activated by Lewis acids has provided a powerful tool to control the stereochemistry of epoxide ring opening. The major theme in all these reactions is that the Lewis acid reagent has a dual character. First, it activates the epoxide ring and second, it provides the nucleophile that usually attacks the epoxide in an intramolecular fashion.[8b]

A plethora of epoxide nucleophilic addition reactions[6] has been developed. An exceptionally developed approach is Jacobsen's methodology. His manganese salen complexes[7] have been renowned catalysts since 1995 for epoxidation of olefins (yields up to 97% with ee's as high as 98%). In the epoxidation reaction, oxygen is coordinated to the high valent manganese atom, making the former highly electrophilic. Jacobsen imagined a similar picture, starting with a metal complex without an oxygen ligand. The question that arose was whether manganese coordinated to the epoxide oxygen activates the epoxide to ring opening (Scheme 1.2). Screening of different metals showed that

(salen)chromium(III) complexes are the most efficient catalyst for epoxide ring opening reaction with different nucleophiles.[8]

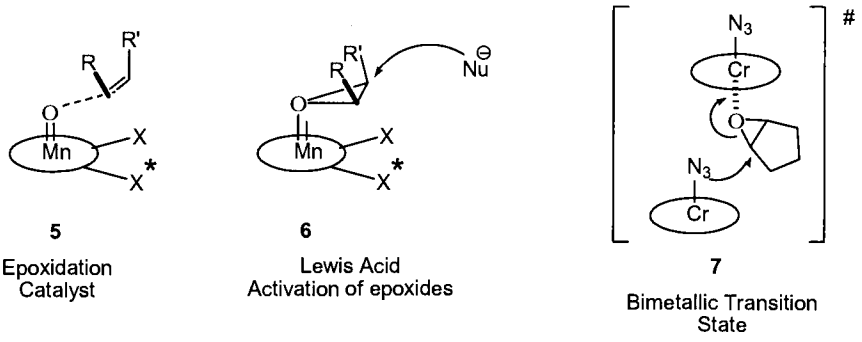

Scheme 1.2 Epoxidation versus Epoxide Ring Opening

Jacobsen employed successfully the salen catalyst in kinetic resolution of epoxides,[9] notably hydrolytic kinetic resolution (HKR).[10]

Mechanistic studies showed that the counterion plays a crucial role in HKR. Namely, the intermediate in HKR is believed to be (salen)Co(OH) aqua complex, which partitions into two reaction pathways; the counterion makes one of them more favorable.

1.2.2 Deoxygenation of epoxides

Deoxygenation of epoxides has been used in the synthesis of complex natural products (Scheme 1.3).[11] However, most work has been focused on the mechanistic relationship with epoxidations.

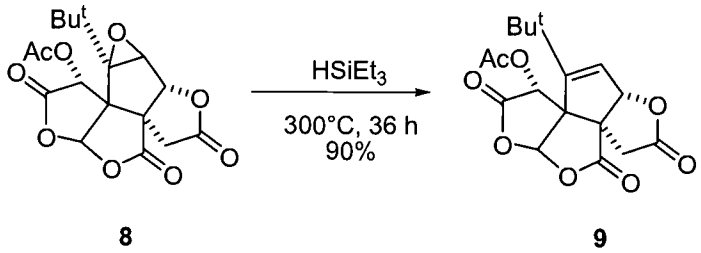

8 9

Scheme 1.3 Deoxygenation step in the total synthesis of (±)-Bilobalide

Epoxide ring opening reactions have been used to perform kinetic resolution of epoxides. In principle, the same is possible with deoxygenation of either epoxides or diols. Epoxides are occasionally used to protect olefins; deoxygenation is crucial to successfully deprotect a protected olefin.[12] Finally, the deoxygenation of renewable biomass feedstocks to more useful materials is a potential application.

Despite the potential, deoxygenation of epoxides has not been used much in the organic synthesis. The reason for this is that many deoxygenating reagents require multi-step procedures, usually stoichiometric amount of reagents, harsh conditions, show low stereselectivity, operate under unknown mechanisms and suffer from functional group incompatibility.

A classical reagent that effects deoxygenation of epoxides at 200 °C is triphenylphosphine.[13] It leads to overall inversion of configuration

(Scheme 1.4). At this temperature many sensitive organic compounds do not survive.

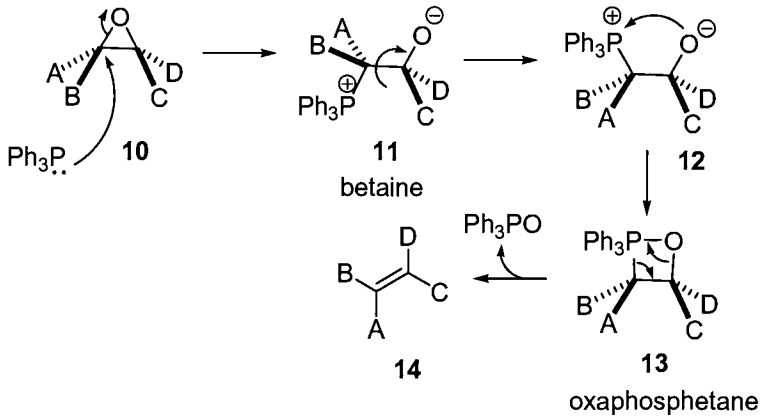

Scheme 1.4 Mechanism of four-center deoxygenation of epoxides

Related phosphorous reagents have been designed that effect deoxygenation at room temperature; they lead to inversion of stereochemistry. Examples are bis(dimethylamino)phosphorous acid[14] and lithium diphenylphosphide.[15] They are stereospecific and work under mild conditions. The drawback of the latter methodology is that it operates under strong basic conditions, demanding protection of sensitive functional groups.

An interesting alternative methodology that effects retention of configuration is that of diphosphorous tetraiodide (P_2I_4).[16] It is very mild and stereospecific reagent (Scheme 1.5).[17]

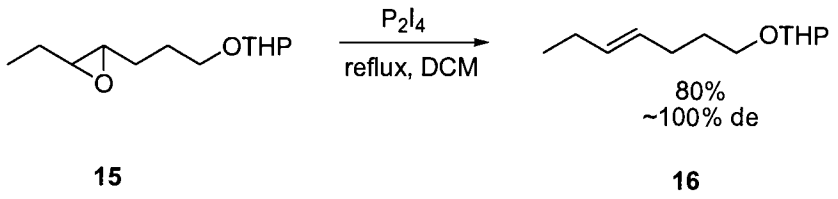

Scheme 1.5 Highly stereospecific deoxygenation of epoxides with P_2I_4

A plethora of selenium and tellurium reagents that effect one step epoxide deoxygenation have been reported. They work below room temperature and proceed with retention of stereochemistry. This example reveals a striking difference between epoxides and seleniranes. First, epoxide ring opening occurs and then selenirane (episelenide) **22** forms, which extrudes the olefin (Scheme 1.6).[18] Tellurium behaves very similarly.[19]

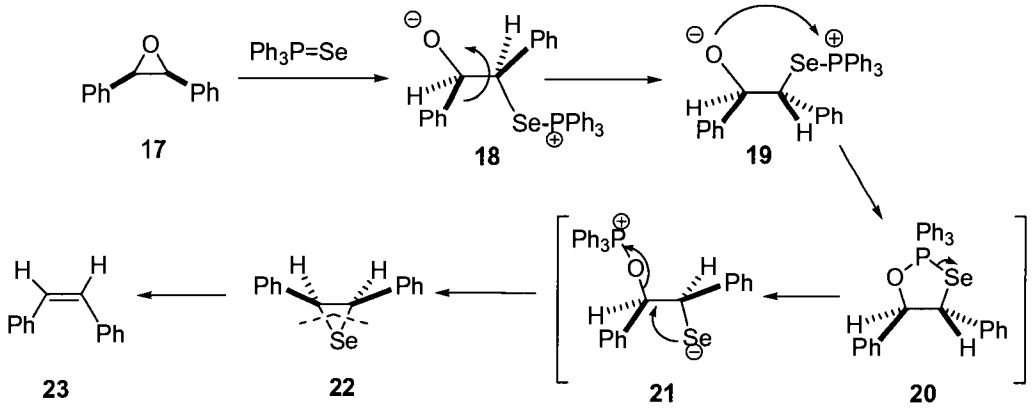

Scheme 1.6 Stereospecific deoxygenation of epoxides with Ph_3P=S

Sharpless in 1972 introduced low-valent, highly reactive and selective tungsten complexes as deoxygenation reagents.[20] The low valent tungsten species, generated from WCl_6 with reducing agents (BuLi, Li and LiI), were never identified. The stereochemical outcome depends on the substrate and on the way low-valent tungsten species is prepared. Although the reagent shows high reactivity and selectivity, it is required in stoichiometric quantity (Scheme 1.7).[21]

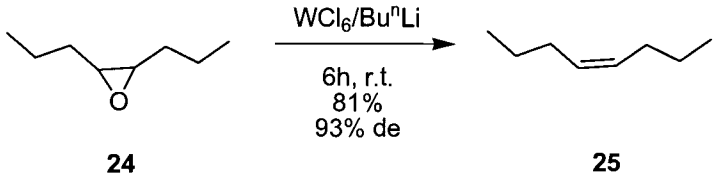

Scheme 1.7 Stereospecific deoxygenation of epoxides with low-valent tungsten species

Transition metal carbonyl complexes are known to deoxygenate epoxides. An archetypical example is dicobaltoctacarbonyl ($Co_2(CO)_8$)[22] which deoxygenates epoxides with inversion (Scheme 1.8).

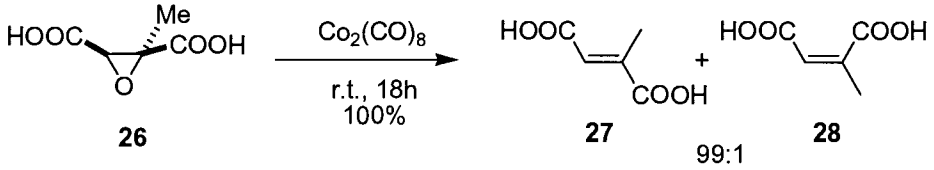

Scheme 1.8 Epoxide deoxygenation with transition metal carbonyl complex

The intermediate **29** is proposed to explain the stereochemical outcome of the reaction. This probably comes about by nucleophilic epoxide ring opening by electron rich cobalt; insertion gives finally the intermediate **29** (Fig 1.1).

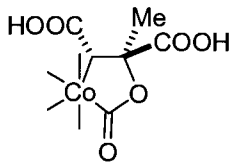

29

Fig 1.1 The intermediate of epoxide deoxygenation with $Co_2(CO)_8$

An interesting alternative metal carbonyl complex is sodium (cyclopentadienyl)dicarbonylferrate.[23] It is very stereospecific and gives inverted olefins in refluxing THF. If reaction with epoxide is followed by addition of sodium iodide, retention of stereochemistry is observed (Scheme 1.9).

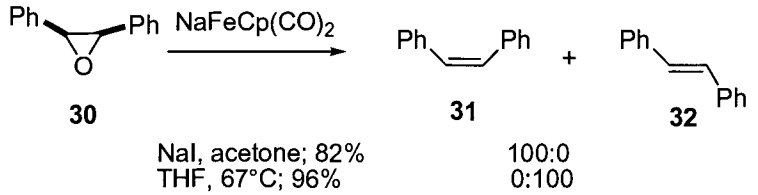

Scheme 1.9 Highly stereospecific epoxide deoxygenation with sodium (cyclopentadienyl)dicarbonylferrate

Titanocene dichloride effects the deoxygenation of epoxides with high stereselectivity and retention of configuration, employing Mg as stoichiometric reductant (Scheme 1.10).[24] Carbonyl groups, alkenes, ethers and acetals are not affected under the reaction conditions.

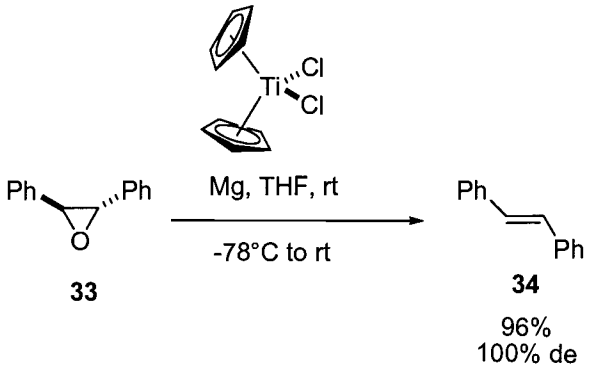

33 **34**

96%
100% de

Scheme 1.10 Titanocene dichloride catalyzed deoxygenation of epoxides

The last example stands out for being *catalytic in the metal complex* (Scheme 1.10). In order to design such a catalytic cycle, the catalyst properties must be adjusted by picking an appropriate metal or adjusting the ligand sphere, so oxygen atom transfer from the substrate to the metal is feasible. The strength of the metal oxygen bond usually is decisive. If the metal oxygen bond is too stable, the metal oxide intermediate will be the thermodynamic sink and catalysis is not viable. At the same time, the metal oxygen bond should be stable enough to make feasible oxygen transfer from the substrate to the catalyst and from the oxidized catalyst

intermediate to stoichiometric reductant. In case of tungsten, W-O is so strong that is very hard to reduce, making this a bad metal with which to design a catalytic cycle.

1.3 Hard and soft acids and bases

In 1963, Pearson[25] introduced a useful classification of substances into "hard" and "soft" acids and bases. The two classes are identified by their affinities (expressed as constants of equilibrium, K) towards halide ion bases:

- Hard acids bond in the order: $I^- < Br^- < Cl^- < F^-$
- Soft acids bond in the order: $I^- > Br^- > Cl^- > F^-$

From this definition, a general line can be drawn. In general, hard acids tend to bind to hard bases and soft acids tend to bind to soft bases. The reason lies in the nature of the interaction. Namely, hard acid-base interactions are mainly electrostatic, whereas soft acid-base interactions are mainly covalent.[26]

1.4 Ligand metal interaction

The hard/soft principle is useful, though in essence empirical. Molecular orbital theory is a quantum mechanical approach that explains in quantitative manner the nature of metal ligand interaction.[27] It gained

ground with advances in computer software and hardware, becoming indispensable to a modern organic chemist.[28]

A typical feature of the transition metals is their affinity to form complexes with so called π- acceptor ligands via back bonding. A very common ligand of this sort is carbon monoxide (CO). The metal-carbon bond has at least fractional π character.[29]

As opposed to a metal-CO interaction, where the metal-carbon bond is partially a second order bond, metal oxygen bonds are at least fully double. Actually, in many cases the bond order is probably >2 because there are two filled p π symmetry orbitals on the oxygen atom, which can nicely overlap with d π symmetry orbitals on the metal atom (Fig. 1.2).[30]

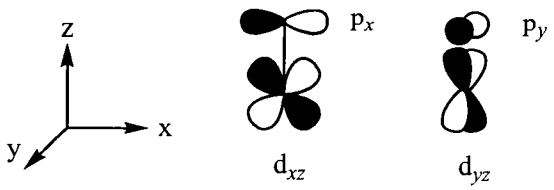

Fig. 1.2 d orbital of metal overlapping with p atomic orbitals of oxygen atom

A quintessential example of interest is methyltrioxorhenium(VII), $MeReO_3$. From the MO diagram few important conclusions can be drawn (Fig 1.3).

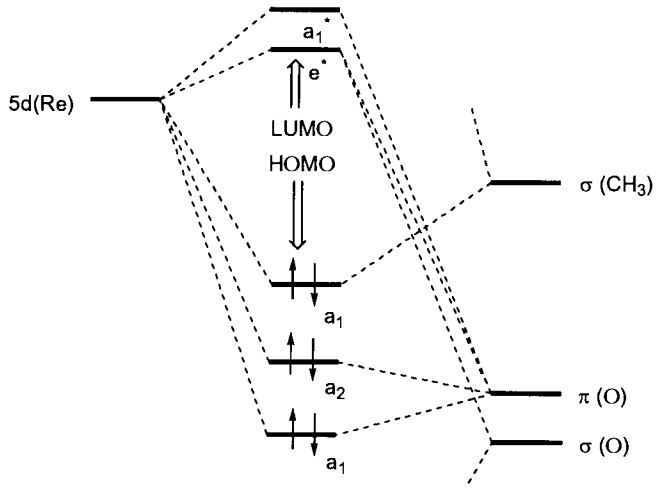

Fig. 1.3 Simplified MO diagram of methyltrioxorhenium(VII)

HOMO is oxygen centered, whereas LUMO is metal centered orbital. This implies that Re atom is the electrophilic site and most likely attacked by nucleophiles. The LUMO energy can decrease by changing methyl with another ligand making the LUMO more oxygen centered and the oxygen atom more electrophilic site. An example is $[Tp'ReO_2Ph]OTf$, where a migration from σ bonded Ph to rhenium atom to oxygen atom occurs (Scheme 1.11).[31]

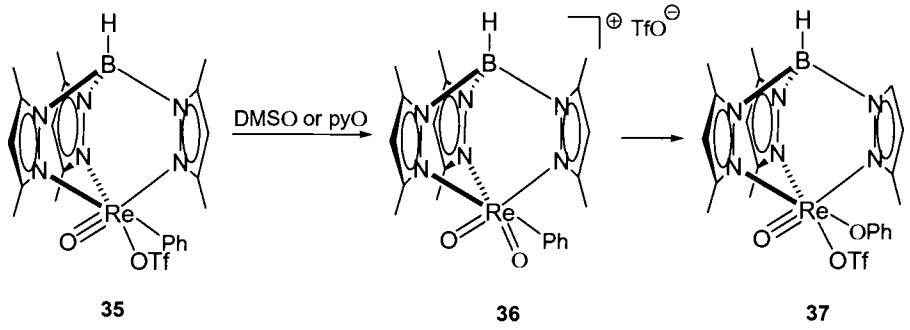

35 36 37

Scheme 1.11 A migration of Ph from rhenium center to the oxo ligand

1.5 Organorhenium Oxides- Methyltrioxorhenium

In the middle of the transition metals lies the VII B group, otherwise know as manganese triad (manganese, technetium and rhenium).[32] While manganese is a relatively common element, technetium and rhenium[33] are very rare elements, the former being the first element to have been produced artificially[34] and the latter being the last naturally occurring element to be discovered.

This triad is wealthy in the number of known compounds. In terms of organic chemistry, organometal oxides thereof are the most important, especially in case of rhenium (Fig 1.4).[35]

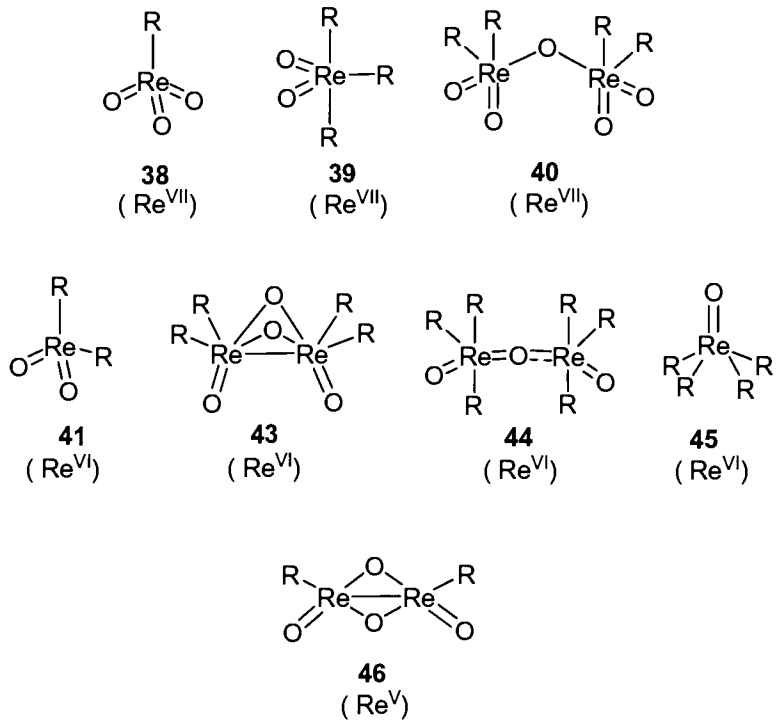

Fig 1.4 Eight different types of neutral organorhenium oxides

Class **38** is the best understood and the most important class; as far as 1997, 38 organorhenium oxides of type **38** had been prepared. Dirhenium heptaoxide (Re_2O_7) is the main entrance to these classes of compounds.[36] While Re_2O_7 homologs (Mn_2O_7, Tc_2O_7) have molecular structures, Re_2O_7 has a polymeric solid state structure like most insoluble metal oxides (WO_3, MoO_3). Its structure is unique. In the solid[37] state, it consists of equal number of nearly regular tetrahedral and of highly distorted octahedral centers, which share oxygen corners (Fig 1.5, **46**). In

the gas phase, it consists of two equivalent rhenium atoms in tetrahedral environment (Fig 1.5, **47**).

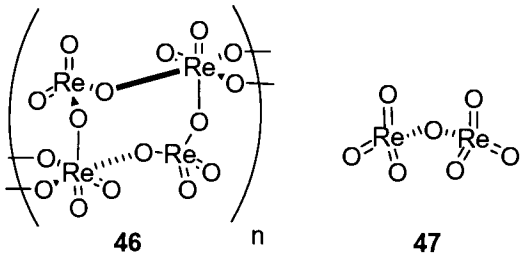

Fig 1.5 Re_2O_7 solid (**46**) and gas (**47**) phase state geometries

The polymeric structure of Re_2O_7 is cleaved by aprotic, organic donor solvents such as MeCN, THF or DME (Scheme 1.12).

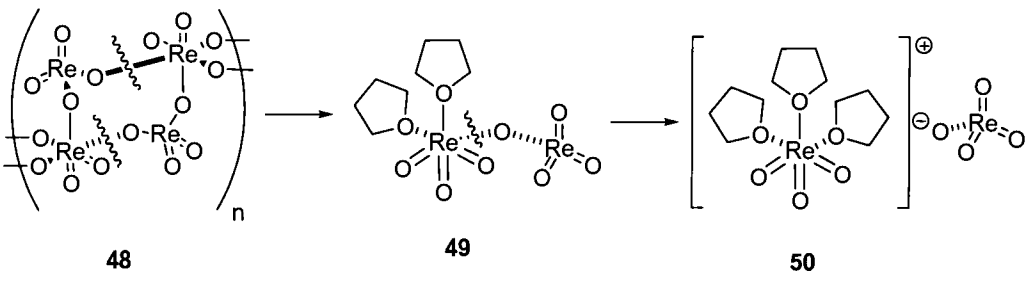

Scheme 1.12 Breaking of a polymeric Re_2O_7 structure by organic donor solvents

50 can be alkylated (arylated) with organotin, organozinc and organomagnesium reagent to give rise to a plethora of compounds of type **38.** The drawback of this approach is that half of rhenium is lost. A more efficient approach is to prepare *in situ* a mixed anhydride, RCO_2ReO_3 and use it as perrhenyl synthon instead (Scheme 1.13).[38]

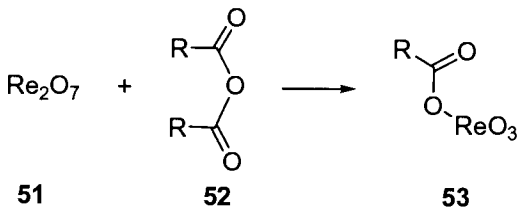

Scheme 1.13 A mixed anhydride as perrhenyl synthon

The simplest member of this class, methyltrioxorhenium, $MeReO_3$ (hereafter referred as MTO) is one of the best studied organometallic compounds.[39] Ever since its serendipitous discovery[40] in 1979, it was noticed that it bears unique properties. Further studies undertaken by Herrmann et. al. [41] showed that MTO is an excellent catalyst for alkene epoxidation using H_2O_2 as terminal oxidant. In addition, MTO is a catalyst of a myriad of important organic reaction (Fig 1.6).[42]

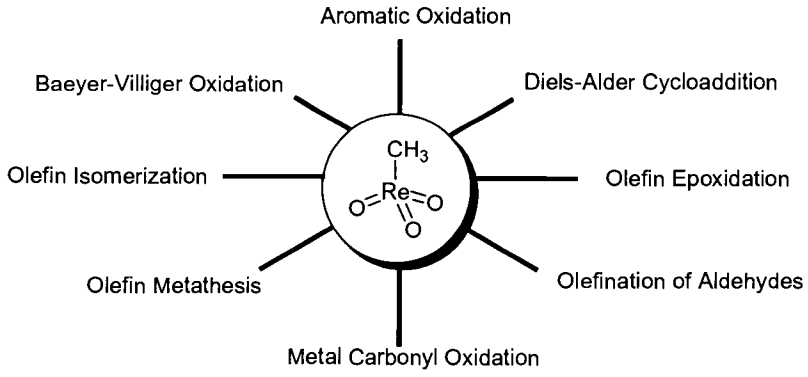

Fig 1.6 Main organic reaction catalyzed by MTO

One of the best studied catalytic reactions involving MTO is the epoxidation of olefins. MTO is an efficient epoxidation catalyst. It is very active at both low concentration of MTO (typically 0.1-1 mol %) and H_2O_2 (concentration < %5); it works well over a large temperature range (usually -10°C – 100°C; even at -30°C); its selectivity can be modified by use of certain additives (co-ligands);[43] it is commercially available, air stable, soluble in water (low pH) and in organic solvents and it's effective as either a homogenous or a heterogeneous catalyst. The kinetic model of the catalytic cycle has been worked out in detail.[44]

OsO_4 is a well documented cis-dihydroxylation reagent for olefins, affording osmium (VI) 1, 2-diolates (Scheme 1.14, Eq. 1.1).[45] Technetium forms similar metallacycles in the same manner (Scheme 1.14, Eq. 1.2).[46] Unlike technetium and osmium, rhenium behaves differently.[47] Similar rhenium-containing diolates are known; however, they are accessible via condensation reaction with diols[48] and ring opening (expansion) of epoxides[49] (Scheme 1.14, Eq. 1.3).

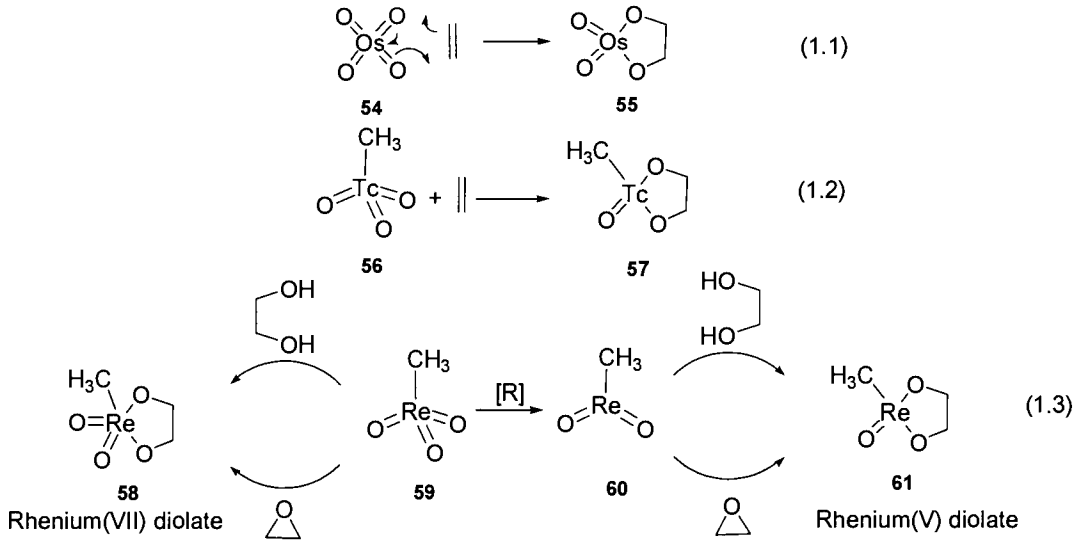

Scheme 1.14 Osmium, Technetium and Rhenium diolates

1.6 Cycloreversion of Rhenium Diolates

An interesting impact on MTO chemical and physical properties is observed by changing methyl ligand with more electron rich ligand, Cp^* (η^5- pentamethylcyclopentadienyl) (Fig 1.7).[50] The reason for this impact is the nature of the ligand. While Me is a strong σ donor, Cp^* is a moderately good π donor and donates four more electrons. The first impact is observed in Re-O bonds. In Cp^*ReO_3, this bond is longer and weaker. MTO is unstable under strong basic condition and forms easily adducts with tertiary amines.

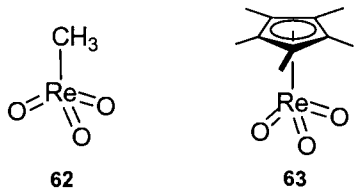

62 63

Fig 1.7 MTO versus Cp^*ReO_3

On the other hand, Cp^*ReO_3 can survive both LiOH and concentrated HCl in THF solution for several days at room temperature and does not form isolable Lewis base adducts. The most striking difference is in their chemistry. Whereas MTO in presence of H_2O_2 epoxides olefins, Cp^*ReO_3 does not. In addition, Cp^*ReO_3 dihydroxylates strained olefins only, giving rise to rhenium (V) diolates.[51] In the case of unstrained olefins, the formed diolates are thermodynamically unstable and cyclorevert to olefin. MTO fails to bishydroxylate strained or unstrained olefins.

1.6.1 Mechanistic implication of the Cycloreversion

OsO_4 has been a reagent of choice for alkene bishydroxylation for much of the last century. Its empirical advancement and utility in organic synthesis has outpaced its mechanistic understanding. The latter it is even nowadays shrouded with mystery despite immense research time devoted

in this area. Generally, two mechanisms have been proposed in order to explain experimental data:

1) a concerted [3+2] cycloaddition[52] and 2) a stepwise mechanism involving an osmaoxetane intermediate, **69** (Scheme 1.15).

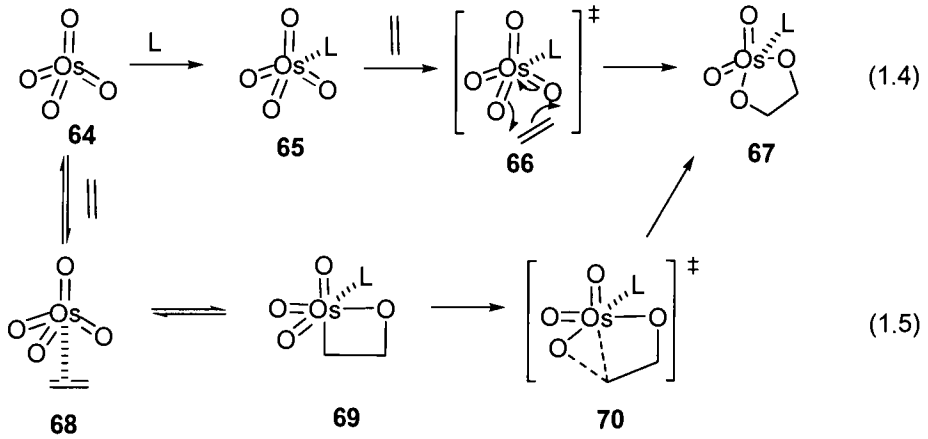

Scheme 1.15 Two mechanistic themes of alkene bishydroxylation by OsO_4

The first mechanistic theme is based on Criegee's pioneering work and supported by the Woodward-Hoffman rules.[53] Many workers in this area, notable Corey, argue that [3+2] cycloaddition is more consistent with observed enantioselectivity.[54] The osmaoxetane mechanism came into play by drawing an analogy with chromyl chloride epoxidation of olefins[55] and olefin metathesis.[56] In 1997, Sharpless et. al.[57] combined kinetic isotopic effect (KIE) measurements with high level DFT

calculation to unravel the mechanism. Measured[58] and calculated KIEs were remarkably similar and thus supported the [3+2] mechanism. In addition, transition state energies for osmaoxetene formation and expansion were calculated to be higher for the stepwise [2+2] mechanistic pathway than observed experimentally. These results argued strongly in favor of [3+2] mechanism but could not rule out [2+2] pathway. The main reason for this is a truncated model[59] used for modeling transition state and thus the calculated KIEs may not reflex the real picture. In addition, the [3+2] mechanism does not explain observed electronic effects[60] in this reaction and temperature dependence of the enantioselectivity[61] that implies a stepwise mechanism.

Cycloreversion of rhenium (V) diolates are important because of the presumed mechanistic kinship to OsO_4 alkene bishydroxylation. Interest in this reaction was spurred by the fact that $LReO_3$ is isoelectronic with OsO_4; thus cycloreversion of rhenium (V) diolates is the microscopic reverse of formation of **67** (Scheme 1.15). In accordance to the principle of microscopic reversibility,[62] rhenium (V) diolates must cycloreverse by the same mechanism **67** (Scheme 1.15) is formed. Much work has been devoted to the reaction mechanism. Gable's[63] work stands out for being

the most comprehensive in this area. A fairly large amount of data favors an asynchronous concerted [3+2] mechanism (Scheme 1.16, Eq. 1.7, **80**).[64] Alternative polar mechanisms are very unlikely to operate in this system, because very high stereospecificity[65] and rate solvent independence[66] is observed.

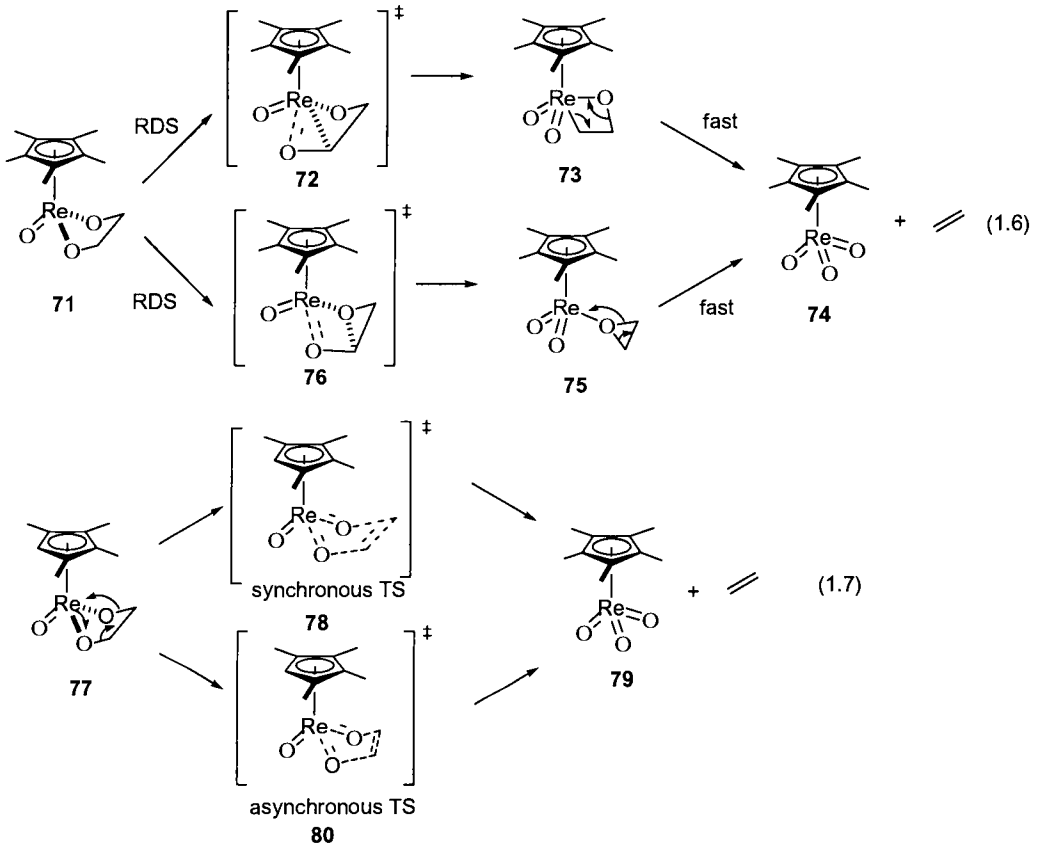

Scheme 1.16 Rhenium (V) diolate cycloreversion mechanism

Experimental and computational evidence that support asynchronous mechanisms versus a stepwise [2+2] mechanism is the following:

1) Strain/Reactivity Studies: The strain in the newly formed double bond has no effect on the rate of olefin excision.[67] A rationale for this is that in the rate determining step the double bond has not formed yet.
2) Conformational/Reactivity Studies: A kinetic study of olefin excision from several diolates showed a strong dependence of the rate on the conformation of diolate.[68] The excision was inhibited if the ring assumed an eclipsed conformation and promoted if it assumed a staggered conformation. Computational work showed that LUMO of the diolate has mostly metal d character. One C-O bond (the "axially" oriented one) is roughly parallel to one of LUMO lobes around the metal center (Fig 1.8).[69]

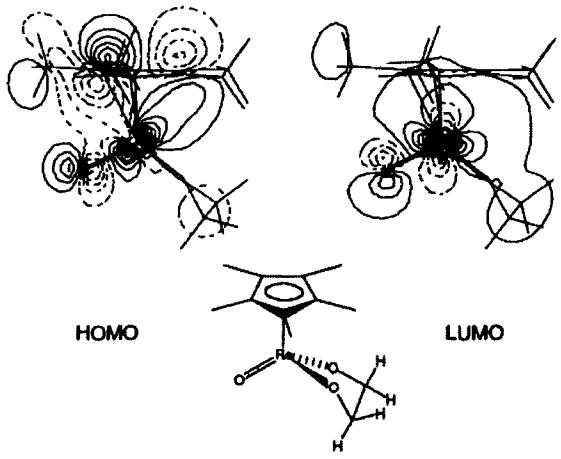

Fig 1.8 Frontier Orbitals of $Cp^*Re(O)(OCH_2CH_2O)$ from EHT Calculation
(From Gable, K. P et. al. *J. Am. Chem. Soc.* **1996**, *118*, 2625. By permission of the publisher)

3) Linear Free-Energy Relationship (Hammett Studies):[70] Hammett studies with phenylethanediolates showed that an electronic buildup occurs at transition state on the benzylic carbon. Modeling the transition state showed that indeed one of two C-O bond is much longer then the other.[71] Furthermore, symmetric diolate loses symmetry as it goes through transition state; this was observed as a V-shaped Hammett plot for diphenylethanediolates.[72]

4) Kinetic Isotope Effects:[73] Kinetic studies showed KIEs greater than unity at both α and β carbons (k_H/k_D = 1.076±0.005 at the α position and 1.017±0.005 at the β position).[74] Had the stepwise

rhenaoxetane intermediated mechanism (Scheme 1.16, Eq. 1.6) been operating, one would have predicted KIE in one carbon bigger than unity and on the other carbon approximately equal to unity. KIEs are in favor of an asynchronous but concerted mechanism.

Overall, the data consistently suggests asynchronous cleavage of the two C-O bonds. Early on, it was presumed that this better fit the stepwise mechanism (1, 2, 3), but KIE studies definitively showed that it is an asynchronous, but concerted process with very flexible (physical and electronically) transition state. This fits with Sharpless findings on bishydroxylation mechanism of olefins.[75]

Extensive kinetic measurements and modeling led Gable to propose a mechanism of epoxide deoxygenation mediated by rhenium(V) dioxo complex (Scheme 1.17).[76] In the first step $Tp'Re^{VII}O_3$ is reduced with Ph_3P in a very fast manner giving $Tp'Re^{V}O_2$, which is the active catalyst. Water retards the turnover frequency by converting $Tp'Re^{V}O_2$ into its dihydroxy adduct **81** (Scheme 1.17). Introduction of molecular sieves drives the equilibrium toward active species **82**. Cleverly engineered competition experiments proved that $Tp'Re^{V}O_2$ coordinates to the

epoxide. Driven by sterics, the coordinated epoxide expands under kinetic control giving the diolate **84.** Kinetic treatment of the data proved that diolate cycloreversion alone cannot explain the rate of olefin excision. Direct oxygen transfer was introduced to explain the kinetics. After **84** reaches steady state concentration, the rate of epoxide deoxygenation depends only on the diolate concentration.

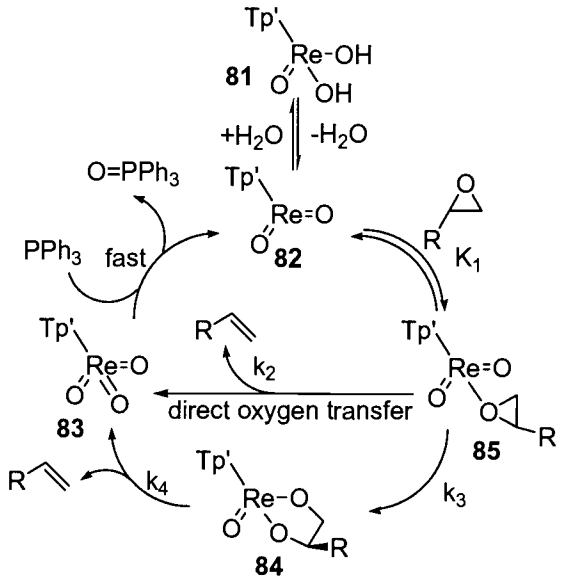

Scheme 1.17 Kinetics and mechanism of Rhenium catalyzed O atom transfer

1.6.2 Synthetic utility and limitations[77]

Trost's[78] and Larock's[79] organic reaction compendiums are the first resource that the synthetic organic chemist turns to. The fact that the latter do not make any mention of rhenium-catalyzed epoxide

deoxygenation shows how little attention this chemistry has received from the synthetic community. This is so for aforementioned reasons. However, the late advent in understanding the mechanism of rhenium (VII) trioxo catalyzed epoxide deoxygenation will without doubt change this picture in the near future.

In 1996, Cook and Andrews[80] reported catalytic deoxygenation of vicinal diols with Cp^*ReO_3 using Ph_3P as stoichiometric reductant. Under these conditions Cp^*ReO_3 is reduced to $Cp^*ReO_2/(Cp^*ReO)_2(\mu - O)_2$. Epoxides are deoxygenated by this rhenium catalytic system, but the turnover frequency is low. Turnover frequency was increased by increasing Ph_3P concentration to impractical concentration. The reason for the catalytic cycle shutting down was found to be formation of a novel tetranuclear cluster rhenium complex that is catalytically inactive.[81] It was reckoned that one way of inhibiting the clustering is bulking up the rhenium ligand sphere.[82] This ligand should minimally perturbs the reactivity of the metal center, but should inhibit the clustering. Ligands of choice were so-called scorpionates (polypyrazolylborates), notably hydridotris(3, 5-dimethyl-1H-pyrazoly)borate (Tp') which have long been know as "cyclopentadienyl equivalent" (Fig 1.9).[83]

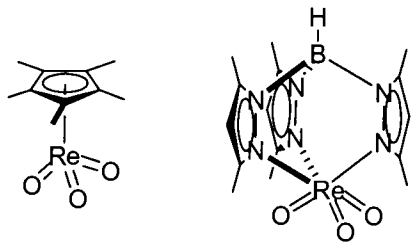

86 **87**

Fig 1.9 Cp^*ReO_3 versus $Tp'ReO_3$

As mentioned before, relatively few methods exist for deoxygenation of epoxides which operate under mild conditions.[84] A rhenium-based catalytic system operates under neutral conditions; it requires only a mild coreagent (Ph_3P) as stoichiometric reductant and operates under low catalyst loading (5 mol-% or less); THF, ether, MeCN, benzene are good solvents to run the catalysis in; byproduct (Ph_3PO) is easily removed with column chromatography; reaction runs usually at 75°C and for more stubborn substrates usually 105°C will suffice to push the reaction to completion; the reaction is highly stereospecific (with few exceptions such as trans-2-butene). Usually terminal epoxides are more readily deoxygenated that internal ones; likewise, more substituted epoxide deoxygenate less readily, with some exceptions. Epoxides with electron withdrawing functionality are more reactive. Nitro and hydroxyl functional groups interfere; protecting OH as silylether resulted in

efficient catalysis. Esters, halogens, conjugated double bonds, nitrile, do not interfere at all.

1.7 Conclusion and Outlook

If the carbonyl functional group is virtually the backbone of organic synthesis, the epoxidation is at least one of main muscles.[85] Epoxides are very versatile intermediates. One of the most important reactions that epoxides undergo is epoxide ring opening reaction. Worthwhile mentioning is Jacobsen's catalyst. Its success is mainly due to understanding of the kinetic model of the catalytic cycle in detail. The deoxygenation reaction is a related reaction that epoxides undergo and it is formally the reverse of the epoxidation. This reaction is occasionally used in the synthesis of complex natural products. A plethora of reagents that effect deoxygenation of epoxides have been developed. All, but very few are plagued by multi-step procedures, usually require stoichiometric and harsh conditions, show low stereselectivity, operate under unknown mechanisms and suffer from functional group incompatibility.

In contrast to epoxidation, very few methodologies exist for catalytic epoxide deoxygenation, not to mention asymmetric epoxide

deoxygenation. High oxidation state rhenium compounds are emerging as useful candidates to fill this gap. As opposed to its neighbors, which are either good epoxidation (titanium,[86] vanadium[87] and chromium[88]) or bishydroxylation (manganese,[89] ruthenium,[90] and osmium[91]) reagents, the rhenium trioxo complexes are remarkably adjustable and thus promising catalysts for epoxidation and bishydroxylation reactions.

In the following chapter we are going to describe the design of new chiral rhenium (VII) trioxo complexes. Chiral rhenium (VII) trioxo complexes that we set out to prepare can be divided in two groups: 1) chiral complexes void of stereogenic centers and 2) chiral complexes with stereogenic centers.

-Chapter 2-

Designing Chiral Rhenium Trioxo Complexes

2.1. Introduction

An important guide to designing the chiral rhenium (VII) trioxo complexes is the mechanism for translating the stereogenic properties of the auxiliary to the reaction site. The first step in rhenium epoxide deoxygenation is coordination of the epoxide to the rhenium (V) electrophilic center (Scheme 1.17). In order to deoxygenate epoxides in an asymmetric fashion the epoxide coordination has to be facially differentiated. If we examine the top view of a generic $Tp'Re^{V}O_2$ species we notice that it is symmetric, thus it will not be facially discriminative towards the coordinated epoxide. Installation of even a chiral entity at position C5 would not impact the way epoxide is coordinated to rhenium (V). This site is too remote from the reaction site. The main way to distort this symmetry is by bulking up the pyrazole ring at position C-3. This will tilt otherwise parallel three pyrazole rings, giving rise to an asymmetric environment (Fig 2.1). To install asymmetry we have used bulky

trispyrazolylborates that either exhibit atroisomerism or contain a stereogenic center.

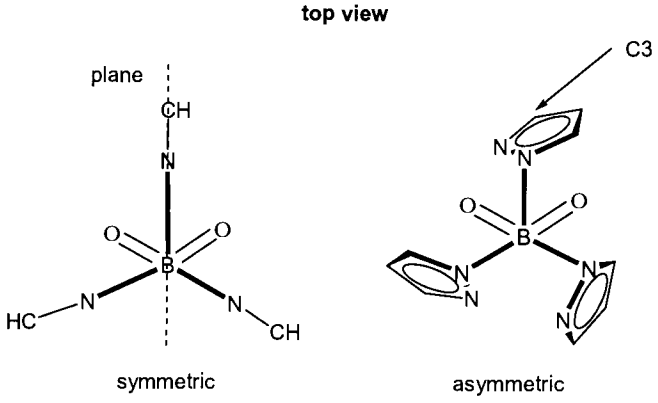

Fig 2.1 The mechanism of translating stereogenic information

2.2 Scorpionates[92]

In chapter 1 scorpionates (polypyrazolylborates) were briefly mentioned as ligands of choice. They are well-established ligand systems, known for over 30 years. They are represented by general formula **1** (Fig. 2.2).

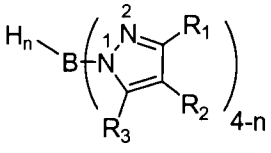

1

Fig. 2.2 A generic polypyrazolylborate ligand

R_1, R_2, R_3 can be alkyl, aryl, heteroaryl, halo, cyano, fused benzo- and naphto- rings, etc. giving rise to a huge number of polypyrazolylborates. This pliability bestows on them very adjustable sterics and electronics, thus a predicable coordinative chemistry.

Trispyrazolyborates are tridentate C_{3v} symmetry ligands that coordinate strongly to a metal, impacting its sterics and electronics, and leaving other coordinating sites free for other chemistries of interest. The coordination to a metal is reminiscent of the way a scorpion grips on its prey, hence the name scorpionates (Fig 2.3).

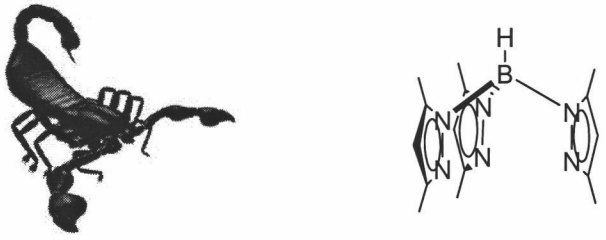

Fig 2.3 The resemblance of a scorpion with scorpionates-trispyrazolylborates

Although there are more than 170 reported scorpionates, trispyrazolylborate (Tp) and 3,5-dimethypyrazolylborate (Tp') are the most commonly used. The latter are known as homoscorpionates.

These ligands are usually prepared by heating a mixture of alkaline metal borohydrides and a corresponding pyrazole (PzH). The substitution is controlled by limiting the reaction temperature (Scheme 2.1).[93]

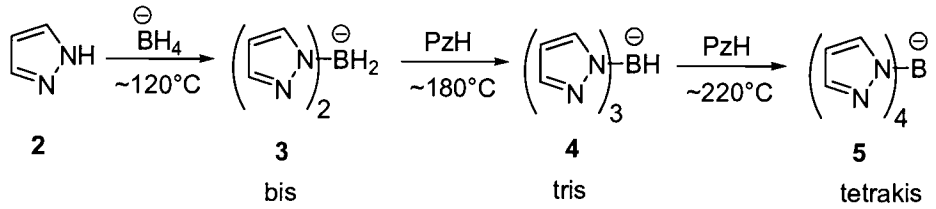

Scheme 2.1 A generic synthetic route to polypyrazolylborates

A salient feature of scorpionates is their resemblance to Cp ligand. Both ligands are uninegative, each donates 6 electrons (the former has heptacity equal to 3 whereas the latter equal to 5) and occupy 3 coordinative sites. The similarity ceases here. Scorpionates bear many unique features:

- They belong to the C_{3v} point group, whereas Cp belongs to the C_{5v} point group.
- There are 10 substitutable sites in Tp. This offers wider range of modification of Tp ligands.
- The alkali metal salts of Tp ligands are air-stable solids; on the contrary, such Cp salts are air-sensitive.

- The "free acids", TpH are also stable compound and acts as ligands. By contrast, cyclopentadiene (CpH) itself is a ligand but unstable and notorious for dimerizing.

2.3. Atropisomerism

The term "conformational isomers" is used to denote any one of a number of momentary configurations of the molecule that results from rotation around single bonds.[94] Conformational isomers, such as the gauche (Fig 2.4, **6**) and anti butane (Fig 2.4, **7**) are discrete entities. The energy barrier between these two isomers at room temperature is so low (~3.4 kcal/mol) that it is impossible to isolate them. Any attempt to do so will result in reforming the equilibrium mixture. It takes an energetic barrier of about 16-20 kcal/mol to prevent equilibration of two conformational isomers at room temperature.[95]

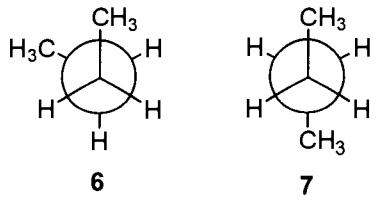

6 **7**

Fig 2.4 The gauche and anti conformational isomers of n-butane

Lowering temperature freezes the equilibrium and makes possible to distinguish conformational isomers. A case in point is 1,4-dimethylcyclohexane (Scheme 2.2). At room temperature the two methyls are equivalent on average and indistinguishable by physical methods. However, at -60 ° C the methyl groups become discernible by the ^{13}C NMR and ^{1}H NMR spectroscopy.

8 9

Scheme 2.2 Two conformational isomers of 1,4-dimethylcyclohexane

The UV spectrum of biphenyl has a strong absorption band at λ_{max}= 249 nm (ε = 15000) because of an excited state involving delocalization of π electrons across the two benzene rings (Fig 2.5).

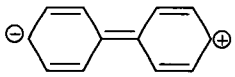

10

Fig 2.5 Excited state of biphenyl

Introducing a single methyl group in the ortho position shifts the absorption maximum to λ_{max}= 237 nm and lowers the extinction

coefficient to ε = 10500.[96] Introduction of the second methyl group in ortho' position causes the complete disappeared of the absorption band.[97] The reason for this is that the 2,2'-dimethylbiphenyl molecules spend most of their time in a conformation that deviates from the planar geometry. In accordance to the Franck-Condon principle,[98] the excited state must therefore deviate from the planar geometry. Although the rotation around the carbon-carbon bond is dampened, the resolution of different conformational isomers is not possible. Bulking up the biphenyl with bigger groups can dampen the rotation around the carbon-carbon bond and make the resolution possible at root temperature. Classical examples are diphenic acid derivatives, the first resolved biphenyl derivates (Fig 2.6).[99]

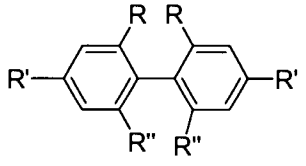

11

11a R= NO_2, R'= H, R"=COOH
11b R= R'=NO_2, R"=COOH
11c R= H, R'=NO_2 , R=COOH

Fig 2.6 Resolvable diphenic acid derivatives

Diphenic acid derivates were among the first examples of optically active organic compound void of a stereogenic center.[100]

2.4 Chiral Rhenium Trioxo Complexes

Guided by the mechanism for translating the stereogenic properties, we set out to prepare a chiral complex where the source of asymmetry was the restricted rotation around a carbon-carbon bond. The simplest scorpionate that exhibits atropisomerism was envisioned to stem from 2-methylacetophenone **12**. If resolution of the atropisomers is a problem, the remedy would be simple installation of an appropriate functionality on C6 of the benzene ring. From the synthetic point of view, one would start with commercially available 2-methyl-6-nitroacetophenone (Scheme 2.3).

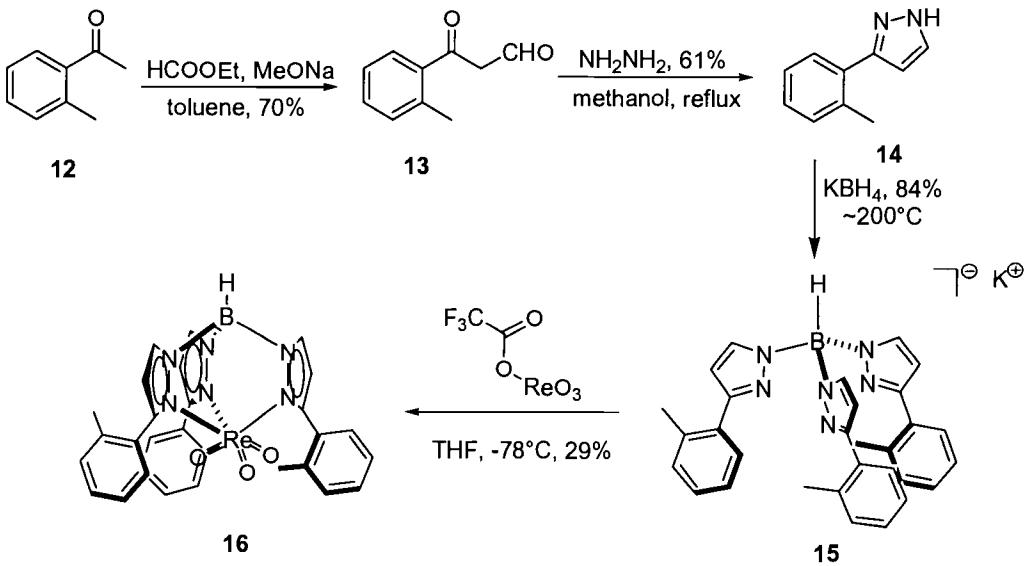

Scheme 2.3 The preparation of hydrido-tris-(3-o-tolyl-1H-pyrazolyl)borate based rhenium(VII) trioxo complex

The strategy laid above (Scheme 2.3) is a general strategy for preparing unsubstituted,[101] 3-monosubstituted,[102] 4-monosubstituted,[103] 3,4-disubtituted,[104] 3,5-disubtituted,[105] 4,5-disubstituted,[106] trisubstituted[107] and boron-substituted[108] scorpionates. By designing the ketone **12**, different functionalities can be installed in carbon 3, 4 and 5 of the pyrazole ring. Another option is monoalkylation of the β-keto aldehyde **13.** The β-keto aldehyde **13** annulates with hydrazine giving a substituted pyrazole.[109] The pyrazole **14** undergoes acid-base chemistry with alkaline metal (sodium or potassium) borohydrides giving bis, tris or tetrakispyrazolylborates depending on the temperature at which the reaction is run.[110] Finally, using trifluoroacetyl perrhenate as a source of rhenium (VII), simple ligand exchange gives the rhenium trioxo complex **16**.[111]

IR spectroscopy is a very reliable tool to show the presence of a B-H and a Re=O bond. $TpReO_3$ shows a conspicuous, strong B-H stretch at 2529 cm^{-1} (Fig 2.7). This prototypical rhenium (VII) trioxo complex is prepared by reacting 1 equivalent of hydrido-tris(pyrazoly)borate with mixed anhydride $CF_3COOReO_3$ at room temperature.[63] This reaction runs

very smoothly at room temperature with no change in color giving a white fluffy solid.

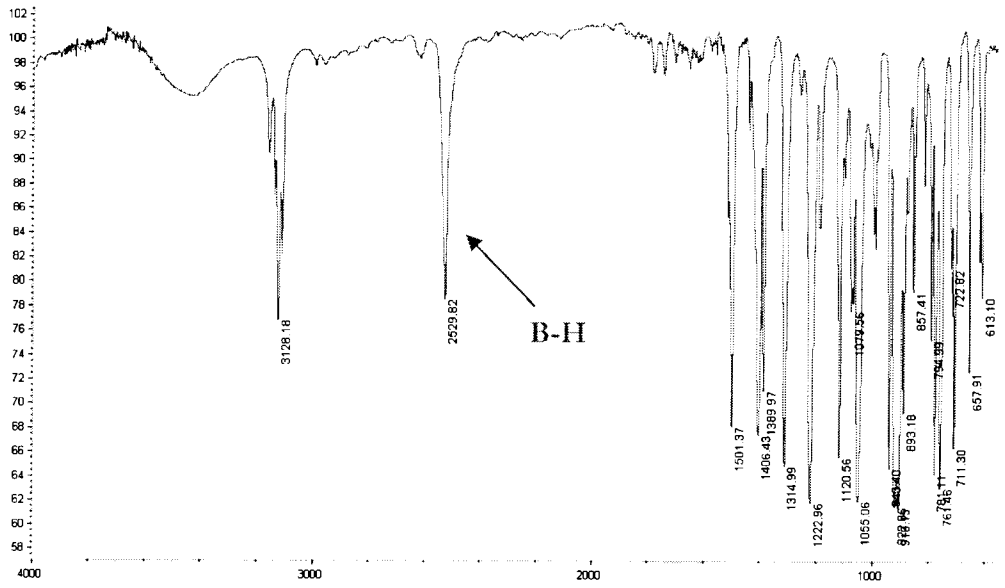

Fig 2.7 The IR spectrum of $TpReO_3$

When the same methodology was pursued to prepare **16,** there was no visible precipitation of the product. We always obtained a dark colored (green or pink) solution that after washing with methanol gave a white to gray solid. IR spectroscopy conclusively showed that this is $KReO_4$. Due to steric congestion, an electron transfer reaction at room temperature was likely competing with coordination of scorpionate to the rhenium trioxo center. To probe this hypothesis we tried to prepare hydrido-tris-(3,5-diisopropyl-1H-pyrazolyl) borato (trioxo) rhenium(VII) under the same conditions. At the outset of the reaction, the solution turned yellow and

with time it became dark green. No visible product precipitated. A very fine white to gray solid was obtained, that was characterized as $KReO_4$ (IR). It was deemed that running the reaction at low temperature will slow down the competing electron transfer reaction. Reacting the borate **15** with $CF_3COOReO_3$ at -100°C gave the same results. Pleasingly, running the reaction at -78°C for at least 10 h proved to be successful, though the desired reaction was much slower. A white to gray solid was obtained (procedure A) that showed a moderately strong B-H stretch at 2510 cm^{-1} and a Re=O stretch at 919 cm^{-1} (Fig 2.8).

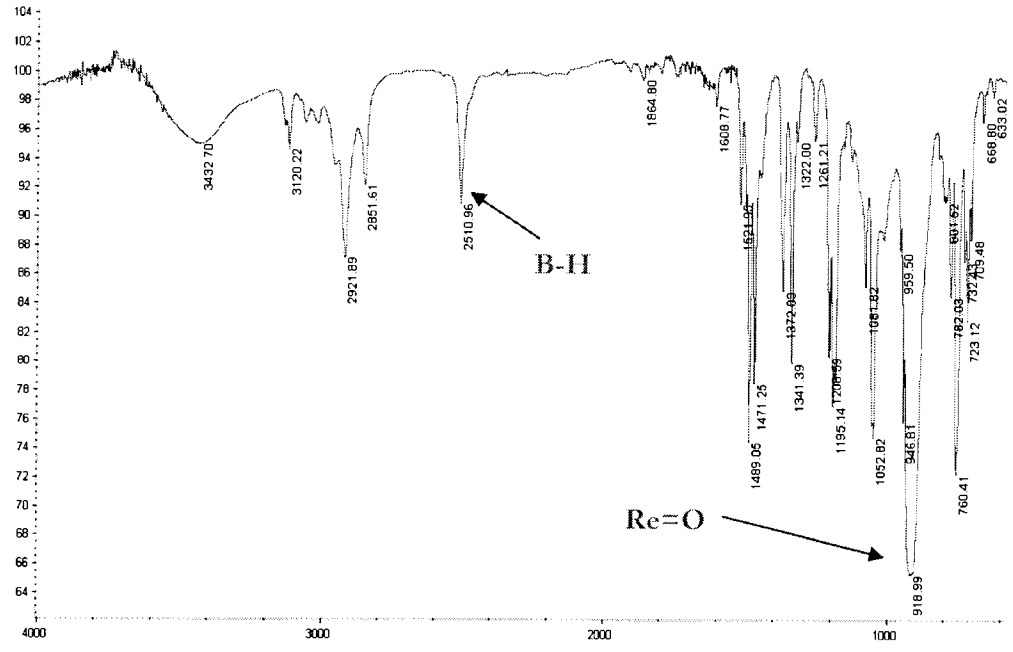

Fig 2.8 IR spectrum of **16** (Procedure A)

The ^1H NMR (DMSO) spectrum showed that at room temperature the rotation around carbon-carbon bond is so fast on the NMR time scale that all pyrazoles and methyls are indistinguishable (Fig 2.9). HRMS analysis (FAB) detected a molecular ion $[C_{30}H_{28}BN_6O_3Re]^+$ 719.1932.

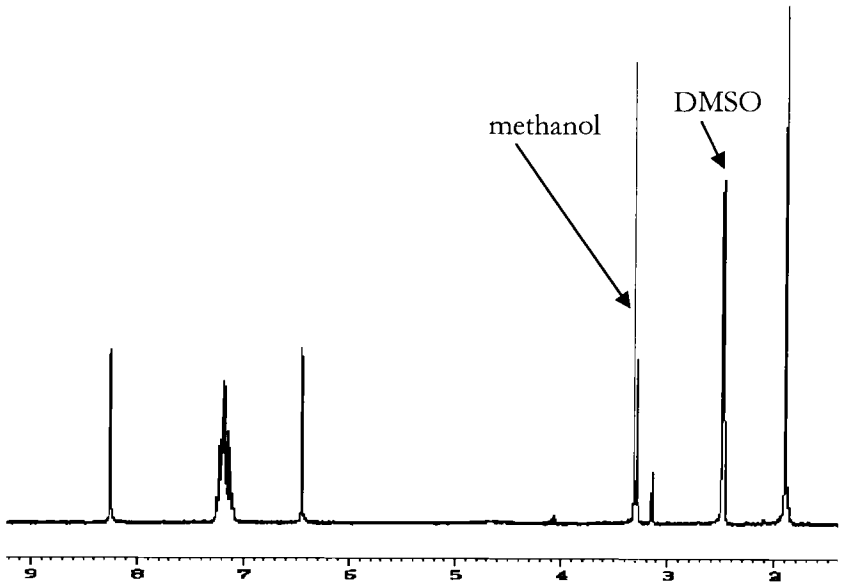

Fig 2.9 ^1H NMR of rhenium(VII) Trioxo complex **15** (Procedure A)

Rhenium (VII) trioxo complex **16** is insoluble in most organic solvents; DMSO proved to be only good solvent. This posed an obstacle for running NMR at lower temperatures, because of the melting point of DMSO (m.p. 18°C). A solution to this problem was converting the complex into rhenium (V) ethane-1,2-diolate, a more soluble complex with almost unperturbed conformational propensity of the ligand on rhenium. Usually rhenium (V) ethane-1,2-diolate complexes are light

blue. This is exactly what we have recorded when we tried to prepare the diolate from rhenium (VII) trioxo complex **16**. Compared to $TpRe^{V}(O)(OCH_2CH_2O)$, the IR spectrum shows a broad and a weak characteristic B-H stretch at 2496 cm^{-1}. Flash chromatography purification of rhenium(V) ethane-1,2-diolate (V) proved to be difficult compared to very easily flash chromatography purification of $TpRe^{V}(O)(OCH_2CH_2O)$. Under the same condition the R_f of the former was much bigger. A conclusive piece of evidence came from the ^1H NMR. Carbinolic proton peaks were missing (two multiplets above 3.0 ppm), meaning that we had been unsuccessful in making the diolate. This also called into question identification of rhenium (VII) trioxo complex **16**.

Serendipitously, in pursuit of preparing rhenium (VII) trioxo complex **16,** we reacted 2.6 equivalents of the borate **15** with trifluoroacetyl perrhenate at -78°C (Procedure B) (Scheme 2.3). A deep green solution emerged with time. To our surprise, a careful separation gave a white to gray solid that showed a doubled IR band: 2551 and 2516 cm^{-1} (Fig 2.10). HRMS analysis (FAB) detected molecular ion $[C_{30}H_{28}BN_6O_3Re]^+$ 719.2000.

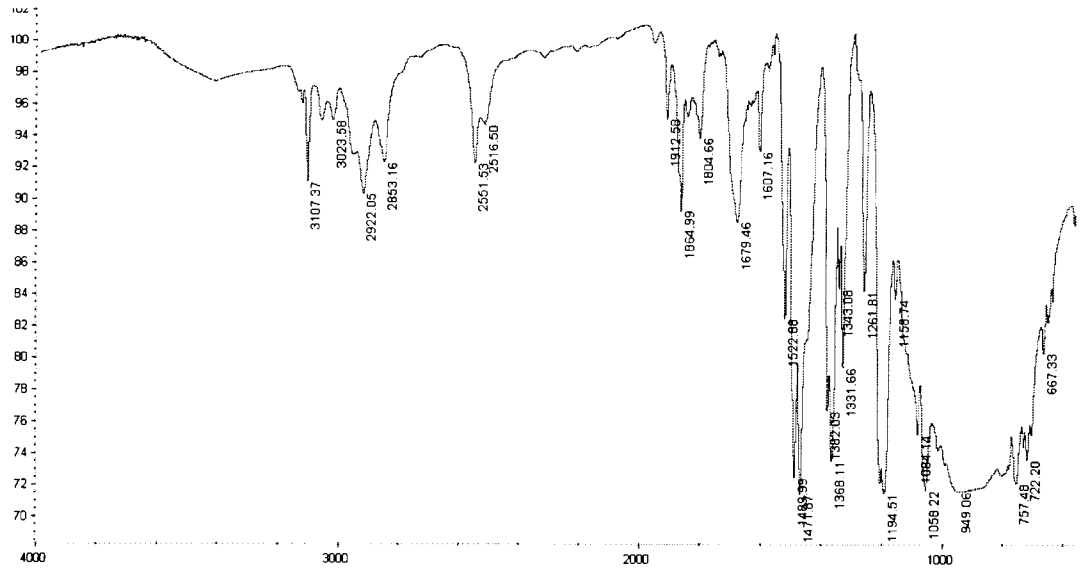

Fig 2.10 IR of rhenium (VII) trioxo complex **15** (Procedure B)

^{1}H NMR (DMSO-d_6) shows two methyl peaks and two pairs of vinylic peaks (Fig 2.11, a). The rhenium (V) ethane-1,2-diolate (V) **18** prepared from this complex (Scheme 2.4) showed the expected B-H stretch at 2506 cm^{-1} and the expected carbinolic peaks (Fig 2.11, b).

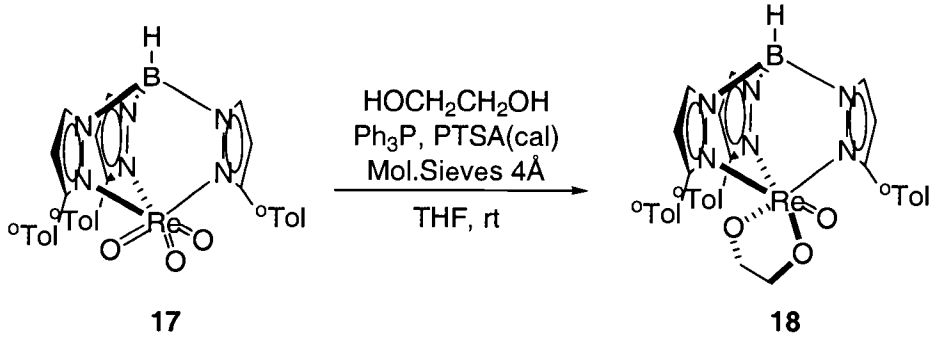

17 **18**

Scheme 2.4 The preparation of hydrido-tris-(3-o-tolyl-1H-pyrazolyl)borato(ethane-1,2-diolato)(oxo)rhenium(V) complex

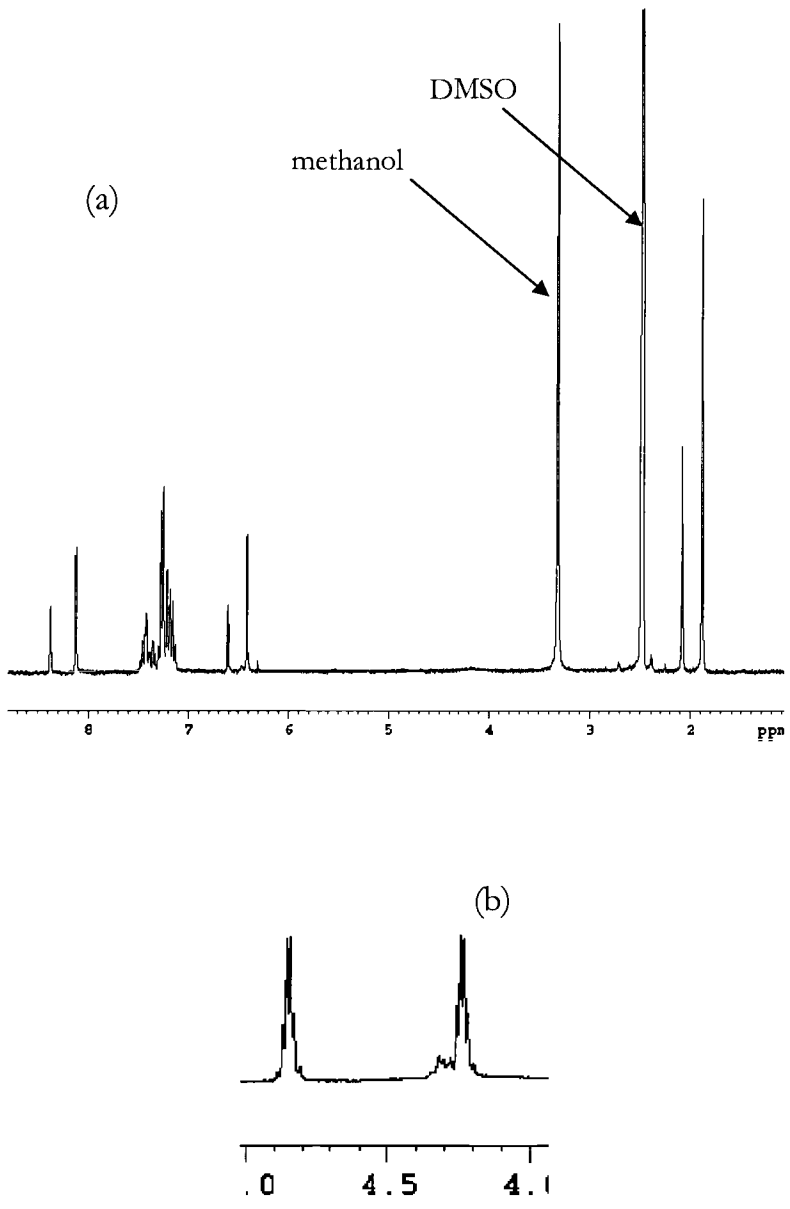

Fig 2.11 (a) ^{1}H NMR of o-tolylpyrazolylborate base rhenium(VII) trioxo complex (b) ^{1}H NMR of hydride-tris(o-tolylpyrazolyl)borato(1,2-ethandiolato)rhenium (V) carbinolic region

If there is a free rotation around carbon-carbon bonds one would expect to observe only one methyl and two vinylic doublets in the ^{1}H NMR spectrum at room temperature. Species **19** would have been very good explanation. The fact that we are observing two methyls peak (1:2) and four vinylic doublets, made us think that species **20** is the only observed species (Fig 2.12). **20** has two syn methyls (d and e) that on the average ^{1}H NMR time scale appear as one peak.

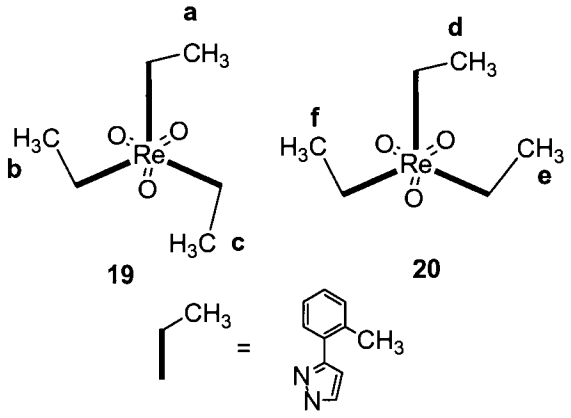

Fig 2.12 Top view of two diastereomeric o-tolylpyrazolylborate based rhenium(VII) complexes

2.4.1 nOe and 2D NMR Studies

The nOe is a through-*space* effect.[112] It can be used to determine which ^{1}H is positioned near a second ^{1}H. This can be particularly powerful for determining spatial shape of the molecule.

The ^{1}H NMR spectrum of the diolate **18** suggests that in the solution different diolate atropisomers coexist (Fig 2.13). The small humps at 3.5 ppm and 3.9 ppm were initially thought to be impurities. Careful column purification and recrystalization of the diolate failed to remove them. Particularly informative was the vinylic doublets pattern.

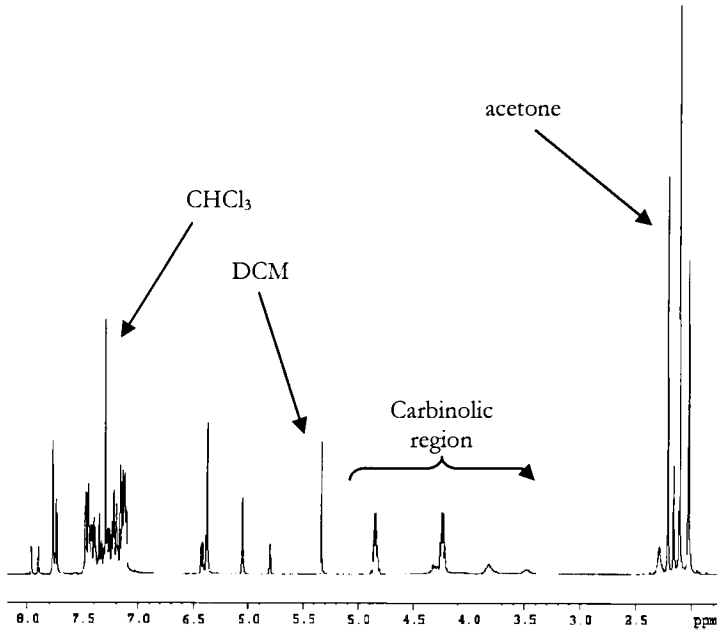

Fig 2.13 ^{1}H NMR of the diolate

2D NMR (COSY) and coupling constant analysis showed that there are 10 coupled vinylic doublets (5 pairs of doublets) (5.5-8.0 ppm) (Fig 2.14).

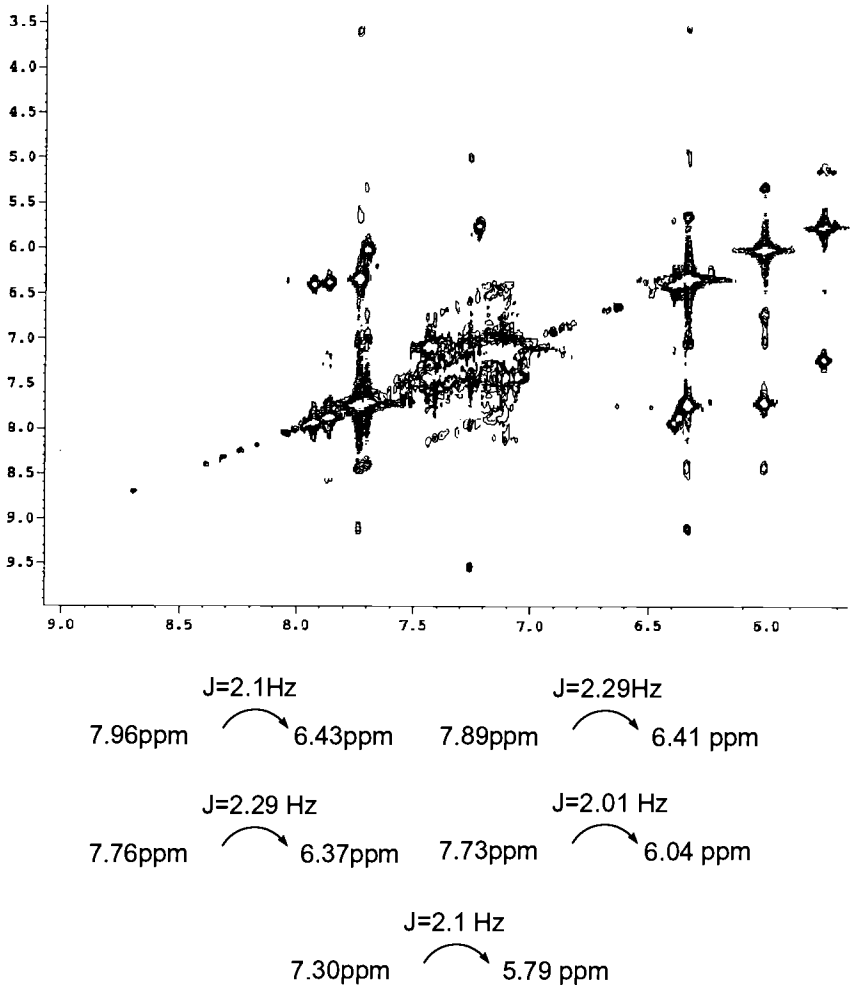

Fig 2.14 COSY spectrum of the diolate-low-field region

A rationale for this pattern can be coexistence of two major diolate species in the solution (Fig 2.15). This explains the presence of two pairs of carbinolic humps in the ^{1}H NMR spectrum of the diolate (Fig 2.13).

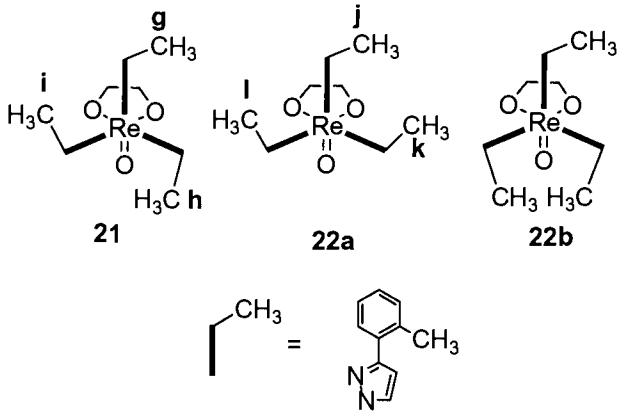

Fig 2.15 Major diolate species present in the solution

The species **21** is the major species observed in the solution. On the average NMR time scale, it has C_1 symmetry, thus it will have three pairs of the vinylic peaks (7.76, 7.73, 7.30, 6.04, 6.37, 5.79 ppm) and three singlets for three methyls. However, the methyl **i** and **h** overlap in the ^{1}H NMR spectrum giving the biggest peak in downfield region at 2.1 ppm. The methyl **g** appears as an independent singlet (2.02 ppm).

On the other hand, the species **22a** is the minor species observed in the solution. It has C_s symmetry, (implying that the methyl **j**-like tolyl ring rotates fast) thus it will have two pairs of the vinylic peaks (7.96, 7.89, 6.43, 6.41 ppm). The methyls **l** and **k** overlap in the ^{1}H NMR spectrum with methyls **i** and **h** (2.1 ppm). The methyl **j** appears as an independent weak singlet (2.17 ppm). Species **22b** is symmetry equivalent with species **22b**.

nOe experiments revealed an interesting conformational behavior of the diolate in the solution. The first methyl (2.02 ppm) (Fig 2.16, **b**) interacts strongly with two vinylic hydrogens (7.76 ppm and 6.04 ppm) and with ortho hydrogen of the benzene ring (7.34 ppm). According to COSY, these two vinylic protons come from two different pyrazole rings. In addition, there is a very weak interaction with carbinolic protons (4.81 ppm, 4.23 ppm). On the other hand, two other methyls (2.10 ppm, 2.16 ppm) (Fig 2.16, **c** and **d**) interact with one vinylic proton from different pyrazole rings (6.37 ppm and 6.41 ppm) (according to COSY). In addition, when the peak at 2.10 ppm is irradiated, a weak interaction with carbinolic peaks (4.81 ppm, 4.23 ppm) and another vinylic peak (7.76 ppm) is detected.

A rationale for the ^{1}H NMR spectrum is that the first two methyl peaks stem from **21**. In addition, the biggest vinylic doublets (7.76, 7.73, 7.30, 6.04, 6.37, 5.79 ppm) come from **21** as well as two carbinolic peaks (4.81 ppm, 4.23 ppm). The weak methyl peak at 2.17 ppm comes from **22a** as well as four weak vinylic doublets (7.96, 7.89, 6.43, 6.41 ppm). The two humps at 3.5 ppm and 3.9 ppm are the carbinolic peaks of **22**a. There is no observable interaction with these hydrogens when the methyl at 2.17

ppm is irradiated. This is because **22**a is present in low concentration in the solution. Accordingly to above picture, the peak at 2.1 ppm contains two methyls of **22a**. We should expect some interaction when this peak is rradiated with carbinolic hydrogens of **22a** (3.5 ppm, 3.9 ppm). We observe none, because of low concentration of species **22a** in the solution.

The carbinolic protons show interesting behavior. The one at 4.81 ppm (Fig 2.16, **f**) interacts with other carbinolic proton at 4.23 ppm and vinylic protons at 7 .77 ppm. On the other hand, other carbinolic protons at 4.25 ppm (Fig 2.16, **g**) interact with other carbinolic protons only. This supports the rationale laid down above. In addition, this suggests that one of the carbinolic carbons is tilted above compared to the other one and interacts with the methyl. Molecular modeling supports this picture.

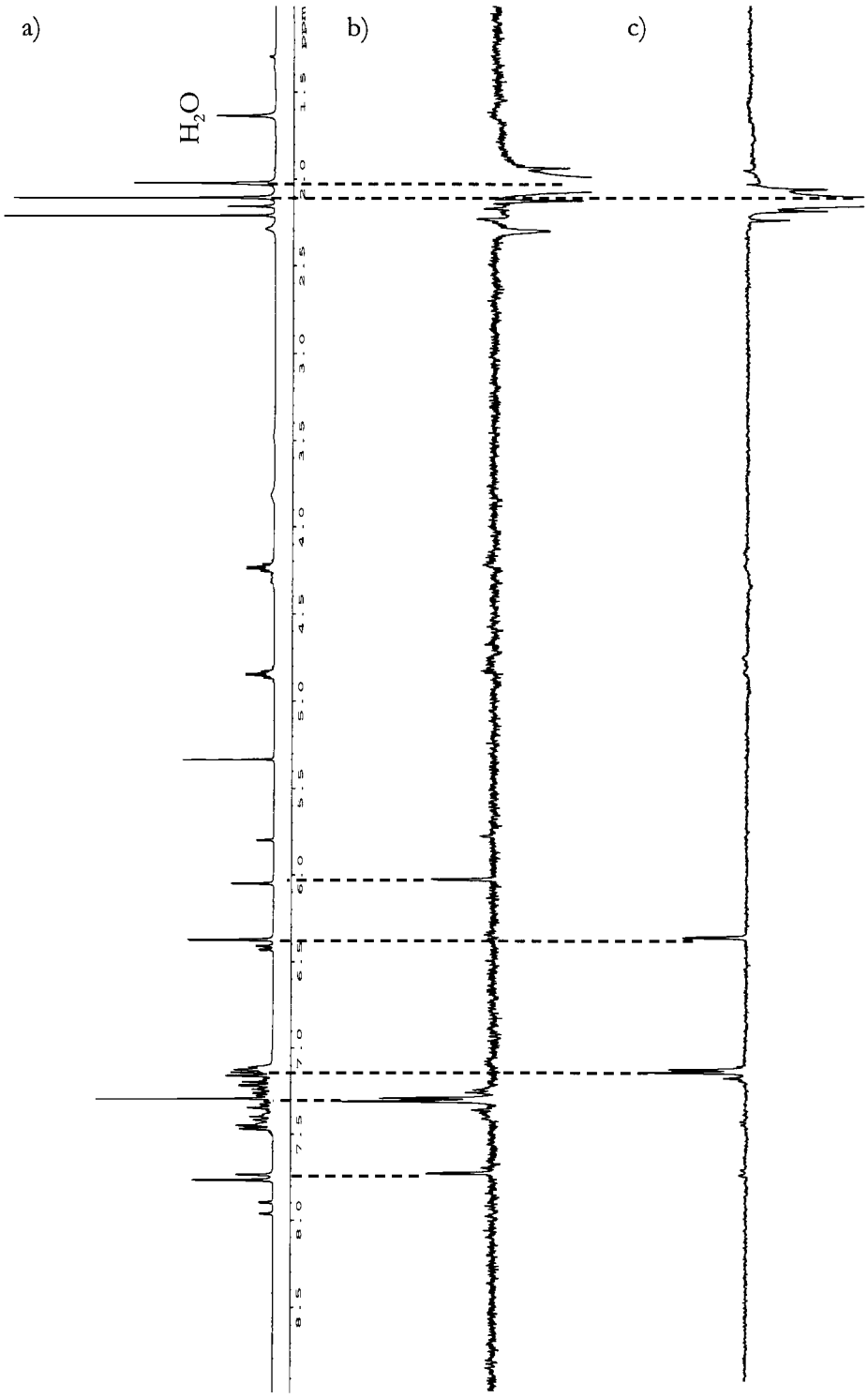

Fig 2.16 nOe Spectrum of the diolate **18**

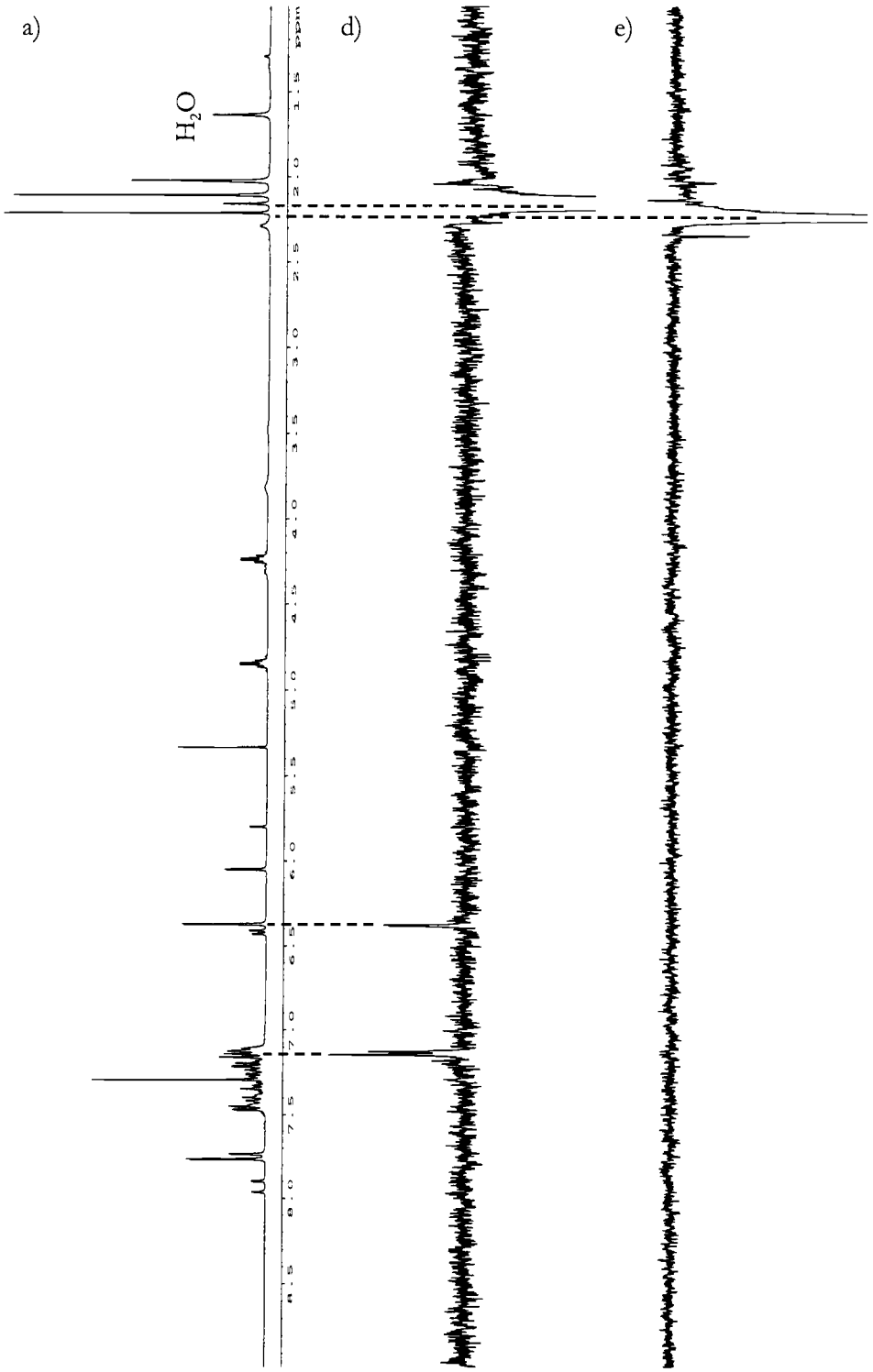

Fig 2.16 nOe Spectrum of the diolate **18** (continued)

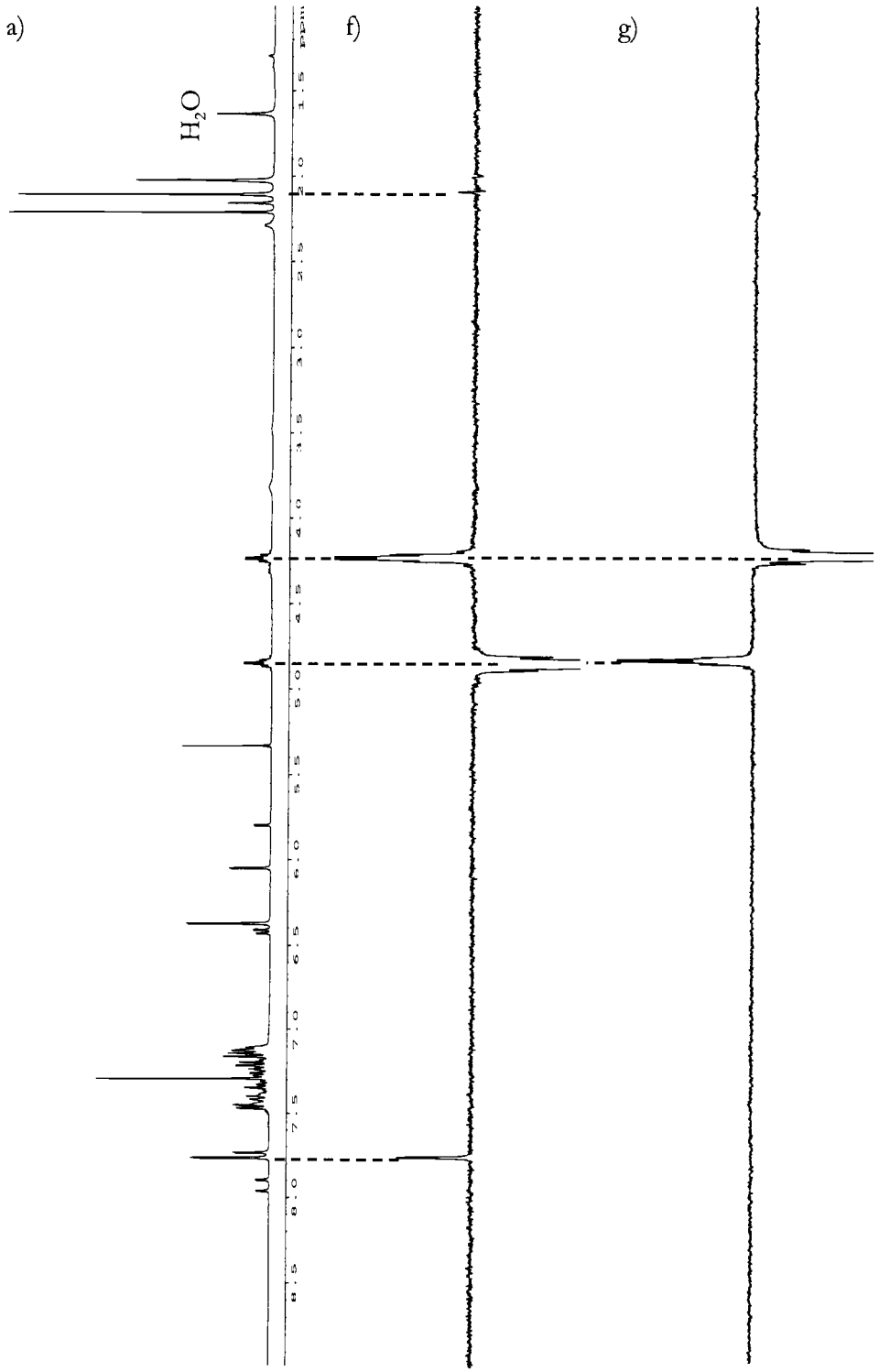

Fig 2.16 nOe Spectrum of the diolate **18** (continued)

2.4.2 Evaluation of Rates and Activation Enthalpies with NMR

When two species undergo a rapid exchange on the NMR time scale, the chemical shifts (δ) and coupling constants (J) are averaged over all species (Eq. 2.1).

$$\delta = \sum_i n_i \delta_i \qquad J = \sum_i n_i J_i \tag{2.1}$$

where n_i is the corresponding mole fraction.

A quintessential example is 1-isopropyl-2-methylnaphtalene (Scheem 2.5). Two methyls at room temperature appear in the ^{1}H NMR spectrum as a doublet. Lowering temperature to -45 °C causes splitting of the doublet into two doublets of different chemical shifts.

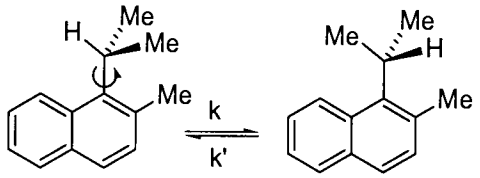

23 **24**

Scheme 2.5 Indistinguishable methyls due to fast rotation

The relative distribution of **23** and **24** is related to the system temperature in accordance to the known thermodynamic equation (Eq. 2.2):[113]

$$K = \frac{k}{k'} = \frac{[24]}{[23]} = \exp(-\Delta G^\circ / RT) \tag{2.2}$$

$\Delta G°$ difference in standard state Gibb's free energy
R gas constants
T absolute temperature

The Eyring equation (Eq. 2.3) gives the relationship between the rate constant and the system temperature.

$$k = (\kappa T / h)\exp(-\Delta G^{\#} / RT) \qquad (2.3)$$

$\Delta G^{\#}$ free energy of activation
κ Boltzmann constant
h Planck's constant

As mentioned above, if the exchange is fast, the signals of **23** and **24** will average out and if the exchange is slow the signals of **23** and **24** will be observed. Between these two extremes, broadening of NMR signals transpires. This phenomenon is called coalescence and the temperature that occurs, the coalescence temperature (T_c). The rate constant at coalescence is given approximately by (Eq. 2.4).

$$k_{T_c} = \frac{\pi}{\sqrt{2}}|\delta_a - \delta_b| \qquad (2.4)$$

where δ_a and δ_b are chemical shifts at the slow exchange condition.

If T_c is given in kelvin (K) and the shifts in Hz, then the free energy of activation is given (in KJ/mol) by (2.5).

$$\Delta G^{\#} = 19.1*10^{-3} * T_c(9.997 + \log T_c - \log|\delta_a - \delta_b| \qquad (2.5)$$

A superior method to the one outlined above is the complete bandshape (CBS) method.[114] It utilizes all the information contained in the spectrum, and it is therefore much less sensitive to errors. It consists of fitting of the real spectrum with a calculated spectrum usually aided by appropriate computer software.

The rotation barrier is an important parameter in designing a ligand that exhibits atropisomerism. Because of sparingly solubility of the rhenium trioxo complex in most of solvents but DMSO, we decided to use the diolate thereof to estimate the rotation barrier. Chloroform-d (m.p. -64°C) was not a good solvent, because the solution froze at about -65°C. The best solvent for this proved to be dichloromethane-d_2, which has a freezing point -95°C, though sample dissolved in chloroform was more responsive to the temperature change (Fig 2.17). The ^{1}H NMR was taken at 15, 5, -5, -15, -25, -35, -45, -55, -65, -75, -85, -95, -100, -110, -125 and -130°C. The sample froze at -130°C (the spectrum flattened out).

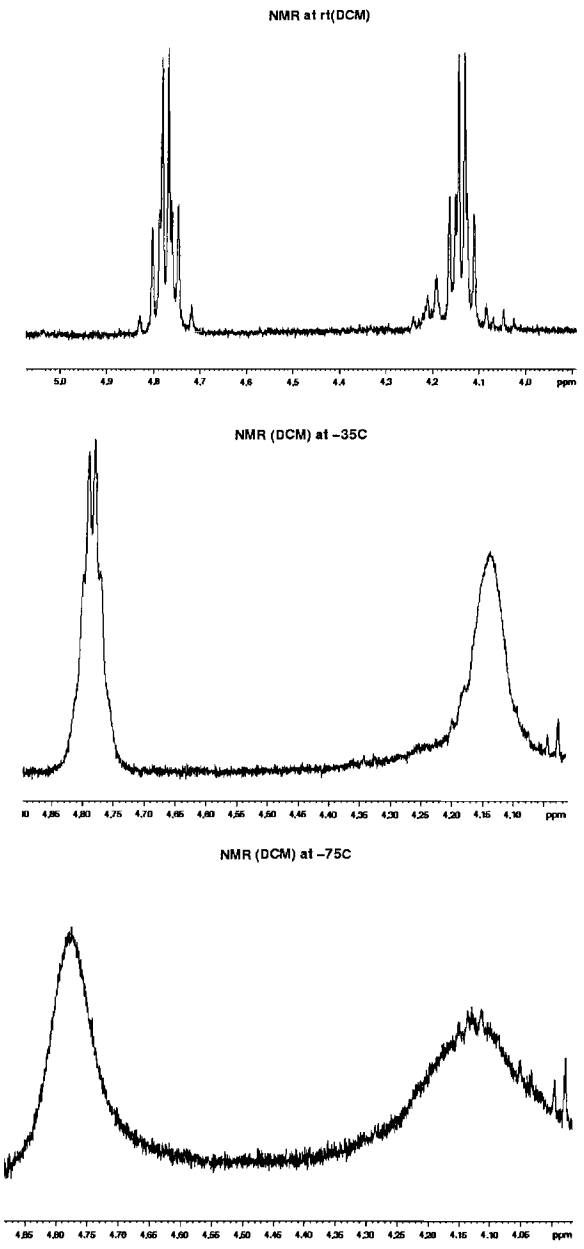

Fast rotation
(25°C)
(a)

Near fast rotation
(-35°C)
(b)

Coalescence
(-75°C)
(c)

Fig 2.17 Low temperature ^{1}H NMR measurements

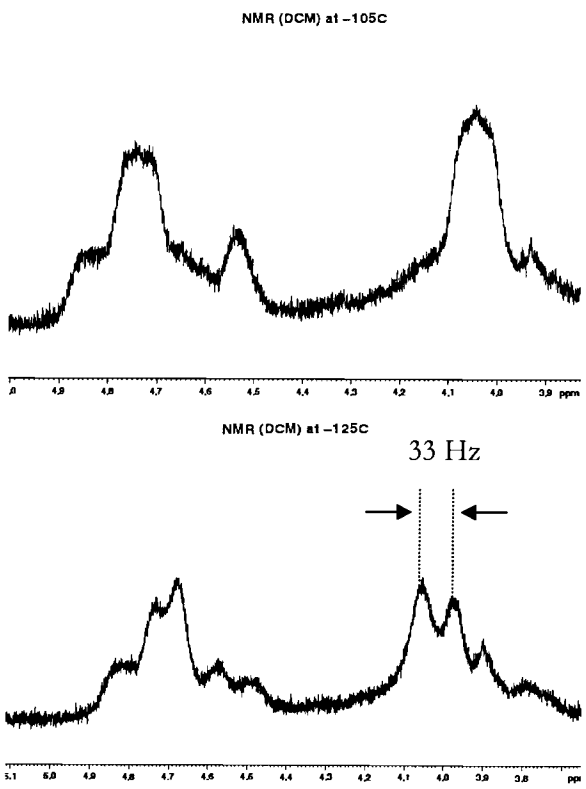

Fig 2.17 Low temperature ^{1}H NMR measurements (continued)

The carbinolic hydrogens at room temperature (Fig 2.17, a) appear as AA'BB' spin pattern in the ^{1}H NMR spectrum as a results of fast rotation of the o-tolyl rings. The two exo carbinolic hydrogens are chemically equivalent and magnetically inequivalent. The same applies for the endo hydrogens. The endo carbinolic hydrogens are closer to the polar Re=O bond and thus appear more upfield in the ^{1}H NMR spectrum

compared to the exo carbinolic hydrogens (Fig 2.18). Nuclear Overhauser experiments of systems such as Re(V) diphenylethan-1,2-diolates are a prime precedent.[115]

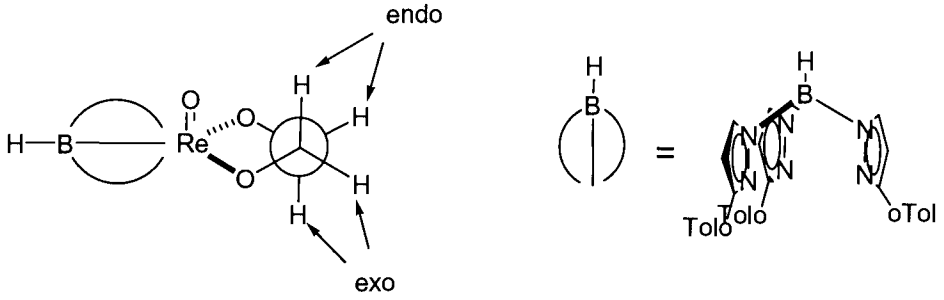

Fig 2.18 Two distinct carbinolic hydrogens in rhenium(V) ethan-1,2-diolates **17**

At low temperatures, the o-tolyl rotation slows down making the two endo hydrogens not any more chemically equivalent. The same applies for the exo hydrogens. Under these conditions, the carbinolic hydrogens appear as ABCD spin pattern. This means that two multiplets should split out into 4 different multiplets. This prediction starts taking hold at t= -125°C (Fig 2.17, f). At ~-130°C the sample froze preventing us to obtain a better estimate of "the freezing rotation" temperature. However, we think -125°C is close to "the freezing rotation" temperature. At this temperature, we chose the right chemical shift for gauging splitting, because this multiplet was more clearly split. With simple

inspection, we measured splitting in Hz ($|\delta_a - \delta_b| = 33$ Hz) (Fig 2.17, f). Plugging this constant and T_c=198±5 K in equation (2.5), we obtain the energetic barrier of rotation around carbon-carbon bond.

$$\Delta G^{\#} = 40.6 \pm 0.543 \text{ kJ/mol } (9.72 \pm 0.130 \text{ kcal/mol})$$

2.4.3. Evaluation of the Dihedral Angle with NMR

Based on valence bond calculations of the contact electron spin-nuclear spin interaction of ethane, Karplus[116] and Conroy proposed an equation that relates the dihedral angle with two vicinal proton scalar coupling constant ($^3J_{HH}$):

$$^3J_{HH} = A\cos\theta + B\cos 2\theta + C \qquad (2.6)$$

where A, B, C are constants with the values 4.22, -0.5 and 4.5, respectively. $^3J_{HH}$ for θ = 0° and 180° are generally about 2-4 Hz bigger than the calculated values. The empirical constants A=7, B=-1 and C=5 have been proposed to give improved results.[117]

The scalar coupling constant depends on the electronic interactions. Thus the coupling constant depends on C-H and C-C distance, the C-C-H bond angle and, most importantly, on electronegativities of substituents bound to the carbon atoms. The

improved Karplus equation that takes into consideration electronegativities is due to Haasnoot (Eq. 2.7):[118]

$$^{3}J_{HH} = P_1 \cos^2\theta + P_2 \cos 2\theta + \sum_i \Delta\chi_i \{P_4 + P_5 \cos^2(\xi\phi + P_6 \mid \Delta\chi_i \mid)\} \quad (2.7)$$

where $\Delta\chi_i$ is the difference of Huggins electronegativities between substituent i and hydrogen, ξ_i is ± 1 depending on the orientation of the substituents, and P_1= 13.86, P_2= -0.81, P_4= 0.56, P_5=-2.32, and P_6= 17.9°.

The Karplus-Conroy equation (2.7) is a powerful tool for estimating the dihedral angle. The ^{1}H NMR first order spectrum provides us with coupling constants that can be used for calculating dihedral angles. In our case, we wanted to estimate dihedral angle (θ) in the carbinolic site of the molecule (Fig 2.19).

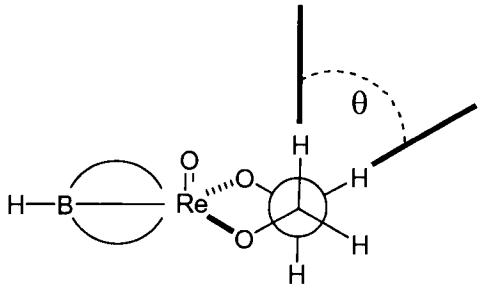

Fig 2.19 Dihedral angle of interest in the diolate **18**

The region in the ^1H NMR spectrum that contains the information is AA'BB' spin pattern, thus very hard to accurately extract coupling constants from. A popular remedy to this dilemma is simulation of the ^1H NMR spectrum and then extracting information needed. Using NMR Utility Transform software (NUTS)[119] we successfully simulated the NMR region of interest (Fig. 2.20).

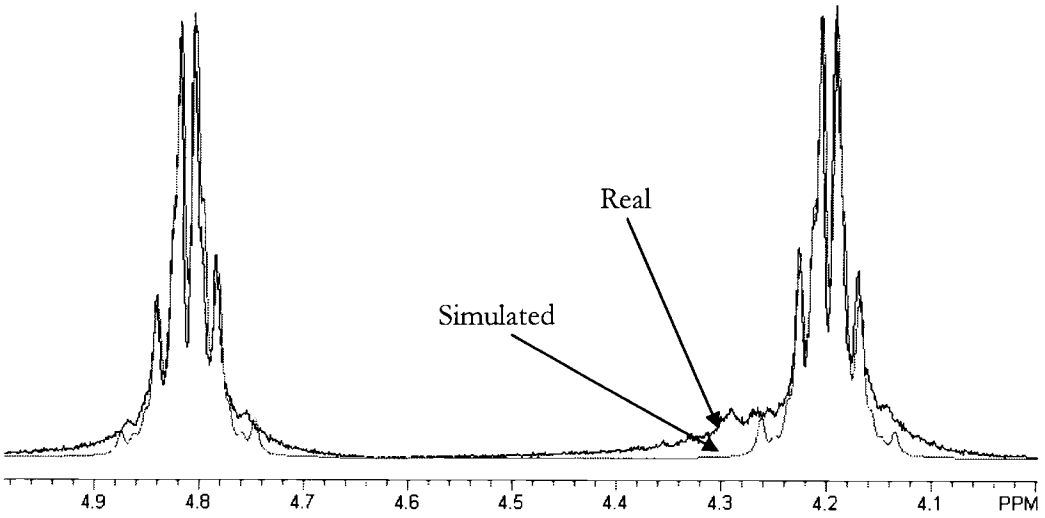

H_1 = 4.813 ppm
H_2 = 4.809 ppm
H_3 = 4.203 ppm
H_4 = 4.197 ppm

$J_{1,2}$ = 7.023 Hz
$J_{1,3}$ = -11.03 Hz
$J_{1,4}$ = 6.439 Hz
$J_{2,3}$ = 7.229 Hz
$J_{2,4}$ = -11.10 Hz
$J_{3,4}$ = 7.006 Hz

Fig. 2.20 The simulated and real ^1H NMR spectrum region of interest and estimated chemical shifts and coupling constants

$J_{1,4}$ is the most important coupling constant in terms of estimating the dihedral angle. As we are dealing with substituents different from hydrogen, we had to use Haasnoot modified Karplus Eq. (2.7).[120] Instead of solving the formidable equation (2.7) for θ, it is possible to plot $J_{14}=f(\theta)$ (Fig 2.21) and then extract the dihedral angle. Simple inspection of the graph shows that the dihedral angel (θ) is about 15°. Other possible angles predicted by the Karplus curve (125°, 210°, 310°) are precluded by the cyclic structure of the diolate.

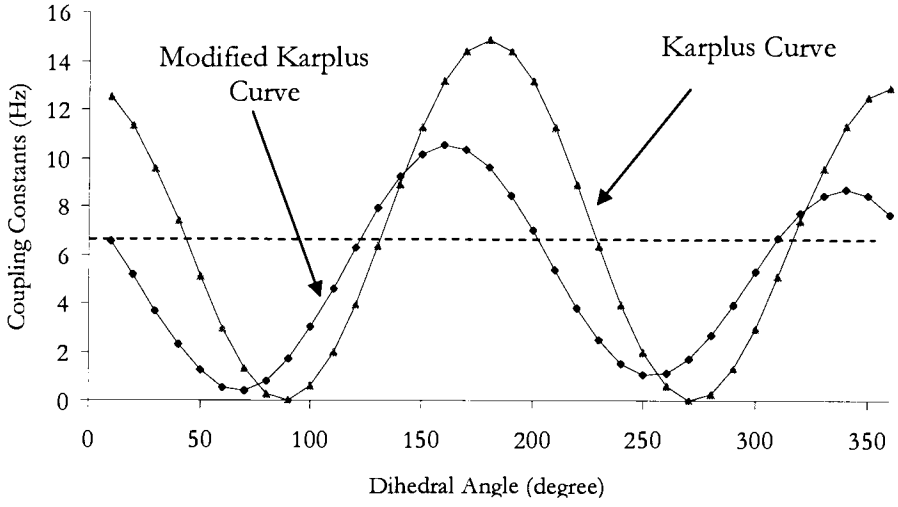

Fig 2.21 Original Karplus and Modified Karplus curve with electronegativities related correction

2.4.4 Computational Conformational Analysis

Molecular mechanics (MM) and Quantum Mechanics (QM) are two computational methodologies of widespread use to establish molecular

equilibrium and transition state geometries, conformation, heats of reaction, activation energies and vibrational frequencies.[28c] MM is the simplest and least costly (the fastest), thus commonly employed. It can be applied to molecules containing 1000 or more atoms.[28b] The basic premise behind MM is the high degree of transferability of geometry parameters (bond length, bond angles, etc) from one molecule to another. The calculation reference point of MM calculations is the ideal geometry, where the bond distances, bond angles, dihedral angles and non-bonded interactions are ideal. It is mainly used for calculating equilibrium geometry.

QM is based on numerical solution of the Schrödinger's equation:

$$\left[\frac{-h^2}{8\pi^2 m}\nabla^2 - \frac{Ze^2}{r}\right]\Psi(x,y,z) = E\Psi(x,y,z) \qquad (2.8)$$

where m mass
r distance from the nucleus
Z nuclear charge
Ψ wavefunction
E energy
∇^2 the Laplacian operator

Among QM methods, the semi-empirical model is parameterized with experimental data and at MNDO, AM1 and PM3 level can be applied to molecules up to 200 atoms.[28b] It is computationally a cheap approach and

is quite successful for calculating equilibrium energies and moderately good for modeling of transition state geometries. The *Ab initio* model stands out for thermodynamic and kinetic comparisons, molecular equilibrium and transition state modeling. This model is more costly than the semi-empirical model, and for molecules above 100 atoms it becomes impractical.[28b] Due to separation of electron motions ("Hatree-Fock approximation"), this model is not good for comparison between reactants and transition states. The Density Funtional model (DFT) provides an estimate of electron correlation energies and is thus superior to the Hartee-Fock (HF) model and represents the most reliable computational model to date.

The best model for solving the problem at hand is the one that consistently reproduces known data. Before we mapped energies of different conformations of our ligand for rotation around carbon-carbon bond, first we had to find a similar system that has been studies experimentally and use it as a benchmark for our model. We chose 2,2'-dimethylbiphenyl because this system has been studied in detail experimentally[121] and computationally[122] (Fig 2.22).

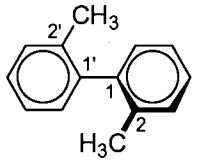

25

Fig 2.22 2,2'-dimethylbephenyl

Geometries were initially optimized at the HF/3-21G level and B3LYP/6-31-G level, and finally optimized at the B3LYP/6-31**G level. The fully optimized atropoisomer dihedral angles were systematically changed and with applied constraint on the dihedral angle reoptimization was run again (Table 2.1).

Table 2.1 Energies relative to the most stable atropoisomers of **25**

	Dihedral Angles (2'-1'-1-2)					
Energy(kcal/mol)[a]	**0**	**45**	**60**	**90**	**120**	**135**
B3LYP/6-31**G	28.24		1.924	1.286	0.2880	
B3LYP/6-31+G* [c]	168.8	5.370		0		2.820
HF/3-21G	37.71		3.177	1.517	1.609	
HF/6-31G* [c]	219.3	7.3800		0.0100		4.520
MMFF94s[b]	39.19		1.600		0.814	
	180	**240**	**270**	**300**		
B3LYP/6-31**G	16.15	0.296	0	1.887		
B3LYP/6-31+G* [c]	16.7200					
HF/3-21G	23.66	1.693	0	3.835		
HF/6-31G* [c]	21.79					
MMFF94s	27.79	0.815	0	1.600		

a) Shaded areas contain our calculations; (b) We did MM calculation just for comparison. (c) Friedrich Grein *J.Phys Chem A*, **2002**, *106*, 3823

From Table 2.1 the planar atropoisomer energies stand out for being the most erratic when compared to other calculations. Energies of other atropoisomers are very similar to our calculations. Overall, our calculated data are closer to the experimental data, what proves our model as a good computational model (Table 2.2, Fig 2.23).

Table 2.2 Rotational energies and twist angles of **25**

	Exp	Calculated(DFT)[c]	Literature[d]
Twist Energy (kcal/mol)	14.60 [a, b]	16.15	16.72
Twist Angles (degree)	109.7[b]	91.6	90.8

(a) W. Theilacker and H. Bohm *Angew. Chem., Int. Ed.* **1967**, *9*, 251.
(b) K. Mullen, W. Heinz, F. G. Klarmer, W. R. Roth, I. Kindermann, O. Adamczak, M. Wette and J. Lex *Chem. Ber.* **1990**, *123*, 2349.
(c) Our calculations.
(d) Friedrich Grein *J.Phys Chem A*, **2002**, *106*, 3823. θ =0° is not included in calculation.

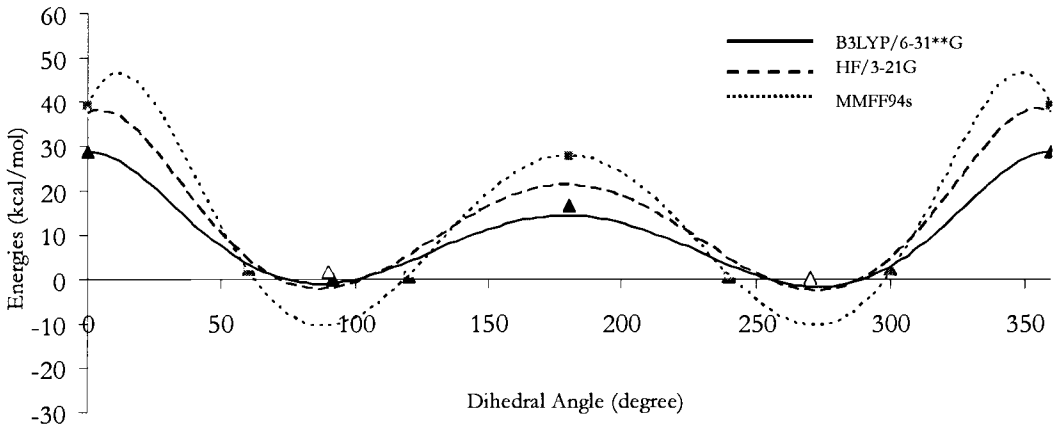

Fig 2.23 Calculated rotational curves at different levels for **25**

Using the same model for our ligand (Fig 2.24), we calculated optimized energies of each atropoisomer. The LACVP basis set, incorporating a

Hay-Wadt effective core potential[144] for rhenium was used. Phenyl groups were rotated at the same time for the same angle in the same direction.

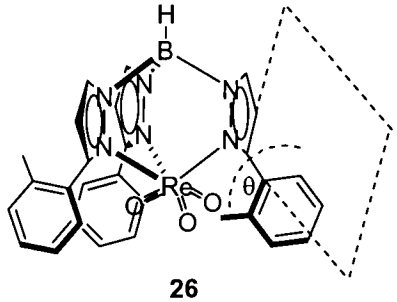

26

Fig 2.24 The dihedral angle of interest in our ligand

Calculated energies relative to the global minimum are laid down in Table 2.3 and plotted in Fig. 2.25.

Table 2.3 Energies relative to the most stable atropoisomers

Dihedral Angle(degree)	Energy(kcal/mol)
70.0	45.5
80.0	13.8
90.0	8.25
97.0	0
100	0.56
120	3.71
180	51.5
200	43.9
240	8.95
270	1.03
280	2.66
290	14.9
300	26.9

Twist Angle (degree)	Twist Barrier (kcal/mol)
97.0	16.7

The calculated twist barrier is 50 kcal/mol. As we rotated three phenyls at the same time, 50:3 = 16.7 kcal/mol to a first approximately is the twist energy for rotating one phenyl and keeping other two fixed.

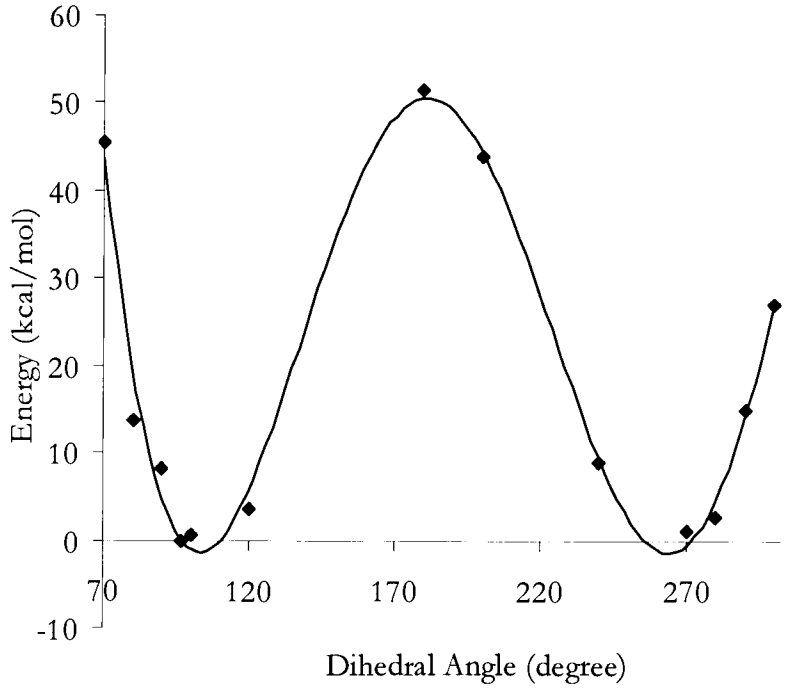

Fig 2.25 Calculated rotational curve for **26**

Using the same model for the diolate (by rotating one phenyl group at a time, while holding two others fix) the twist angle and the twist barrier relative to the global minimum were calculated (Table 2.4 and Fig 2.26).

Table 2.4 Calculated conformational parameters for the diolate

Twist Angle (degree)	Twist Barrier (kcal/mol)
82.0	8.06

Table 2.4 Calculated conformational parameters for the diolate (continued)

Dihedral Angle(degree)	Energy(kcal/mol
82.0	0
102	0.520
240	0.700
220	1.56
122	1.99
142	2.00
200	3.95
162	4.82
180	8.06
170	6.49
190	5.86
230	1.03
200	5.90

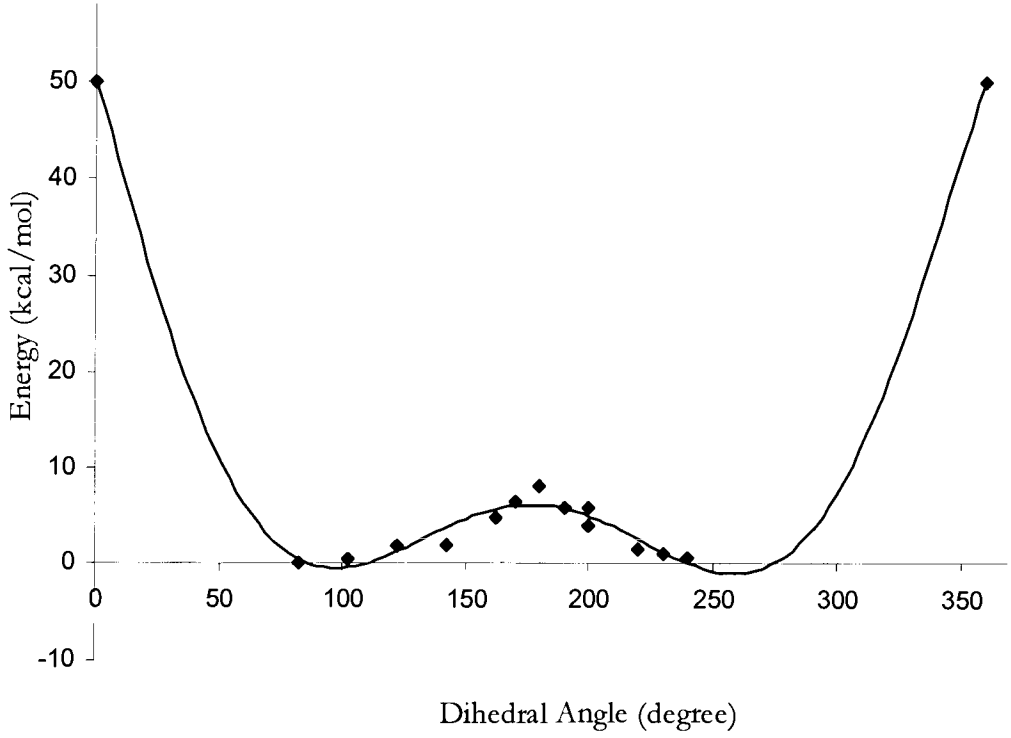

Fig 2.26 Calculated rotational curve for the diolate

As the dihedral angle approached 0° and 360°, the calculating algorithm failed to converge. This is because the conformations were getting very high in energy, because of clashing between the methyl group and the diolate ring or the Re=O bond. For plotting purpose, we alleged that energies of these two conformational extremes are 50 kcal/mol.

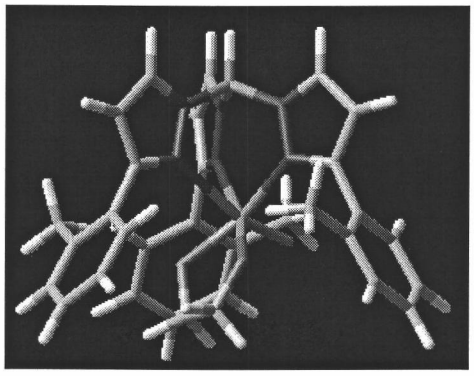

Fig 2.27 DFT optimized molecular model of the diolate **18**

The dihedral angle was calculated to be θ =26.4° (Fig 2.27). As the calculation were done for gas phase, we optimized the diolate **18** including solvent presence to gauge the solvent effect on the calculation output. Two solvent were used: 1) CCl_4 (μ=2.238 D), θ =26.8° and 2) $ClCH_2CH_2Cl$ (μ=10.65 D), θ =26.8°. Although the diolate **18** was calculated to be 1.2 times more stable in CCl_4 and 6 times more stable in $ClCH_2CH_2Cl$, its conformational properties do not change a lot. This

makes our calculation for the diolate **18** in gas phase applicable for solution phase.

Inspection of optimized model of **18** revealed that there were no nOe vulnerable hydrogens. As an example, it is shown only part of our model inspection (Fig 2.28). This is so because the optimized structure is a static geometry of the global energetic minimum.

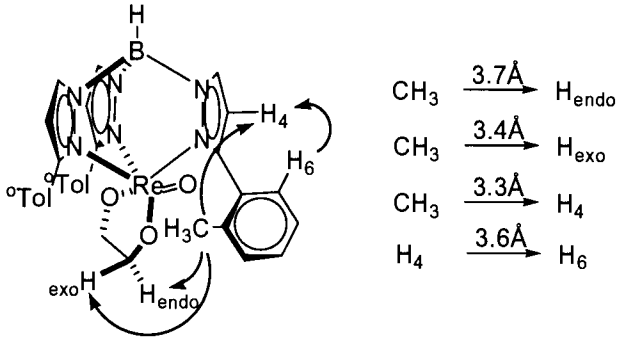

Fig 2.28 nOe vulnerable hydrogen analysis

Not surprising, by changing dihedral angles between pyrazole and benzene rings we have notices that nOe vulnerable hydrogens emerge. This shows that the optimized diolate model being the most stable conformation of the diolate **18,** it does not tell us anything about the infinite number of fleeting conformations that the diolate **18** takes. The latter contain many nOe vulnerable hydrogens.

2.5. Camphor based and related rhenium (VII) trioxo complexes

Transition metals catalyze many important organic reactions. Asymmetric catalytic cyclopropanation of olefins with organic diazo compounds has been utilized a lot in the organic synthesis.[123] A classical example is due to Nozaki et. al. in 1966.[124] The ability of trispyrazolylborates to firmly coordinate to metals throughout the periodic table and their steric and electronic adjustability has spurred on the interest in using them in asymmetric synthesis ever since their discovery. A synthesis of a couple of chiral poly(pyrazolyl)borates has been reported (Fig 2.29).[125]

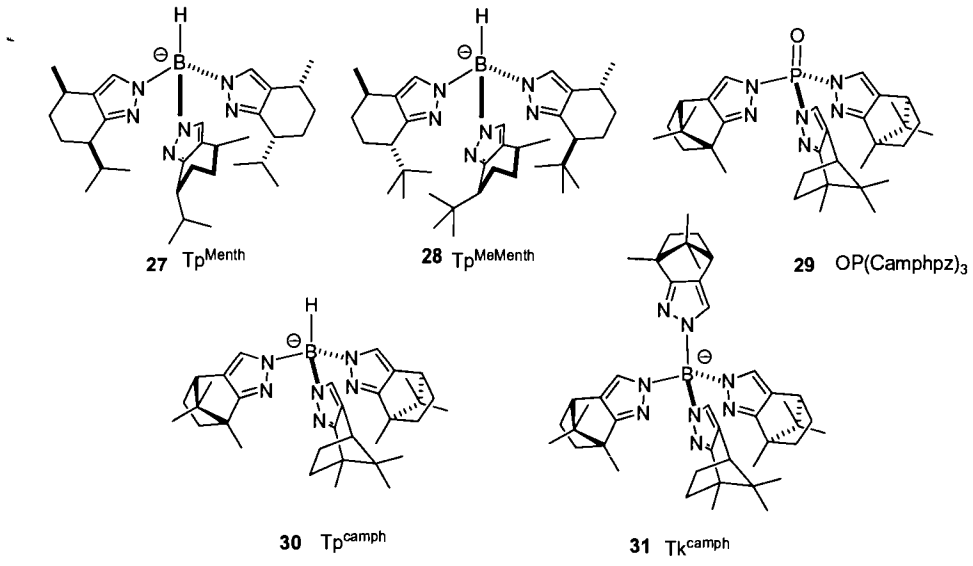

Fig 2.29 Chiral poly(pyrazolyl)borates and their analogs

Reports on ligand **30** are controversial.[126] Failure to prepare **30** made Tolman prepare a phosphorous trispyrazolylborate analog **29** instead.[127] Singh et. al. reported synthesis of **30** from (-)-camphor (Scheme 2.6).[128]

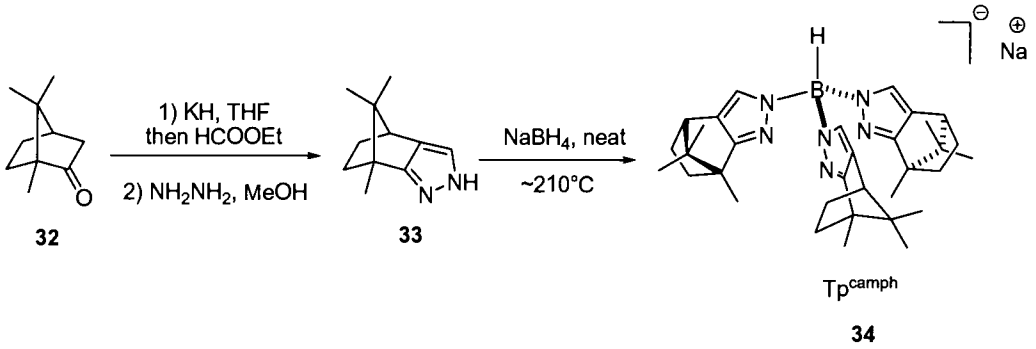

Scheme 2.6 Synthesis of $Tp^{Camph}Na$

Tolman et. al. reported a catalyzed cyclopropanation of styrene with ethyl diazoacetate in presence of 3mol % $[(\eta^3\text{-}\mathbf{29})Cu(CH_3CN)]BF_4$ (Scheme 2.7). Yields and stereoselectivity (cis/trans) were moderate with ee's% up to 60%.[129] Singh used **30** in enantioselective cyclopropanation of olefins with ee's % up to 40%.[130] Similarly Brunner[131] acquired ee's % up to 62% by using **31**.[132]

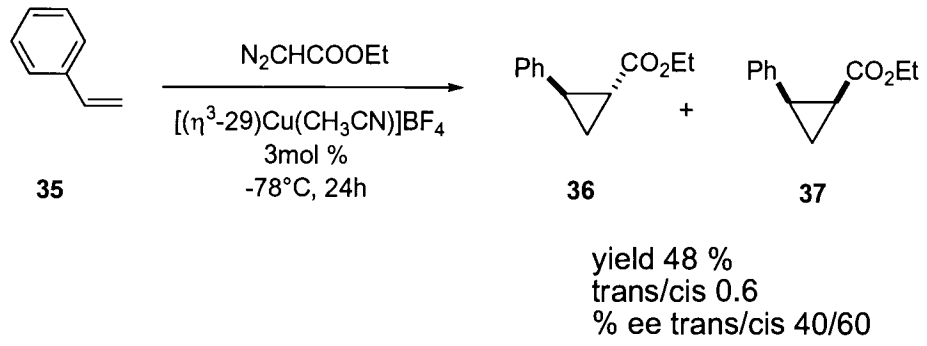

Scheme 2.7 Asymmetric Catalyzed cyclopropanation of olefins

The success of these cyclopropanations (C-atom transfer) suggested high promise for such ligands in our O-atom transfer reactions. All our efforts to reproduce the reported synthesis of **30** were in vain. Trofimenko[133] in his book on scorpionates describes two ways to prepare scorpionates: 1) high melting point pyrazoles and 2) low melting point pyrazoles. In the latter case, usually scorpionates are prepared with the neat method where an excess of pyrazole and metal (sodium or potassium) borohydride are heated; pyrazole serves as a solvent and as a reagent. In the former case, usually the reaction is run in an inert high boiling point solvent. We have tried this approach also by using veratrole (o-dimethoxybenzene) (b.p. 210°C) and decalin (b.p. 190°C) as solvents. In the former case, we obtained after overnight reflux a white solid that was merely insoluble in all ordinary organic solvents and water. The very good solubility in dimethyl sulphate was attributed to a nucleophilic

reaction of some sort. In the latter case, all camphorpyrazole either decomposed or recovered. The fact that the tetrakis scorpionate exist, the rational for failure to prepare the tris scorpionate must be the kinetic instability of the latter. Although the tetrakis scorpionate is more stericly congested than the tris scorpionate, the former is probably formed under kinetic control.

Another scorpionate we were after was (-)–menthone based scorpionate – Tp^{Menth} (Scheme 2.8).

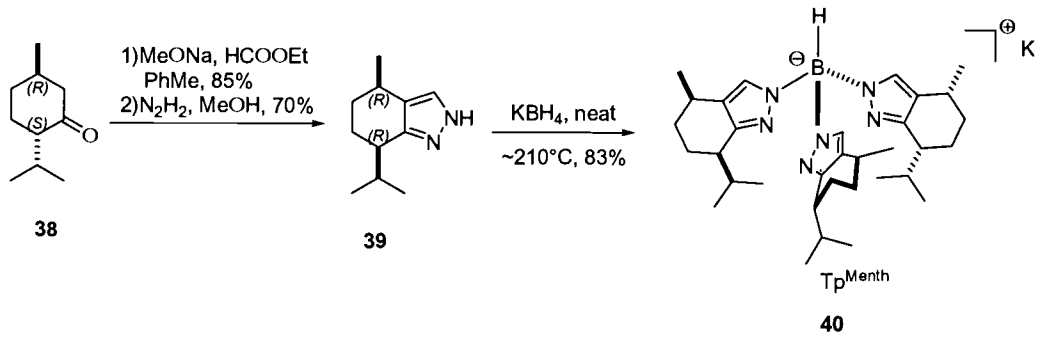

Scheme 2.8 Synthesis of $Tp^{Menth}K$

A single B-H stretch at 2416 cm^{-1} was conclusive piece of information on the presence of the B-H bond. The ^1H NMR spectrum was in concur with the molecular structure **40**. Having this scorpionate at hand, we tried to prepare the rhenium (VII) trioxo complex accordingly. The compound we obtained showed contradicting chemical and physical properties. The

^{1}H NMR spectrum bore all peaks we were expecting. On the other hand the IR spectrum was lacking the characteristic B-H stretch. The finger print region was almost void of bands. There was merely one big band at ~900 cm^{-1}. When we tried to prepare the diolate from this complex we obtained a blue compound (as all diolates) that was lacking characteristic carbinolic CH peaks in the ^{1}H NMR spectrum.

2.6. Outlook and conclusion

Guided by the mechanism of rhenium (VII) catalyzed epoxide deoxygenation and the mechanism of transferring the stereogenic information of the auxiliary to the reaction site, we have managed to design a general model for preparing chiral rhenium (VII) complexes.

Due to difficulties in preparing chiral scorpionates and rhenium (VII) trioxo complexes, we have successfully synthesized only one chiral rhenium (VII) trioxo complex. The conformational properties of this complex were studied experimentally (NMR measurements) and theoretically (Molecular Modeling). These studies will aid in preparing similar chiral rhenium (VII) trioxo complexes. The experimental energetic barrier of the rotation in the case of biphenyl is 2.0 kcal/mol, whereas in

the case of 2,2'-dimethylbiphenyl is 14.6 kcal/mol. Assuming only the steric factor is involved in restriction of the rotation around carbon-carbon bond, it is very easily calculated that the energetic cost of one ortho methyl in biphenyl is 6.3 kcal/mol. From our work, the energetic barrier of the rotation in the case of the diolate **18** is 9.72 kcal/mol. To a first approximation, installation of methyl on the carbon 6 of the o-tolyl ring will raise the energetic barrier of the rotation to 16 kcal/mol. This is the energetic threshold for optical resolution of optically active atropisomers at room temperature.

The difference in spectroscopic and chemical properties of rhenium (VII) trioxo complexes **16** prepared by the original and the modified methodology took us by surprise. This is unprecedented. A rationale to this outcome might be that when we react one equivalent of the borate **15** with trifluoroacetate perrhenate (Scheme 2.2) a tetragonal cluster rhenium (VII) trioxo complex is formed. Its T symmetry would explain one B-H stretch and very simple ^{1}H NMR spectrum. Diolate formation would be hampered by steric congestion on the rhenium sphere, though reduction of rhenium (VII) to rhenium (V) would transpire giving a light blue product. High resolution mass spectrometric

analysis of this rhenium (VII) trioxo complex spotted a monomeric molecular ion probably due to decomposition of the cluster complex under high electron bombardment. A way to probe this hypothesis would be to react this rhenium (VII) trioxo complex with excess of the borate **15,** which should tear apart the clustered complex into the monomeric rhenium (VII) complex.

The camphor based scorpionate was the first scorpionate we were interested in. Reportedly, it is prepared from cheap and enantiomerically enriched (R)-camphor. Due to bicyclic carbon skeleton, it is very easy to retain stereogenic centers throughout the synthesis of this scorpionates. Unfortunately, we have not succeeded in preparing this scorpionate. Admittedly Singh (personal commutation) notes that they had a hard time to prepare this scorpionate due to difficulties in controlling the right reaction temperature. The plethora of similar scorpionates, notably the menthone based scorpionate, suggest that this scorpionate can be prepared. The future work will focus on more careful adjusting of the reaction condition.

The menthone based scorpionate was successfully synthesized, but the menthone based rhenium (VII) trioxo complex was showing

contradicting physical and chemical properties. This is not surprising. The same dichotomy was noted in our initial efforts to prepare tolyl based rhenium (VII) trioxo complex. More careful adjusting of reaction condition is needed (especially the reaction temperature).

-Chapter 3-

Conclusion

Epoxides are an important class of organic compounds for stereocontrolled synthesis. Their inherent strain in the three member ring and the polarity of the C-O bond imparts reactivity to the epoxide functional group toward different reactions. This and the ease of their synthesis make epoxides extremely useful synthons.

Epoxide deoxygenation reaction is an important reaction from mechanistic and synthetic perspective. Compared to epoxide ring opening reactions, epoxide deoxygenation has not been developed so much.

Rhenium (VII) trioxo complexes have spurred on our interest from mechanistic and synthetic points to view. Over the last year, we have been striving to design chiral rhenium (VII) complexes. We successfully designed, synthesized and spectroscopy characterized hydrido-tris-(3-o-tolyl-1H-pyrazolyl)borato(trioxo)rhenium(VII). The asymmetry of this complex arises from a restricted rotation around the carbon-carbon bond. Extensive NMR measurements, in particular low temperature NMR experiments and high level DFT modeling lead us to a useful

conformational analytical description of our complex. This model will be very useful for future studies on similar complexes.

Due to steric congestion and electron transfer competing reaction, we have not been able to prepare menthone based rhenium (VII) trioxo complex. We have proved that the reaction temperature is crucial in slowing down the competing electron transfer reaction. The reaction temperature that worked in case of hydrido-tris-(3-o-tolyl-1H-pyrazolyl)borato(trioxo)rhenium (VII) (-78°C) did not yield results. A more careful adjustment of the reaction temperature is needed. A future work will concentrate on this issue.

We have been hampered to prepare a very appealing camphor based rhenium (VII) trioxo complex from (+) –camphor by failure to prepare the related scorpionate. The preceding work on the synthesis of scorpionate strongly suggests that this scorpionate can be prepared, inasmuch as there have been reported two papers on synthesis and usage thereof in asymmetric cyclopropanation of olefins. Our work on synthesis of this scorpionate will be used in the future work.

-Chapter 4-

Experimental

4.1 General Methods

All reactions were performed under an inert atmosphere using standard Schlenk[134] or vacuum line techniques and a nitrogen-filled glovebox (Vacuum-AMTOspheres Co. HE 493), except when noted. All solvents were dried, degassed and distilled prior to use. THF was distilled from Na/benzophenone, toluene and hexane from P_2O_5. [135] HCOOEt was left over K_2CO_3 for 30min and then distilled from P_2O_5. Veratrole was dried with activated MS (4 Å, Fisher) and distilled from CaH_2. Decaline was distilled from sodium. Molecular sieves (4 Å, Fisher) were crushed and activated by heating at 120 °C overnight prior to use. Infrared spectra were run on a Nicolet Magna-IR560. Starting reagents were used as purchased from Aldrich or Acros (Fisher) except when noted. All deuterated solvents were purchased from Cambridge Isotopes. Silica gel (32-63 mesh) used for flash column chromatography was purchased from Selecto, Inc.

4.2 NMR Measurements

The ^{1}H NMR and ^{13}C NMR spectra were recorded on a Brüker DP300 (operating at 300.13 MHz for proton or 75.409 MHz for carbon), whereas nOe and low temperature NMR experiments were run on a Brüker DPX400 (operating at 400.134 MHz for proton or 100.614 MHz for carbon). ^{1}H chemical shifts are referenced using the residual solvent protons and are reported relative to TMS (tetramethylsilane). ^{13}C chemical shifts are reported relative to TMS and are referenced to solvent peaks.

4.3 Synthetic Procedures

(Z)-3-(hydroxymethylene)-1,7,7-trimethylbicyclo[2.2.1]heptan-2-one

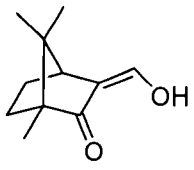

It was synthesized according to Tolman.[136] (R)-(+)-camphor (10.1 g, 0.0660 mol) was added to an oil slurry of KH (44.6 g, 0.330 mol, 30.0 % oil suspension washed with hexanes) in THF (70.0 mL). Gas evolution commenced immediately. The mixture was refluxed for 15 min until gas

evolution ceased and was then cooled to room temperature. Ethyl formate (22.0 mL, 0.270 mol) was syringed in slowly; the mixture was stirred with mechanical stirrer for an additional 16 h. After quenching with t-butanol and thereafter with diluted aqueous solution of ethanol, the water layer was separated and acidified to pH=1 with concentrated HCl. An oil separated and was extracted with diethyl ether (3 X 50.0 mL); the extracts were dried with $MgSO_4$, and the solvent was removed under reduced pressure to afford a pale tan solid (6.07 g, 0.0340 mol, yield= 50 %).

^{1}H NMR ($CDCl_3$, 25 °C): δ 6.80 (s, 1H), δ 2.45 (d, J=3.8 Hz, 1H), δ 1.95-2.11 (m, 1H), δ 1.75-1.60 (m, 1H), δ 1.45-1.35 (m, 1H), δ 0.95 (s, 3H), δ 0.90 (s, 3H), δ 0.85 (s, 3H).

4,5,6,7-tetrahydro-7,8,8-trimethyl-2H-4,7-methanoindazole

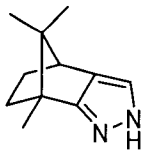

(Z)-3-(hydroxymethylene)-1,7,7-trimethylbicyclo[2.2.1]heptan-2-one (6.07 g, 0.0340 mol) and $N_2H_4 \cdot H_2O$ (3.27 mL, 0.0674 mol) were dissolved in methanol (500 mL) and refluxed for 17 h. 100 mL solvent was removed

under reduced pressure, and 100 mL water was poured in. A lightly yellow solid precipitated. All volatiles were removed under reduced pressure, giving a light yellow solid (5.07 g, 0.0290 mol, yield= 85%).

^{1}H NMR ($CDCl_3$, 25°C): δ 7.30 (s, 1H), δ 2.78 (d, J=3.9 Hz, 1H), δ 2.10-00 (m, 1H), δ 1.90-1.80 (m, 1H), δ 1.30 (s, 1H), δ 1.26-1.11 (m, 1H), δ 0.95 (s, 1H), δ 0.65 (m, 1H).

^{13}C NMR ($CDCl_3$, 25°C): δ 166.6, δ 126.6, δ 120.4, δ 61.4, δ 50.4, δ 47.5, δ 34.1, δ 28.2, δ 20.8, δ 19.6, δ 11.1.

Potassium hydrido-tris(4,5,6,7-tetrahydro-7,8,8-trimetheyl-2H-4,7-methanoindazolyl)borate

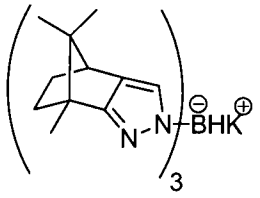

Neat Procedure: **(A)** Potassium borohydride (0.0734 g, 0.00136 mol) and 4,5,6,7-tetrahydro-7,8,8-trimetheyl-2H-4,7-methanoindazole (1.00 g, 0.00568 mol) were poured in a flask (25 mL) and heated slowly with a mineral oil bath under Ar atmosphere with constant stirring. At 140-150°C 4,5,6,7-tetrahydro-7,8,8-trimetheyl-2H-4,7-methanoindazole melted and soon a vigorous evolution of hydrogen commenced. Kept heating at

210°C with stirring until the melt froze. The solid was broken and washed with hot pet. ether. The product was the recovered 4,5,6,7-tetrahydro-7,8,8-trimetheyl-2H-4,7-methanoindazole (according to IR). **(B)** Sodium borohydride (0.141 g, 0.00370 mol) and 4,5,6,7-tetrahydro-7,8,8-trimetheyl-2H-4,7-methanoindazole (1.97 g, 0.011 mol) were poured in a flask (25 ml) and heated slowly with a mineral oil bath under Ar atmosphere at 210°C. Hydrogen evolution commenced when the mixture melted. The melt froze at 160°C. The solid was the recovered starting material (IR). **(C)** Sodium borohydride (0.0350 g, 0.000900 mol) and 4,5,6,7-tetrahydro-7,8,8-trimetheyl-2H-4,7-methanoindazole (0.500 g, 0.00287 mol) were poured in a flask (25 ml) and heated slowly with a mineral oil bath under Ar atmosphere. This time I used stoichiometric amounts and heated at 160°C with stirring. Hydrogen evolution commenced and in 30 minutes the melt froze. The product was the recovered starting material.

Solvent Procedure: **(A)** 4,5,6,7-tetrahydro-7,8,8-trimetheyl-2H-4,7-methanoindazole (1.00 g, 0.00568 mol) and potassium borohydride (0.0770 g, 0.00143 mol) were poured in veratrole (10 mL). The mixture was stirred under Ar and heated with a sand bath at 210°C overnight.

Soon everything dissolved giving a yellow solution that with time was becoming lighter in color. The next day a white solid precipitated. The product was merely insoluble in anything. IR spectrum was lacking B-H stretch reported by Singh et al.[137]**(B)** 4,5,6,7-tetrahydro-7,8,8-trimetheyl-2H-4,7-methanoindazole (0.5 g, 0.00284 mol), potassium borohydride (0.05 g, 0.00925 mol) were poured in decaline (25 mL). The mixrure was stirred under Ar and heated with a sand bath at 210°C overnight. No product precipitated. A white to gray to white solid precipitated when acetonitrile was poured in the solution; the solid was unidentifiable (IR and NMR). The mother liquor was let overnight in a fridge. No crystals precipitated. Removal of all decaline under high vacuum gave nothing at all.

(3S, 6R)-3-isopropyl-6-methyl-2-oxocyclohexanecarbaldehyde

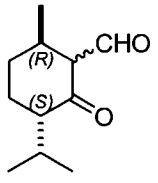

It was prepared according to a literature method.[138] Toluene (50.0 mL) and sodium methoxide (11.7 g, 0.220 mol) were poured into a 3-neck 1000 mL flask. The flask was immersed in an ice–water bath (~ 5°C) and

the mixture was stirred using a mechanical stirrer. A solution of ethyl formate (10.0 mL, 9.00 g, 0.120 mol) in toluene (25.0 mL) was syringed slowly into the flask while the stirrer was on. The mixture was stirred for an additional 10 minutes. A solution of (-) menthone (10.0 g 0.0650 mol, 11.2 mL) of in toluene (20.0 mL) was syringed in slowly. The mixture was stirred for 16 hour, letting the mixture temperature rise to room temperature. A light yellow sticky solid was quenched with ice cold water while keeping the flask in an ice bath. The toluene layer was separated from the water and washed with 50.0 mL of 2.00 M sodium hydroxide. The water layers were joined and acidified with concentrated HCl until pH=1. An oil separated slowly and was extracted with ether (3 x 50.0 mL). The layer was dried with $MgSO_4$ and then evaporated to a red to brown oil, which was purified by chromatography using hexane: acetone (25:1 mixture) on silica gel (Scientific Adsorbents Inc., 32-63) and thereafter distilled under reduce pressure ($P \sim 10^{-5}$mm Hg, b.p. 70-80°C). A light yellow oil was obtained (10.0 g, 0.0550 mol, yield= 85 %).

^{1}H NMR ($CDCl_3$, 25°C): δ 8.72 (s, 1H), δ 2.70-2.60 (ddd, 1H), δ 2.55-2.40 (m, 1H), δ 2.40-2.34 (m, 1H), δ 1.67 (m, 4H), δ 1.10 (d, J= 7.0 Hz, 3H), δ 0.98 (d, J= 7.0 Hz, 3H), δ 0.83 (d, J= 7.0 Hz, 3H).

(4R,7R)-4,5,6,7-tetrahydro-7-isopropyl-4-methyl-2H-indazole

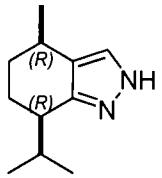

(3S, 6R)-3-isopropyl-6-methyl-2-oxocyclohexanecarbaldehyde (10.0 g, 0.0550 mol) was dissolved in methanol (30.0 mL). $N_2H_4 \cdot H_2O$ (2.76 g, 2.68 mL, 0.0550 mol) was syringed in and the mixture was refluxed for 2 hours. All volatiles were removed under reduced pressure giving rise to thick red to brown oil. The latter is dissolved into dichloromethane (20.0 ml) and washed with water and finally dried with $MgSO_4$. After removal of dichloromethane under reduced pressure, the product was distilled under reduced pressure (b.p. 125°C, 10^{-5} mmHg).[139] A thick yellow oil was obtained (6.90 g, 0.0387 mol, yield= 70.0 %, 90% de according to ^{1}H NMR).

^{1}H NMR ($CDCl_3$, 25 °C): δ 7.35 (s, 1H), δ 2.80-2.70 (ddd, 1H), δ 2.65-2.50 (m, 1H), δ 2.15-2.00 (m, 1H), δ 1.80-1.70 (m, 1H), δ 1.70-1.60 (m, 1H), δ 1.55-1.40 (m), δ 1.20 (d, J= 7.0 Hz, 3H), δ 1.02 (d, J= 7.0 Hz, 3H), δ 0.88 (d, J= 7.0 Hz, 3H).

Potassium hydrido-tris-[(4R,7R)-4,5,6,7-tetrahydro-7-isopropyl-4-methyl-2H-indazolyl]borate

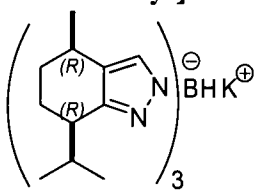

(4R,7R)-4,5,6,7-tetrahydro-7-isopropyl-4-methyl-2H-indazole (5.80 g, 0.0330 mol) and 0.360 equivalent of KBH_4 (0.640 g, 0.0120 mol) were poured into 50.0 mL round bottom flask and heated with a sand bath to 210°C under Ar. When hydrogen evolution ceased, the mixture was cooled to 150°C and quenched with cold toluene. Toluene was removed under reduced pressure giving rise to thick oil. The latter was dissolved into dichloromethane and again evaporated, giving a white glassy solid (6.96 g, 0.0120 mol, yield= 83 %).

IR(KBr): 2953, 2416 (υBH), 1648, 1556, 1454, 1368, 1310, 1241, 1171, 996, 948, 921, 525 cm^{-1}.

^{1}H NMR ($CDCl_3$, 25°C): δ 7.30 (s), δ 7.23 (s), δ 7.18 (s), δ 7.15 (s), δ 2.80-2.75 (m), δ 2.75-2.65 (m), δ 2.65-2.50 (m), δ 2.45-2.41 (m), δ 2.10-1.90 (m), δ 1.80-1.65 (m), δ 1.60-1.40 (m), δ 1.17 (d, J= 7.0 Hz), δ 1.10 (d, J=7.0 Hz), δ 1.02 (d, J=7.0 Hz), δ 0.90 (d, J=7.0 Hz), δ 0.87 (d, J=7.0 Hz), δ 0.75 (d, J=7.0 Hz). **^{13}C NMR ($CDCl_3$-d^6, 25°C):** δ 152.2, δ 138.3, δ

130.6, δ 129.4, δ 128.6, δ 125.7, δ 122.0, δ 121.4, δ 40.8, δ 40.6, δ 40.2, δ 39.3, δ 33.5, δ 33.2, δ 31.5, δ 31.2, δ 30.5, δ 30.3, δ 28.6, δ 28.1, δ 27.1, δ 26.6, δ 23.2, δ 22.8, δ 22.5, δ 22.0, δ 21.5, δ 21.3, δ 20.7, δ 20.5, δ 19.3, δ 19.1, δ 18.0, δ 17.0.

Hydrido-tris-[(4R,7R)-4,5,6,7-tetrahydro-7-isopropyl-4-methyl-2H-indazolyl]borato(trioxo)rhenium(VII)

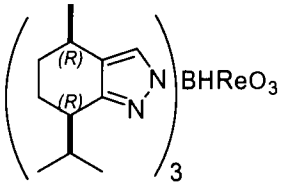

It was prepared according to Mayer[140] with modification. Re_2O_7 (0.500 g, 1.03 mmol) and THF (25.0 mL) were poured in 50.0 mL Schlenk bottle. The mixture was let to warm to room temperature and stirred well until all the oxide was dissolved. The colorless or light green solution was cooled down to -78°C with acetone-dry ice slurry; thereafter $(CF_3CO)_2O$ (0.150 mL, 1.06 mmol) was syringed in slowly while the solution was being stirred. The mixture was warmed to room temperature and stirred well until a colorless solution was obtained. The solution was again cooled down to -78°C with acetone-dry ice slurry and potassium hydrido-tris-[(4R,7R)-4,5,6,7-tetrahydro-7-isopropyl-4-methyl-2H-indazolyl] borate

(1.16 g, 2.00 mmol) in a solution of THF (10.0 mL) was syringed in slowly with constant stirring. The mixture was stirred for at least 10 hours at -78°C. The solution turned brown chocolate color slowly. A very fine white to gray solid was obtained and washed with sufficient methanol (0.360 g, 0.463 mmol, yield=15%, de 70% according to ^{1}H NMR). This was scarcely soluble in organic solvents and water. DMSO barely dissolved it.

IR(KBr): B-H stretch is missing.

^{1}H NMR (DMSO-d^6, 25°C): δ 7.67 (s, 1H), δ 7.44 (s, 2H), δ 2.75-2.60 (m), δ 2.20-2.00 (m), δ 1.75-1.55 (m), δ 1.40-1.30 (m), δ 1.11 (d, J=6.8 Hz, 9H), δ 0.95 (d, J=6.7 Hz, 9H), δ 0.74 (d, J=6.7 Hz, 9H).

Hydrido-tris-[(4R,7R)-4,5,6,7-tetrahydro-7-isopropyl-4-methyl-2H-indazolyl]borato(ethane-1,2-diolato)(oxo) rhenium(V)

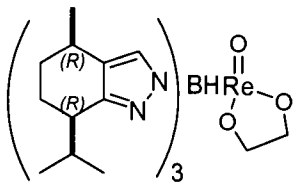

It was prepared according to Gable[141] with modifications. Hydrido-tris-[(4R,7R)-4,5,6,7-tetrahydro-7-isopropyl-4-methyl-2H-indazolyl]borato (trioxo) rhenium(VII) (50.0 mg, 0.0643 mmol), triphenylphosphine

(0.0364 g, 0.140 mmol), p-toluenesulfonic acid monohydrate (~1.00 mg), ground molecular sieves (0.100 g), and ethylene glycol (19.7 μL, 0.360 mmol) were poured into a NMR tube. Thereafter 0.70 mL toluene-d_6 was syringed in the tube and degassed with Freeze-Pump-Thaw technique.[142] A light blue color started rising. ^{1}H NMR showed no presence of carbinolic peaks. The carbinolic peaks did not rise even after heating the tube in an oil bath at 40°C overnight. The tube was opened and the product was purified by chromatography on silica gel (Scientific Adsorbents Inc., 32-63). A solution of dichloromethane and hexane (1:1) was used to wash the blue diolate. Neat ethyl acetate was used to elute the product from the column. Removal of solvent left an unidentifiable (by NMR) solid.

3,5-diisopropyl-1H-pyrazole

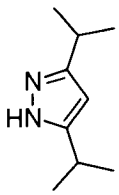

2,6-dimethylheptane-3,5-dione (3.00 g, 0.0190 ml) and $N_2H_4 \cdot H_2O$ (0.940 ml, 0.0190 mol) were dissolved in 30.0 mL methanol and refluxed for 2

hours. Removal of all volatiles gave rise to a white glassy solid (2.36 g, 0.0150 mol, yield= 81 %).

^{1}H NMR ($CDCl_3$, 25°C): 9.00 (broad hump), δ 5.85 (s, 1H), δ 2.95 (sp, J=6.9 Hz, 2H), δ 1.27 (d, J=6.9 Hz, 12H).

Potassium hydrido-tris-(3,5-diisopropyl-1H-pyrazolyl)borate

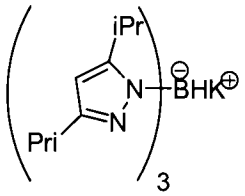

3,5-diisopropyl-1H-pyrazole (2.36 g, 0.0150 mol) and 0.360 equivalent of KBH_4 (0.300 g, 0.00560 mol) were poured into 50.0 mL round bottom flask and heated with sand bath to 210°C under Ar. When hydrogen evolution ceased, the mixture was cooled down to 150°C and quenched with cold toluene. Removal of toluene gave an oil that was dissolved in dichloromethane; removal of dichloromethane under reduced pressure gave a white glassy solid[143] (2.63 g, 0.00470 mol, yield = 100 %).

IR (KBr pellets): 2963, 2468 (υBH), 1566, 1529, 1465, 1421, 1378, 1301, 1261, 1173, 1137, 1105, 1048, 1005, 945, 791, 726, 663 cm^{-1}. **^{1}H NMR**

($CDCl_3$, 25°C): δ 5.86 (s, 1H), δ 5.83 (s, 1H), δ 2.95 (sp, J=7.0 Hz, 2H), δ 1.27 (d, J=7.0 Hz, 12H).

Hydrido-tris-(3,5-diisopropyl-1H-pyrazolyl) borato (trioxo) rhenium(VII)

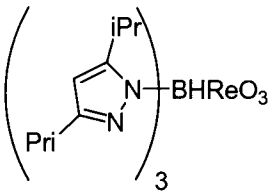

Re_2O_7 (0.500 g, 1.03 mmol) and THF (25.0 mL) were poured in 50.0 mL Schlenk bottle. The mixture was let to warm to room temperature and stirred well until all the oxide was dissolved. The colorless or light green solution was cooled down to -78°C with acetone-dry ice slurry; thereafter $(CF_3CO)_2O$ (0.150 mL, 1.06 mmol) was syringed in slowly while the solution was being stirred. The mixture was warmed to room temperature and stirred well until a colorless solution was obtained. The solution was again cooled down to -78°C with acetone-dry ice slurry and potassium hydrido-tris-(3,5-diisopropyl-1H-pyrazolyl) borate solution in THF (1.08 g, 0.00214 mol dissolved in 10.0 mL THF) was syringed in slowly with constant stirring and let temperature rise to room temperature. A yellow solution was formed that with time became greener (deep green). The

next day a gray to white solid was separated and washed with methanol and THF. The solid was $KReO_4$ (according to IR).

IR(KBr): 911 cm^{-1} (Re=O).

3-oxo-3-o-tolylpropanal

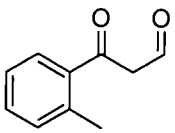

It is prepared by literature method with slight modifications.[144] Toluene (50.0 mL) and sodium methoxide (11.7 g, 0.220 mol) were poured into a 3-neck 1.00 L flask. The flask was immersed in an ice–water bath (~ 5°C) and stirred using a mechanical stirrer.[145] A solution of ethyl formate (10.0 mL, 9.00 g, 0.120 mol) in toluene (25.0 mL) was syringed into the flask slowly. The mixture was stirred for an additional 10 minutes. A solution of 2-methylacetophenon (8.56 mL, 0.0650 mol) in toluene (20.0 mL) was syringed in slowly. The mixture was stirred for 16 hour, letting the mixture temperature rise to room temperature. A lightly yellow sticky solid was quenched with ice cold water. The toluene layer was separated from the water and washed with 50.0 mL 2.00 M sodium hydroxide. The water layers were combined and acidified with concentrated HCl until pH=1. An oil separated and was extracted with ether (3 x 50.0 mL). The

ether layer was dried with $MgSO_4$ and then evaporated, giving a red to brown oil. The product was distilled under reduced pressure (b.p. ~85°C, P~10^{-5} mm Hg). A colorless oil was obtained (7.35 g, 0.0450 mol, yield= 70 % yield).

^{1}H NMR ($CDCl_3$, 25°C): δ 9.90 (t, 1H), δ 8.20 (d, J=4.3 Hz, 1H), δ 7.20-7.60 (m, 4H), δ 5.90 (d, J=4.3 Hz, 1H), δ 4.00 (d, J=2.6 Hz, 1H), δ 2.50 (s, 1H).

3-o-tolyl-1H-pyrazole

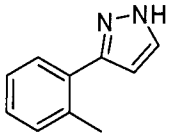

It is prepared by literature method with modifications.[146] 3-oxo-3-o-tolylpropanal (7.35 g, 0.0450 mol) was dissolved in methanol (30.0 mL). $N_2H_4.H_2O$ (2.23 g, 0.0450 mol, 2.31 mL) was syringed in and the mixture was refluxed for 2 hours. All volatiles were removed under reduced pressure giving a thick brown oil. This was dissolved into dichloromethane (20.0 ml) and washed with water and finally dried with $MgSO_4$. After removal of dichloromethane under reduced pressure, the

product was distilled under reduced pressure (b.p. 135°C, P~10^{-5} mm Hg). A colorless thick oil was obtained (4.34 g, 0.0270 mol, yield= 61.0 %).

^{1}H NMR ($CDCl_3$, 25°C): δ 7.55 (d, J=1.9 Hz, 1H), δ 7.20-7.50 (m, 4H), δ 6.40 (d, J=2.0 Hz, 1H), δ 2.40 (s, 2H).

Potassium hydrido-tris-(3-o-tolyl-1H-pyrazolyl)borate

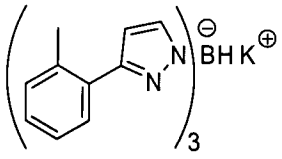

3-o-tolyl-1H-pyrazole (4.34 g, 0.027mol) and 0.36 equivalent of KBH_4 (0.540 g, 0.0100 mol) were poured into 50.0 mL round bottom flask and heated with sand bath to 210°C under Ar. When hydrogen evolution ceased, the mixture was cooled down to 150°C and quenched with cold toluene. A white solid precipitated and toluene was evaporated under vacuum, giving a white solid (4.05 g, 0.00775 mol, yield= 84 %).

IR (KBr pellet): 3105, 3058, 3027, 2412 (υBH), 1954, 1808, 1723, 1605, 1581, 1522, 1493, 1457, 1349, 1301, 1278, 1244, 1189, 1098, 1072, 1043, 1028, 991, 949, 914, 864, 749, 697, 638, 618 cm^{-1}.

^{1}H NMR ($CDCl_3$, 25°C): δ 7.73 (d, J=2.2 Hz, 1H), 7.50 (d, J=2.2 Hz, 1H), δ 7.00-7.40 (m, 9H), 6.40 (d, J=2.2 Hz, 1H), δ 6.30 (d, J=2.2 Hz,

1H), δ 2.40 (s, 2H), δ 2.33 (s, 2H). **^{13}C NMR ($CDCl_3$, 25°C):** δ 136.4, δ 131.2, δ 129.4, δ 128.7, δ 127.4, δ 126.4, δ 126.1, δ 106.0, δ 104.7, δ 21.2.

Hydrido-tris-(3-o-tolyl-1H-pyrazolyl)borato(trioxo)rhenium(VII)

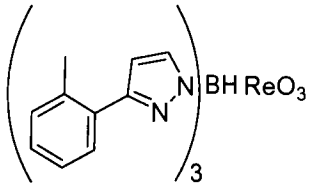

Procedure A: It was prepared according to Mayer[147] with modification. Re_2O_7 (0.500 g, 1.03 mmol) and THF (25.0 mL) were poured in 50.0 mL Schlenk bottle. The mixture was let to warm to room temperature and stirred well until all the oxide was dissolved. The colorless or light green solution was cooled down to -78°C with acetone-dry ice slurry; thereafter $(CF_3CO)_2O$ (0.150 mL, 1.06 mmol) was syringed in slowly while the solution was being stirred. The mixture was warmed to room temperature and stirred well until a colorless solution was obtained. The solution was again cooled down to -78°C with acetone-dry ice slurry and potassium hydrido-tris-(3-o-tolyl-1H-pyrazolyl)borate solution in THF (1.08 g, 2.06 mmol dissolved in 10.0 mL THF) was syringed in slowly with constant stirring. The mixture was stirred for at least 10 hours at -78°C. A very

fine white solid was obtained and washed with sufficient methanol (0.450 g, 0.630 mmol, yield= 29 %).[148]

IR(KBr): 3120, 2921, 2851, 2510 (υBH), 1864, 1608, 1521, 1489, 1471, 1372, 1341, 1322, 1261, 1208, 1195, 1081, 1052, 959, 646, 919 (υReO), 801, 782, 760, 732, 725, 668, 633 cm-1. **^{1}H NMR (DMSO-d_6, 25 °C):** δ 8.30 (d, J=2.3 Hz, 1H), δ 7.01-7.33 (m, 4H), δ 6.45 (d, J=2.3 Hz, 1H), δ 1.89 (s, 3H). **^{13}C NMR (DMSO-d_6, 25°C):** δ 156.2, δ 138.1, δ 132.8, δ 131.1, δ 130.0, δ 129.4, δ 125.5, δ 109.6, δ 20.6. **HRMS (FAB):** calculated mass for $[C_{30}H_{28}BN_6O_3Re]^+$ 719.1938, found 719.1932.

Procedure B: The same as the first generation synthesis, but added 2.60 mmol of potassium hydrido-tris-(3-o-tolyl-1H-pyrazolyl)borate. A white to gray solid obtained (0.537 g, 0.747 mmol, yield= 38 %).

IR(KBr): 3107, 3023, 2922, 2853, 2551 (υBH), 2516 (υBH), 1912, 1864, 1804, 1679, 1607, 1522, 1489, 1471, 1382, 1368, 1331, 1343, 1261, 1194, 1158, 1084, 1058, 1017, 912 (υReO), 803, 757, 733, 722 cm^{-1} . **^{1}H NMR (DMSO-d_6, 25°C):** δ 8.40 (d, J=1.8 Hz, 1H), δ 8.12 (d, J=2.2 Hz, 2H), δ 7.54-7.04 (m, 12H), δ 6.60 (d, J=1.9 Hz, 1H), δ 6.40 (d, J=2.2 Hz, 2H), δ 2.08 (s, 3H), δ 1.88 (s, 6H). **^{13}C NMR (DMSO-d_6, 25°C):** δ 156.2, δ 143.9, δ 138.2, δ 132.7, δ 131.2, δ 129.9, δ 126.8, δ 125.5, δ 109.5, δ 20.6.

HRMS (FAB): calculated mass for $[C_{30}H_{28}BN_6O_3Re]^+$ 719.1952, found 719.2000.

Hydrido-tris-(3-o-tolyl-1H-pyrazolyl)borato(ethane-1,2-diolato)(oxo) rhenium(V)

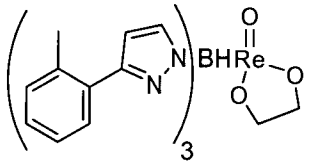

It was prepared according to Gable[149] with modifications. Hydrido-tris-(3-o-tolyl-1H-pyrazolyl)borato(trioxo)rhenium(VII)(50.0 mg, 0.0700 mmol), triphenylphosphine (0.0360 g, 0.140 mmol), p-toluenesulfonic acid monohydrate (~1.00 mg), ground molecular sieves (0.100 g), and ethylene glycol (19.7 μL, 0.360 mmol) were stirred at room temperature for 24 hours in THF (50.0 mL). The very pale blue solution was filtered, and the volatiles removed under reduced pressure. The product was purified by chromatography on silica gel (Scientific Adsorbents Inc., 32-63). A solution of dichloromethane and hexane (1:1) was used to wash the blue diolate. Neat ethyl acetate was used to elute diolate off the column. Removal of solvent left a blue solid.

Procedure A: It was prepared from $LReO_3$ prepared according to procedure A (see above). A blue solid obtained (0.0882 g, 0.118 mmol, yield = 62 %).[150]

IR (KBr): 3053, 2921, 2851, 2496(υBH), 1890, 1583, 1523, 1474, 1432, 1369, 1342, 1306, 1261, 1189, 1155, 1087, 1068, 1055, 1009, 966, 905, 844, 786, 741, 721, 694, 644, 560, 541, 510 cm^{-1}.

^{1}H NMR ($CDCl_3$, 25°C): δ 8.07 (d, J=2.1 Hz, 1H), δ 7.48 (d, J=2.1 Hz, 0.5H), δ 7.44-7.02 (m, 6H), δ 6.41(d, J=2.06 Hz, 1H), δ 5.87 (d, J=2.05 Hz, 0.5H), δ 2.20 (s, 3H), δ 2.05(s, 1.5H).

HRMS (FAB): 746.22 [M+].

Procedure B: It was prepared from $LReO_3$ prepared according to procedure B (see above). A blue solid obtained (0.0187 g, 0.0250 mmol, yield = 36 %).

IR (KBr): 3022, 2919, 2850, 2506 (υBH), 1735, 1654, 1607, 1560, 1532, 1488, 1472, 1380, 1365, 1345, 1260, 1189, 1082, 1055, 1017, 968, 946, 905, 862, 788, 759, 723, 664, 640, 544 cm^{-1}.

^{1}H NMR ($CDCl_3$, 25°C): δ7.96 (d, J=2.1 Hz, 1H), δ 7.89 (d, J=2.3 Hz, 1H), δ 7.76 (d, J=2.3 Hz, 5H), δ 7.73 (d, J=2.0 Hz, 3H), δ 7.51-7.06 (m, 60H), δ 6.43 (d, J=2.2 Hz, 1H), δ 6.41 (d, J=2.3 Hz, 1H), δ 6.37 (d, J=2.3 Hz, 6H), δ 6.04 (d, J=2.0 Hz, 3H), δ 5.79 (d, J= 2.1 Hz, 1H), δ 4.84 (m, 6H), δ 4.24 (m, 6H), δ 2.17 (s, 4H), δ 2.10 (s, 17H), δ 2.02 (s, 12H).

^{13}C NMR ($CDCl_3$, 25°C): δ 160.0, δ 156.7, δ 151.4, δ 147.1, δ 142.0, δ 138.7, δ 138.3, δ 138.1, δ 137.8, δ 134.6, δ 134.2, δ 132.5, δ 132.0, δ 131.8, δ 131.5, δ 130.8, δ 130.5, δ 130.3, δ 129.6, δ 129.2, δ 129.0, δ 128.8, δ 125.9, δ 125.7, δ 125.1, δ 124.4, δ 109.5, δ 108.7, δ 108.5, δ 107.4, δ 107.2, δ 86.8, δ 85.7, δ 20.8, δ 20.7, δ 20.5, δ 20.2.

4.4 Low Temperature NMR Experiments

The NMR sample was prepared by dissolving hydrido-tris-(3-o-tolyl-1H-pyrazolyl)borato(ethane-1,2-diolato)(oxo) rhenium(V) in 0.5 mL deuterated dichloromethane (m.p. -95°C). The sample was cooled with air that was running through a liquid nitrogen filed chamber. Air rate flow was adjusted to have appreciable cooling rate of the sample probe. The ^{1}H NMR was taken at 15, 5, -5, -15, -25, -35, -45, -55, -65, -75, -85, -95, -100, -110, -125 and -130°C. To assure homogeneous magnetic field, readjusting of magnetic field around the sample (shimming) was done each time before the ^{1}H NMR was taken. The sample froze at -130°C (the spectrum flattened out).

4.5 Computations

Computational modeling was performed by running the commercially available Jaguar package in Linux Slackware 10 machine.[151] The LACVP basis set, incorporating a Hay-Wadt effective core potential[152] for rhenium and the 6-31G basis set for all other atoms, was used throughout. All geometry optimizations of the ground state structures were first optimized without polarization or diffuse functions, but were then reoptimized with the added functions (LACVP*+). For calculation of energies of each conformer, energy minimization was performed after an angle constrain by modifying the Z-matrix was applied on each conformer accordingly.

Bibliography

1. Smith. J. G., *Synthesis* **1984**:629.

2. Jørgensen, K. A. *Chem. Rev.* **1989**, *89*, 431.

3. Hodgson, D. M.; Gibbs, A. R.; Lee, G. P. *Tetrahedron* **1996**, *52*, 14361.

4. (a) Hodgson, D. M.; Gibbs, A. R.; Lee, G. P. *Tetrahedron* **1996**, *52*, 14361. (b) Gayet, A.; Bertilsson, S.; Andersson, P. G. *Org. Lett.* **2002**, *4*, 3777. (c) Whitesell, J. K.; Felman, S. W. *J. Org. Chem.* **1980**, *45*, 755. (d) Bertilsson, S. K.; Sodergen, M. J.; Andersson, P. G. *J. Org. Chem.* **2002**, *67*, 1567. (e) Sodergen, M. J.; Bertilsson, S. K.; Andersson, P. G. *J. Am. Chem. Soc.* **2000**, *122*, 6610. (f) Magnus, A.; Bertilsson, S. K.; Andersson, P. G. *Chem. Soc. Rev.* **2002**, *31*, 223. (g) Bertilsson, S. K.; Andersson, P. G. *Tetrahedron* **2002**, *58*, 4665. (h) O'Brien, P. *J. Chem. Soc., Perkin Trans.* **1998**, *1*, 1439.

5. (a) Gansauer, A.; Narayan, S. *Adv. Synth. Catal.* **2002**, *344*, 465. (b) RajanBabu, T. V.; Nugent, W. A. *J. Am. Chem. Soc.* **1994**, *116*, 986.

6. For Denmark's work and related, see: (a) Denmark, S. E.; Barsanti, P. A. *J. Org. Chem.* **1998**, *63*, 2428. (b) Brunel, J. M.; Legand, O;. Reymond, S.; Buono, G. *Angew. Chem., Int. Ed.* **2000**, *39*, 2554. (c) Brunel, J. M.; Reymond, S.; Buono, G. *Tetrahedron: Asymmetry* **2000**, *11*, 4441. (d) Denmark, S. E.; Wynn, T.; Jellerichs, B. G. *Angew. Chem., Int. Ed.* **2001**, *40*, 2255. (f) Fu, G.; Tao, B.; C. Lo, M. *J. Am. Chem. Soc.* **2001**, *123*, 353. (g) Kim, T. J.; Peak, S. H.; Shim, S. Ch.; Cho, Ch. S. *Synlett.* **2003**, *6*, 849. For Shibasaki's work see *(a)* Iida, T.; Yamamoto, N.; Sasai, H.; Shibasaki, M. *J. Am. Chem. Soc.* **1997**, *119*, 4783. (b) Nemoto, T.; Kakei, H.; Gnanadesikan, V.; Tosaki, S.; Ohshima, T.; Shibasaki, M. *J. Am. Chem. Soc.* **2002**, *124*, 14544. (c) Matsunaga, S.; Ohshima, T.; Shibasaki, M. *Adv. Synth. Catal.* **2002**, *344*, 3. (d) Wu, M. and Jacobsen, E.N. Chapter 35 in "Comprehensive Asymmetric Catalysis" Jacobsen, E. N; Pfaltz, A. & Yamamoto, H., 1999, Springer-Verlag. (f) Yamasaki, S.; Kanai, M.; Shibasaki, M. *J. Am. Chem. Soc.* **2001**,123, 1256. For Nugent's work see (a)

Nugent, W. A. *J. Am. Chem. Soc.* **1992**, *114*, 2768. (b) Nugent, W. A. *J. Am. Chem. Soc.* **1998**, *120*, 7139.

7. (a)(R,R)-N,N'-Bis(3,5-Di-tert-butylsalicylidene)-1,2- Cyclohexane di aminomanganese (III) Chloride (b) Larrow, J.F.; Jacobsen, E.N. *Org. Syn.* **1997**, *75*, 1.

8. (a) Martinez, L. E.; Leighton, J. L.; Carsten, D. H.; Jacobsen, Eric N. *J. Am. Chem. Soc.* **1995**, *117*, 5897. (b) Hansen, K. B.; Leighton, J. L.; Jacobsen, E. N. *J. Am. Chem. Soc.* **1996**, *118*, 10924.

9. (a) 8(a). (b) Lebel, H.; Jacobsen, E.N. *Tetrahedron Lett.* **1999**, 40, 7303-7306. (c) Wu, M. H.; Hansen, K. B.; Jacobsen, E. N. Jacobsen *Angew. Chem., Int. Ed.* **1999**, *38*, 2012. (d) Ready, J. M.; Jacobsen, E. N. *J. Am. Chem. Soc.* **1999**, *121*, 6086. (e) Peukert, S.; Jacobsen, E. N. *Org. Lett.* **1999**, *1*, 1245.

10. (a) Schaus, S. E.; Brandes, B. D.; Larrow, J. F.; Tokunaga, M.; Hansen, K. B.; Gould, A. E.; Furrow, M. E.; Jacobsen, E. N. *J. Am. Chem. Soc.* **2002**, *124*, 1307. (b) Breinbauer, R.; Jacobsen, E. N. *Angew. Chem., Int. Ed.* **2000**, *39*, 3604. (c) White, D. E.; Jacobsen, E. N. *Tetrahedron: Asymmetry* **2003**, *14*, 3633. (d) Nielsen, L. P. C.; Stevenson, C. P.; Blackmond, D. G.; Jacobsen, E. N. *J. Am. Chem. Soc.* **2004**, *126*, 1360-1362.

11. Corey, E. J.; Su, W. *J. Am. Chem. Soc.*, **1987**, *109*, 7534. Note: according to Corey the deoxygenation proceeds by a radical chain mechanism involving attack by triethylsilyl on the oxirane oxygen to form olefin and triethylsilyloxy as key propagation steps.

12. Martin, M. G.; Ganem, B. *Tetrahedron Lett.* **1984**, 25, 251.

13. Wittig, G.; Haag, W. *Chem. Ber.*, **1955**, *88*, 1654.

14. Corey, E. J.; Cane, D.E. *J. Org. Chem.* **1969**, *34*, 3053.

15. (a) Vedejs, E. and Fuchs, P. L. *J. Am. Chem. Soc.* **1971**, *93*, 4070. (b) Vedejs, E. and Fuchs, P. L. *J. Am. Chem. Soc.* **1973**, *95*, 822. (c) Vedejs, E.; Karel, J.; Snoble, A. J. and Fuchs, P. L. *J. Org. Chem* **1973,** *38, 1178.*

16. Suzuki, H.; Fuchita, T.; Iwasa, A.; Mishina, T. *Synthesis* **1978**, 905.

17. Martinez, A. G.; Ruiz, M. O. *Synthesis* **1983**, 663.

18. Clive, D. L. J.; Denyer, C. V. *J. Chem. Soc., Chem. Commun.* **1973**, 253.

19. Clive, D. L. J.; Menchen, S. M. *J. Org. Chem.* **1980**, *45*, 2347.

20. Sharpless, K. B.; Umbreit, M. A.; Nieh, M. T.; Flood, T. C. *J. Am. Chem. Soc.* **1972**, *94*, 6538.

21. Kraus, G. A. and Thomas, P. J. *J. Org. Chem.* **1988**, *53*, 1395.

22. Dowd, P.; Kang, K. *J.Chem.Soc.,Chem.Commun.* **1974**, 384.

23. Giering, W. P.; Rosenblum, M.; Tendcrede, J. *J. Am. Chem. Soc.* **1972**, *94*, 7170.

24. Schobert, R. *Angew. Chem. Int. Ed. Engl.* **1988**, *27*, 855.

25. Lowry, H. L.; Richardson, K. S. in "Mechanism and Theory in Organic Chemistry", 3rd Edition, 1987, Harper & Row, p. 319.

26. Shriver, D.; Atkins, P. in "Inorganic Chemistry" 3rd Ed.; W. H. Freeman and Company: New York, 2003; p. 143.

27. Crabtree, R.H. in "The Organometallic Chemistry of the Transition Metals" 3rd Ed.; Wiley Inter Science, 2003; p.13.

28. (a) Young, D. in "Computational Chemistry – A Practical Guide for Applying Techniques to Real World Problems" ; Wiley Inter Science, 2001. (b) "A Brief Guide to Molecular Mechanics and Quantum Chemical Calculations" , Hehre, J. W.; Yu, J.; Klunzinger, P. E.; Lou, L. Wavefunction, Inc., 1998 and references cited therein. (c) "Essentials of Computational Chemistry- Theories and Models", Cramer, J. C. , John Wiley & Sons, LTD., 2002.

29. Collman, J. P.; Hegedus, L. S. in "Principles and Applications of Organotransition Metal Chemistry", 1980, University Science Books. (b) Hegedus, L.S. in "Transition Metals in the Synthesis of Complex Organic Molecules", 1994, University Science Books.

30. Cotton, F. A.; Wilkinson, G.; Murillo, C. A.; Bochmann, M. in "Advanced Inorganic Chemistry", 6th Ed.; 1999, Wiley Inter Science, page 644.

31. Matano, Y.; Northcutt, T. O.; Brugman, J. Bennett, B. K.; Lovell, S. and Mayer, *J.* M. *Organometallics* **2000,** *19,* 2781.

32. Geenwood, N.N. and Earnshaw, A. in "Chemistry of the Elements"; 1984; Pergamon Press.

33. Named after the river Rhine.

34. As its name implies.

35. Herrmann, W. A. and Kuhn, F. E. *Acc. Chem. Res.* **1997**, *30*, 169.

36. (a) Herrmann, W. A. *J. Organomet. Chem* **1995**, *500*, 149. (b) Herrmann, W. A. ; Kuhn, F. E.; Romao, C. C.; Kleine, M. *J. Chem. Ber.* **1994**, *127*, 47. (c) Herrmann, W. A. ; Thiel, W. R.; Kuhn, F. E.; Fischer, R. W.; Kleine, M.; Herdweck, E; Scherer, W.; Mink, *J. Inorg. Chem.* **1993**, *32*, 5188. (d) Herrmann, W. A.; Kuhn, F. E.; Fischer, R. W.; Romao, C. C. *J. Inorg. Chem.* **1992**, *31*, 4431. (f) Herrmann, W. A.; Roesky, P. W.; Kiihn, F. E.; Elison, M.; Artus, G.; Scherer, W.; RomBo, C. C.; Lopes, A.; Basset, J. M. *J. Inorg. Chem.* **1995**, 34, 4701.

37. (a) Krebs, B. ; Muller, A.; Beyer, H. H. *J. Inorg. Chem.* **1969**, *8*, 436.

38. (a) Herrmann, W. A.; Kuhn, F. E.; Fischer, R. W.; Thiel, W. R.; Romao, C. C. *Inorg. Chem.* **1992**, *31*, 4431. (b) Kuhn, F. E.; Herrmann, W. A.; Hahn, R.; Elison, M.; Blumel, J. and Herdtweck, E. *Organometallics* **1994**, *13*, 1601. (c) Herrmann, W. A.; Thiel, W. R.; Kh, F. E.; Fischer, R. W.; Kleine, M.; Herdtweck, E. and Scherer, W. *Inorg. Chem.* **1993**, *32*, 5188.

(d) Matano, Y. Northcutt, T. O.; Brugman, J.; Bennett, B. K.; Lovell, S.; Mayer, J. M. *Organometallics* **2000,** *19,* 2781.

39. Romao, C. C.; Herrmann, W. A. and Kuhn, F. E. *Acc. Chem. Res.* **1997**, *97*, 3197.

40. Baettie, I. R.; Jones, P. J. *J. Inorg. Chem.* **1997**, *18*, 2318.

41. Herrmann, W. A.; Fischer, R.W.; Marz, D. W. *Angew. Chem. Int. Ed. Engl.* **1991**, *30*, 1638.

42. Oxidation reactions catalyzed by MTO: olefins; a) Hoechst A. G.; Herrmann, W. A.; Marz, D. W.; Kuchler, J. D.; Weichselbaumer, G.; Fischer, R. W.; DE 3.902.357, 1989. b) Herrmann, W. A.; Marz, D. W.; Fischer, R. W.; *Angew. Chem. Int. Ed. Engl.* **1991**, *103*, 1706; c) Ref. 41. amines; d) Murray, R. W.; Iyanar, K.; Chen, J.; Wearing, J. T. *Tetrahedron Lett.* **1995**, *36*, 6415. e) Zhu, Z.; Espenson, J. H. *J.Org. Chem.* **1995**, *60*, 1326. e) Murray, R. W.; Iyanar, K.; Chen, J.; Wearing, J. T. *Tetrahedron Lett.* **1996**, *37*, 805. f) Murray, R. W.; Iyanar, K.; Chen, J.; Wearing, J. T. *J. Org. Chem.* **1996**, 61, 8099. sulphides; h) Adam, W.; Mitchell, C. M.; Saha-Moller, C. R. *Tetrahedron* **1994**, *50*, 13121. phosphines; i) Abu-Omar, M. M.; Espenson, J. H. *J. Am. Chem. Soc.* **1995**, *117*, 272. arenes; j) Adam, W.; Herrmann, W. A.; Lin, J.; Saha-Moller, C. R.; Fischer, R. W. and Correira, J. D. G. *Angew. Chem. Int. Ed. Engl.* **1994**, *33*, 2475. Baeyer-Villiger oxidation; k) Herrmann, W. A.; Fischer, R. W.; Correira, J. D. G. *J. Mol. Cat.* **1994**, **94**, 213. phenols; l) Adam, W.; Herrmann, W. A.; Lin, J.; Saha-Moller, C. R.; *J.Org. Chem.* **1994**, *59*, 8281.

43. Adolfsson, H.; Converso, A.; Sharpless, K. B. *Tetrahedron Lett.* **1999**, *40*, 3991.

44. Al-Ajlouni, A. M.; Espenson, J. H. *J. Am. Chem. Soc.* **1995**, *117*, 9243.

45. (a) Schroder, M. *Chem. Rev.* **1980**, *80*, 187. (b) DelMonte, A. J.; Haller J., Houk, K. N.; Sharpless, K. B.; Singleton, D.; Strassner, T.; Thomas, A. A. *J. Am. Chem. Soc.* **1997**, *119*, 9907. (c) Norrby, P. O.; Gable, P. K. G. *J. Chem. Soc., Perkin Trans. 2*, **1996**, 171. (e) Lohray, B. B.; Bhushan, V.

Tetrahedron Lett., **1992**, *33*, 5113. (f) Kolb, H. C.; VanNieuwenhze, M. S.; Sharpless, K. B. *Chem. Rev.* **1994**, *94*, 2483.

46. Herrmann, W. A.; Kiprof, P.; Alberto, R.; Baumgartner, F. *Angew. Chem. Int. Ed. Engl.* **1990**, *29*, 189.

47. Takacs, J.; Kiprof, P. Riede, J.; Herrmann, W. A. *Organometallics* **1990**, *9*, 782.

48. (a) Takacs, J.; Cook, M. R.; Kiprof, P.; Kuchler, J. G.; Herrmann, W. A. *Organometallics* **1991**, *10*, 316-320. (b) ref. 47. (c) Herrmann, W. A.; Kusthardt, U. and Herdtweck, E. *J. Organomet. Chem.* **1985**, *294*, C33. (d) Gable, K. P. *Organometallics* **1994**, *13*, 2486.

49. (a) Zhu, Z.; Al-Ajlouni, A. M.; Espenson, J. H. *Inorg. Chem.* **1996**, *35*, 1408. (b) Ref 44.

50. Herrmann, W. A. Kiprof, P.; Rypdal, K.; Tremmel, J.; Blom, R.; Alberta, R.; Behm, J.; Albach, R. W.; Bock, H.; Solouki, B.; Mink, J.; Lichtenberger, M. D. and Gruhnk, N. E. *J. Am. Chem. Soc.* **1991**, *113*, 6527.

51. Herrmann, W. A.; Marz, D.; Herdtweck, E.; Schäfer, A.; Wagner, W.; Kneuper, H. J. *Angew. Chem., Int. Ed. Engl.* **1987**, *26*, 462.

52. Criegee, R. *Justus Liebigs Ann. Chem.* **1936**, *522*, 75.

53. Woodward, R. B.; Hoffmann, R. "The Conservation of Orbital Symmetry" Verlag Chemie Academic Press, 1971.

54. Corey, E. J.; Noe, M. C. *J. Am. Chem. Soc.* **1996**, *118*, 11038.

55. Sharpless, K. B.; Teranishi, A. Y.; Bäckvall, J. E. *J. Am. Chem. Soc.* **1977**, *99*, 3120.

56. Crabtree R. H. in "The Organometallic Chemistry of the Transition Metals" 3rd Ed.; Wiley Inter Science, 2003; p.313.

57. Ref. 45b.

58. (a) Beno, B. R.; Houk, K. N.; Singleton, D. A. *J. Am. Chem. Soc.* **1996**, *118*, 9984. (b) Singleton, D. A.; Merrigan, S. R.; Liu, J.; Houk, K. N. *J. Am. Chem. Soc.* **1997**, *119*, 3385.

59. Reportedly, they used as a model reaction the reaction of $OsO_4 \cdot NH_3$ with ethylene and propene.

60. Nelson, D. W.; Gypser, A.; Ho, P. T.; Kolb, H. C.; Kondo, T.; Kwong, H.-L.; McGrath, D. V.; Rubin, A. E.; Norrby, P.-O.; Gable, K. P.; Sharpless, K. B. *J. Am. Chem. Soc.* **1997**, *119*, 1840.

61. Gobel, T.; Sharpless, K. B. *Angew. Chem., Int. Ed. Engl.* **1993**, *32*, 1329.

62. Smith, M. B. and March, J. in "March's Advanced Organic Chemistry-Reactions, Mechanisms, and Structure", John Willey & Sons, INC, 5th Edition, 2001, p. 285.

63. Brown, E. C., Ph.D. Thesis, Oregon State University, Corvallis, OR, 2002.

64. Ref. 45b.

65. Gable, K. P.; Phan, T. N. *J. Am. Chem. Soc.* **1994**, *116*, 833.

66. Gable, K. P.; Juliette, J. J. *J. Am. Chem. Soc.* **1996**, *118*, 2625.

67. Ref. 65.

68. Gable, K. P.; Juliette, J. J. *J. Am. Chem. Soc.* **1995**, *117*, 955.

69. (a) Ref. 66. (b) Gable, K. P.; AbuBaker, A.; Zientara, K.; Wainwright, A. M. *Organometallics* **1999**, *18*, 173.

70. "Physical Organic Chemistry" Issacs, N.; Longman Scientific & Technical: Essex, 1995, p. 149.

71. Gable, K. P.; Zhurzvlev, F. A. *J. Am. Chem. Soc.* **2002**, *124*, 3970.

72. Ref. 69a.

73. "Advanced Organic Chemistry" Carey, F. A.; Sunberg, R. J.; Kluwer Academic / Plenum Publishers: New York, 2000, Part A, p. 222.

74. (a) Zhuravlev, F. Ph.D. Thesis, Oregon State University, Corvallis, OR, 2001. (b) Ref. 71.

75. Ref. 45b.

76. Gable, K. P.; Brown, E. C. *J. Am. Chem. Soc.* **2003**, *125*, 11018.

77. Gable, K. P.; Brown, E. C. *Syn. Lett.* **2003**, *14*, 2243.

78. "Comprehensive Organic Synthesis" Trost, B. M., Fleming, I., Eds.; Pergamon Press: New York, 1991.

79. Larock, R. C. "Comprehensive Organic Transformations"; Wiley-VCH Publishers: New York, 1999.

80. Cook, G. K. and Andrews, M.A. *J. Am. Chem. Soc.* **1996**, *118*, 9448.

81. Gable, K. P.; Zhurzvlev, F. A.; Yokochi, A. F. T. *Chem. Commun.* **1998**, 799.

82. Gable, K. P.; Brown, E. C. *Organometallics* **2000**, *19*, 944.

83. (a) " Scorpionates : the coordination chemistry of polypyrazolborate ligands", Swiatoslaw Trofimenko. River Edge, NJ : Imperial College Press, 1999. (b) Trofimenko, S. *Chem. Rev.* **1993**, *93*, 943.

84. (a) ref. 78. (b) ref. 79.

85. Seebach, D.; Weidman, B.; Wilder, L. in "Modern Synthetic Methods " 1983, Scheffold, R., Ed., Otto Salle Verlag: Frankfurt, **1983**, page.324.

86. Pfenninger, A. *Synthesis* **1986**, 89.

87. Mimoun, H.; Mignard, M.; Brechot, P.; Saussine, L. *J. Am. Chem. Soc.* **1986**, *108*, 3711.

88. Ref. 55.

89. Stewart, R. in "Oxidation in Organic Chemistry", Part A; Wilberg, K. B., Ed.; Academic Press: New York, 1971, Chapter 1.

90. Lee, D. G.; Van den Engh, M. in "Oxidation in Organic Chemistry", Part B; Trahanovsky, W. S., Ed.: Academic Press, New York, 1973, Chapter 4.

91. Schröder, M. *Chem. Rev.* **1980**, *80*, 187.

92. Trofimensko, S. *Chem. Rev.* **1972**, *72*, 497.

93. (a) Trofimenko, S. *J. Am. Chem. Soc.*, **1967**, *89*, 3170. (b) Rheingold, A. L.; Ostrander, R. L.; Haggerty, B. S. and Trofimenko, S. *Inorg. Chem.* **1994**, *33*, 3666.

94. Eliel, E. L. "Stereochemistry of Carbon Compounds", 1962, McGraw-Hill Book Company, p.124.

95. (a) Mihailovic, M. LJ. " Osnovi Teoriske Organske Hemije i Stereohemije", Gradeviska Knjiga, 4 izdanje, p. 204. (b) Kistiakowsky, G. B. and Smith, W. R. *J. Am. Chem. Soc.* , **1936**, *58*, 1043.

96. Braude, E. A.; Sondheimer, F. and Forbes, W. F. *Nature*, **1954**, *173*, 117.

97. O'Shaughnessy, M. T.; Rodebush, W. H. *J. Am. Chem. Soc* **1940**, *62*, 2906.

98. Shriver D.; Atkins P. in "Inorganic Chemistry" 3rd Ed.; W. H. Freeman and Company: New York, 2003; p. 452.

99. Christie, G.H. and Kenner, J. *J. Chem. Soc.* **1922**, *121*, 614.

100. Eliel, E. E.; Wilen, S. H.; Mander, L. N. "Stereochemistry of Organic Compounds", 1994; John Wiley & Sons, INC; p. 1119.

101 (a) Curtis, M. D.; Shiu, K. B.; Butler, W. M. *J. Am. Chem. Soc.* **1986**, *108*, 1550. (b) Trofimenko, S. *Inorg. Synth.* **1970**, *12*, 99.

102. (a) Niedenzu, P. M. Niedenzu; K. R. Warner, *Inorg. Chem.* **1985**, *24*, 1604. (b) Trofimenko, S.; Calabrese, J. C.; Domaille, P.J.; Thompson, J. S. *Inorg. Chem.* **1989**, *28*, 1091. (c) Trofimenko, S.; Calabrese, J. C. *Inorg. Chem.* **1992**, *31*, 4810. (d) Trofimenko, S.; Calabrese, J. C.; Kochi, J. K.; Wolowiec, S.; Hulsberg, F. B.; Reedijk, J. *Inorg. Chem.* **1992**, *31*, 3943.

103. (a) Lobbia, G. G.; Valle, G.; Calogero, S.; Cecchi, P.; Santini, C.; Marchetti, F. *J. Chem. Soc., Dalton Trans.* **1996**, 2475. (b) Trofimenko, S. *J. Am. Chem. Soc.* **1967**, *88*, 6288.

104. Ref. 102b. (b) Rheingold, A. L.; Trofimenko, S.; Haggerty, B. S. *J. Chem . Soc., Chem. Commun.* **1994**, 1973.

105. (a) Ref. 103b. (b) Dias, H. V. R.; Lu, H. L.; Ratcliff, R.E.; Bott, S. G. *Inorg. Chem.* **1995**, *34*, 1975. (c) Renn, O.; Venanzi, L. M., Martelleti, A.; Gramlich, V. *Helv. Chim. Acta* **1995**, *78*, 993.

106. (a) Rheingold, A. L.; Haggerty, B. S.; Yap, G. P. A.; Trofimenko, S. *Inorg. Chem.* **1997**, *36*, 5097. (b) Siddiqi, K. S.; Neyazi, M. A.; Tabassum, S. and Zaidi, S. A. A. *Indian J. Chem.* **1991**, *30A*, 724.

107. (a) Ref. 103b. (b) Ref. 106a.

108. (a) Ref. 103b. (b) Reger, D. L.; Tarquini, M. E. *Inorg. Chem.*. **1982**, *21*, 840.

109. (a) Kashima, C.; Shibata, S.; Yokoyama, H.; Nishio, T. *J. Het. Chem.* **2003**, *40*, 773. (b) Luigi, S.; Lambert, S.; Pirard, J. P.; Noels, A. F. *Synthesis* **2004**, *5*, 663-664.

110. Trofimenko, S. *J. Am. Chem. Soc.*, **1967**, *89*, 3170.

111. See references for Scheme 1.13.

112. Crews, P.; Rodriguez, J.; M. Jaspars "Organic Structure Analysis", 1998, Oxford University Press.

113. "Spectroscopic Methods in Organic Chemistry" Hesse, M.; Meier, H.; Zeeh, B., Georg Thieme Verlag: Stuggart, 1997; p. 99.

114. (a) Sandstrom, J. "Dynamic NMR Spectroscopy"; Academic Press; 1982. (b) Friebolin, H. "Basic One and Two Dimensional NMR Spectroscopy" 3rd Edition, Willey-VCH, 1998; p. 313.

115. Ref. 71.

116. Karplus, M. *J. Am. Chem. Soc.*, **1963**, *85*, 2870.

117. Gunther, H. "NMR Spectroscopy" John Wiley & Sons, 1973, p. 106.

118. Haasnoot, C. A. G.; De Leeuw, F. A. A. M.; Altona, C. *Tetrahedron* **1980**, *36*, 2783.

119. Acorn NMR Inc., 1997.

120. Ref. 118.

121. (a) Theilacker, W.; Bohm, H. *Angew. Chem., Int. Ed.* **1967**, *9*, 251.
(b) Mullen, K.; Heinz, W.; Klarrner, F. G.; Roth, W. R.; Kindermann, I.; Adamczak, O.; Wette, M. and Lex, J. *Chem. Ber.* **1990**, *123*, 2349.

122. Grein, F. *J.Phys Chem A*, **2002**, *106*, 3823.

123. Hegedus, L. S. in "Transition Metals in the Synthesis of Complex Organic Molecules", 1994, University Science Books; p. 183.

124. Pfaltz, A. Chapter 16 in "Comprehensive Asymmetric Catalysis" Jacobsen, E. N; Pfaltz, A. & Yamamoto, H., 1999, Springer-Verlag.

125. LeCloux, D. D.; Tokar, Ch. J.; Osawa, M.; Houser, R. P.; Keyes, M. C. and Tolman, W. B. *Organometallics*, **1994**, *13*, 2855.

126. (a) Personal communication with Prof. Brunner, Prof. Tolman and Prof. Singh. (b) Ref. 8 in Tokar, C. J.; Kettler, P. B. and Tolman, W. B. *Organometallics* **1992**, *11*, 2737. Note: Herein Tolman explicitly notes the failure to prepare **34**. On the other hand, Singh et. al. reports (Ref. 128) preparation and use of **34.**

127. (a) 126b. (b) Personal communication with Prof. Tolman.

128. (a) Babbar, P.; Brunner; H.; Singh, U.P. *Indian J. of Chem.*, **2001**, *40A*, 225. (b) Babbar, P.; Brunner; H.; Singh, U.P.; Hassler, B.; Nishiyama, H. *J. Mol. Cat. A*: *Chemical* **2002**, *185*, 33.

129. Ref. 127.

130. Ref. 128.

131. Brunner, H.; Singh, U. P.; Boeck, Th.; Altmann, S.; Scheck, Th.; Wrackmeyer, B. *J. Organomet. Chem.* **1993**, *443*, C16-C18.

132. Ref. 131.

133. Ref. 83a.

134. "The Manipulation of Air-Sensitive Compounds" Shriver, D. F.; Drezdon, M. A., Wiley: New York, 1986.

135. Perrin, D. D.; Armarego, W. L. F. "Purification of Laboratory Chemical", 3rd ed.; Butterworth-Heinemann: Oxford, U.K., 1988.

136. (a) Ref. 125. (b) Garbisch, E. W. *J. Am. Chem. Soc.* **1963**, *85*, 1696. (c) Singh, U. P.; Babbar, P.; Hassler, B.; Nishiyama, H.; Brunner, H. *J. Mol. Cat. A: Chemical* **2002**, *185*, 33. (d) Ref. 128. (f) Lintvedt, R. L.; Fatta,

A. M. *Inorg. Chem* **1968**, *12*, 2489. (g) *Inorg. Synth.* **1998**, vol. 32, pp51-63, and in particular pp. 55-57.

137. Ref. 128.

138. (a) Potapov, V. M.; Kiryushkina, G. V.; Talebarovakaya, I. L; Shapet'ko, N. N.; Radushnova, I.L. *Zh.Org. Khim* **1973**, *9*, 2134. (b) Ref. 125. (c) Bovens, M.; Tagni, A.; L. M. Venanzi *J. Organomet. Chem.* **1993**, *451*, 28. (d) Kashima, C.; Fukuchi, I.; Hosumi, A. *J. Org. Chem.* **1994**, *59*, 7821. (e) LeCloux, D. D; Keyes, M. C.; Osawa, M. V.; Tolman, W. B. *Inorg. Chem.* **1994**, *33*, 6361 (g) LeCloux, D. D; Tolman, W. B. *J. Am. Chem. Soc* **1993**, *115*, 1153.

139. The product is a thick oil that clogs the condenser. When this happens, a heat gun was used to push down the product. Original literature sources: (a) Faure, A.; Frideling, J. P.; Galy, I.; Elguero, J. *Heterocycles* **2002**, *57*, 307 uses acetylation of the pyrazole, followed by Flash Chromatogaphy, and (b) uses fractional crystallization (Ref. 125) to separate cis and trans isomers. We tried both and none worked out. The b.p difference between cis and trans isomers is about 15 °C and suffices to use fractional distillation to separate the out.

140. Mutano, Y.; Northcutt, T. O.; Brugman, J.; Bennett, B. K.; Lovell, S.; Mayer, J. M. *Organometallics* **2000**, *19*, 2781.

141. (a) Ref. 69b. (b) . Gable, K. P. *Organometallics* **1994**, *13*, 2486.

142. This is the most effective methods for solvent degassing. A solvent in a sealed Schlenk or heavy wall sealed tube is frozen by immersion of the flask in liquid N_2. When the solvent is completely frozen, the flask is opened to the vacuum (high vacuum) and pumped 2-3 minutes, with the flask still immersed in liquid N_2. The flask is then closed and warmed until the solvent has completely melted. This process is repeated (usually three times) and after the last cycle the flask is backfilled with an inert gas or sealed under vacuum. Degassed solvent in a sealed Schlenk flask can usually be kept for 1-2 days.

143. This borate hydrolyses with time and should be used as soon as possible or stored under dry conditions.

144. See the references for preparation of (3S, 6R)-3-isopropyl-6-methyl-2-oxocyclohexanecarbaldehyde

145. Failure to use the mechanical stirrer led to premature ending of the reaction by clogging of the reaction mixture.

146. See references for preparation of (4R,7R)-4,5,6,7-tetrahydro-7-isopropyl-4-methyl-2H-indazole

147. Mutano, Y.; Northcutt, T. O.; Brugman, J.; Bennett, B. K.; Lovell, S.; Mayer, J. M. *Organometallics* **2000**, *19*, 2781.

148. MeOH washes away CF_3COOK; using water for this purpose was a detriment, giving a black sticky unidentified compound.

149. (a) Ref. 141a (b) Ref. 141b.

150. A white solid was always littering the diolate. We believe this is rhenium(III) oxide.

151. Jaguar, v. 4.1. Schrödinger, Inc., Portland, OR.

152. Hay, P. J.; Wadt, W. R. *J. Chem. Phys.* **1985**, *82*, 299.

Appendix
Spectroscopic data

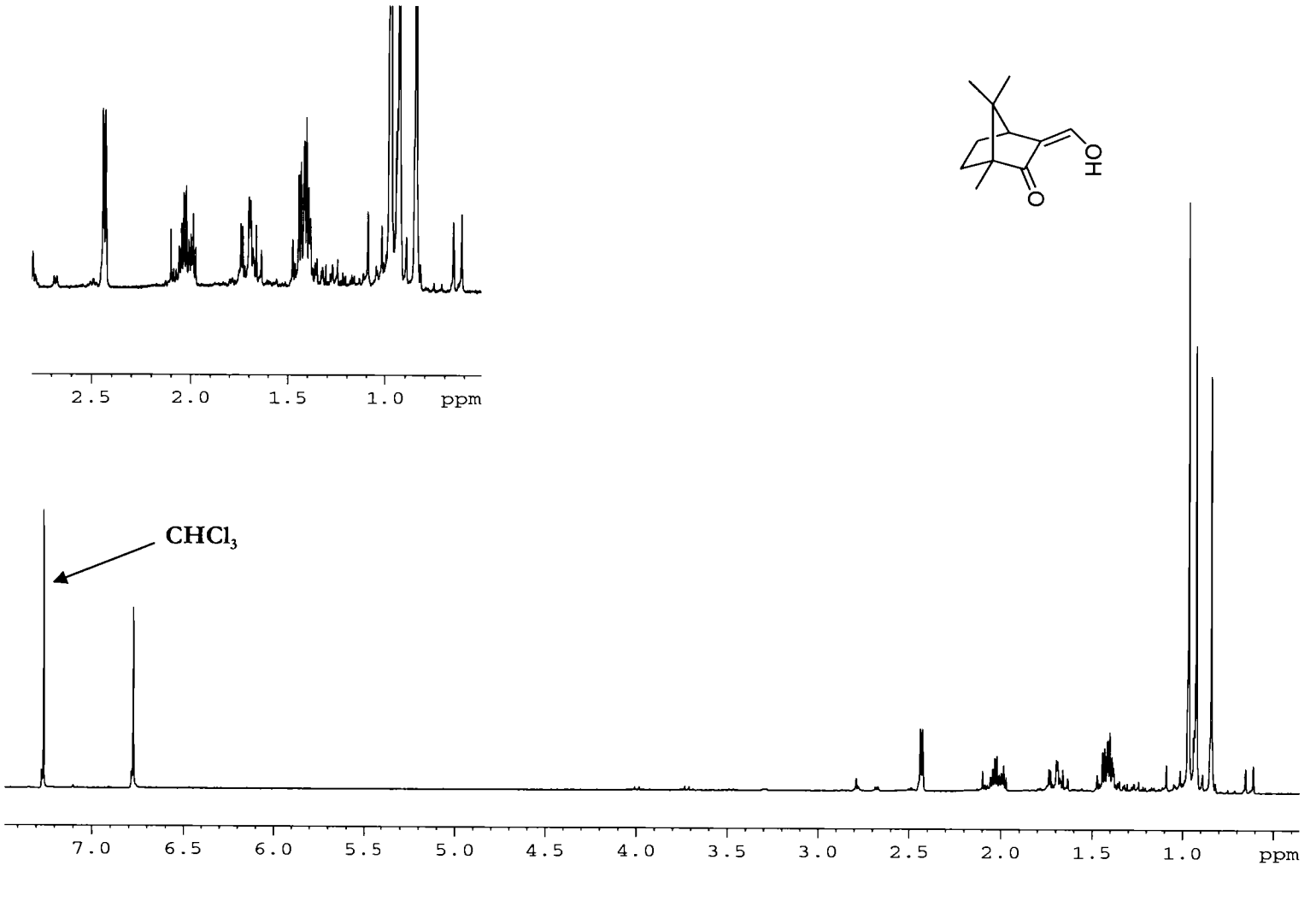
OH
O
2.5
2.0
1.5
1.0
ppm
CHCl3
7.0
6.5
6.0
5.5
5.0
4.5
4.0
3.5
3.0
2.5
2.0
1.5
1.0
ppm

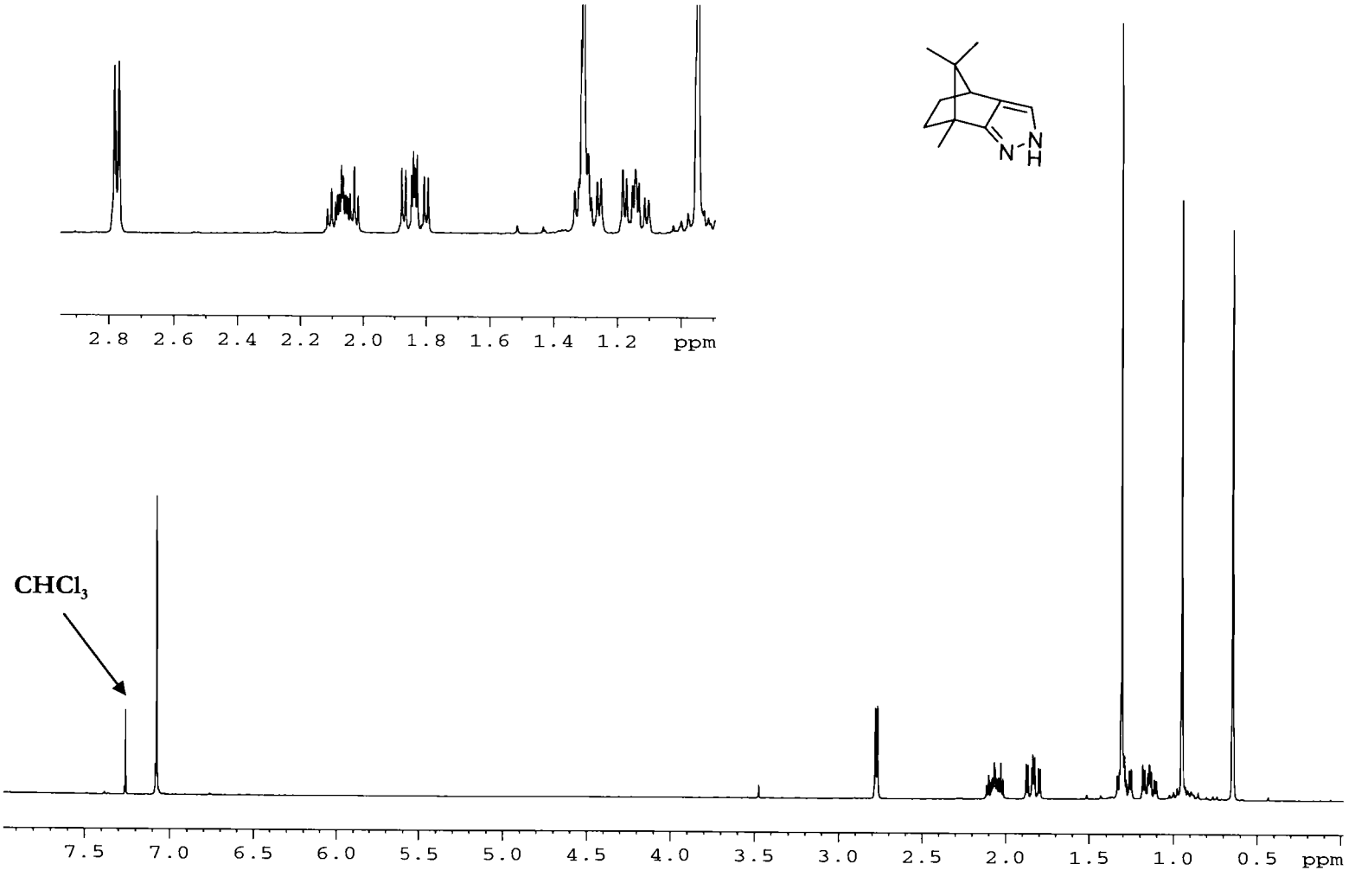
2.8 2.6 2.4 2.2 2.0 1.8 1.6 1.4 1.2 ppm
N
N
H
CHCl3
7.5 7.0 6.5 6.0 5.5 5.0 4.5 4.0 3.5 3.0 2.5 2.0 1.5 1.0 0.5 ppm

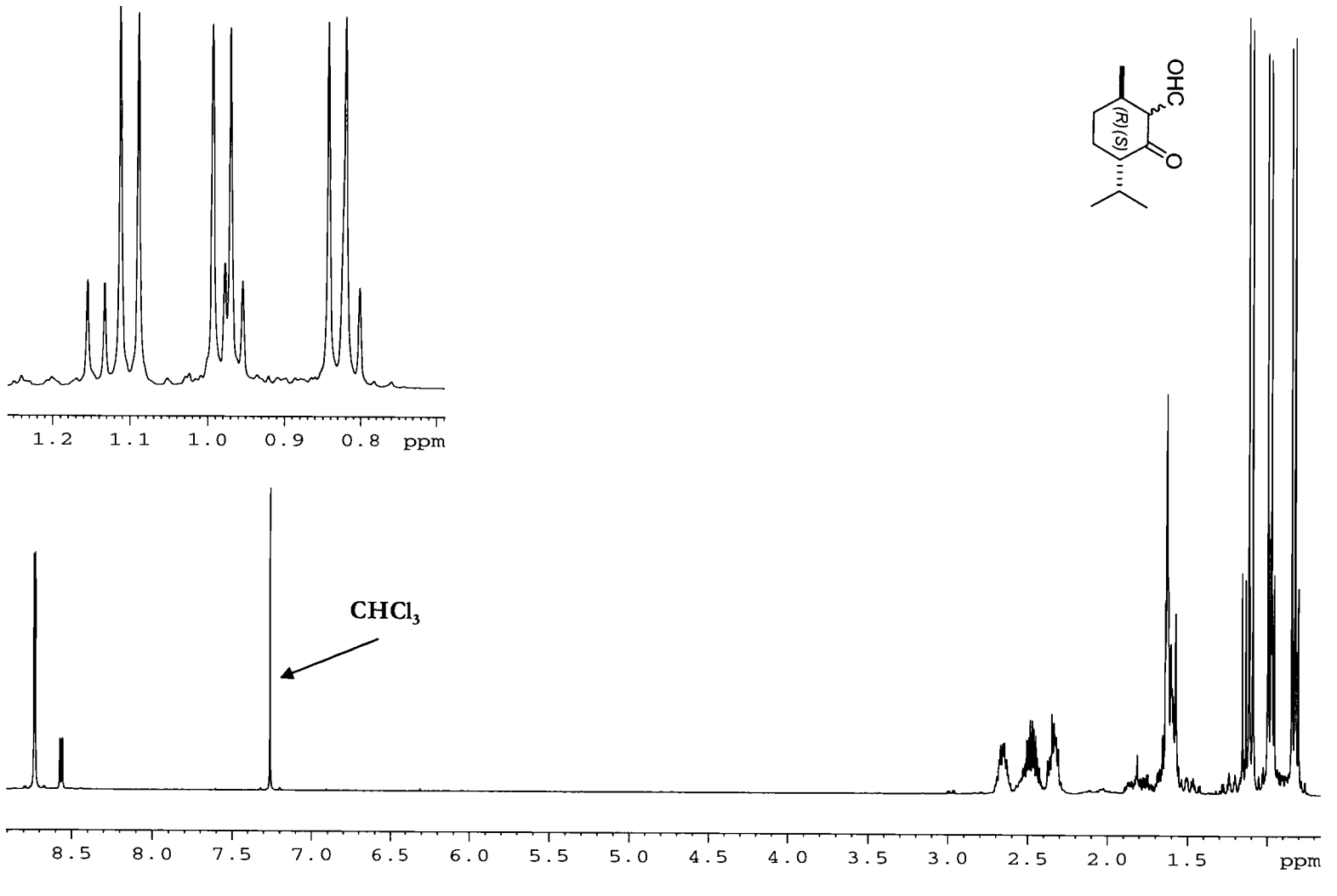
OHC
(R)(S)
O
1.2 1.1 1.0 0.9 0.8 ppm
CHCl3
8.5 8.0 7.5 7.0 6.5 6.0 5.5 5.0 4.5 4.0 3.5 3.0 2.5 2.0 1.5 ppm

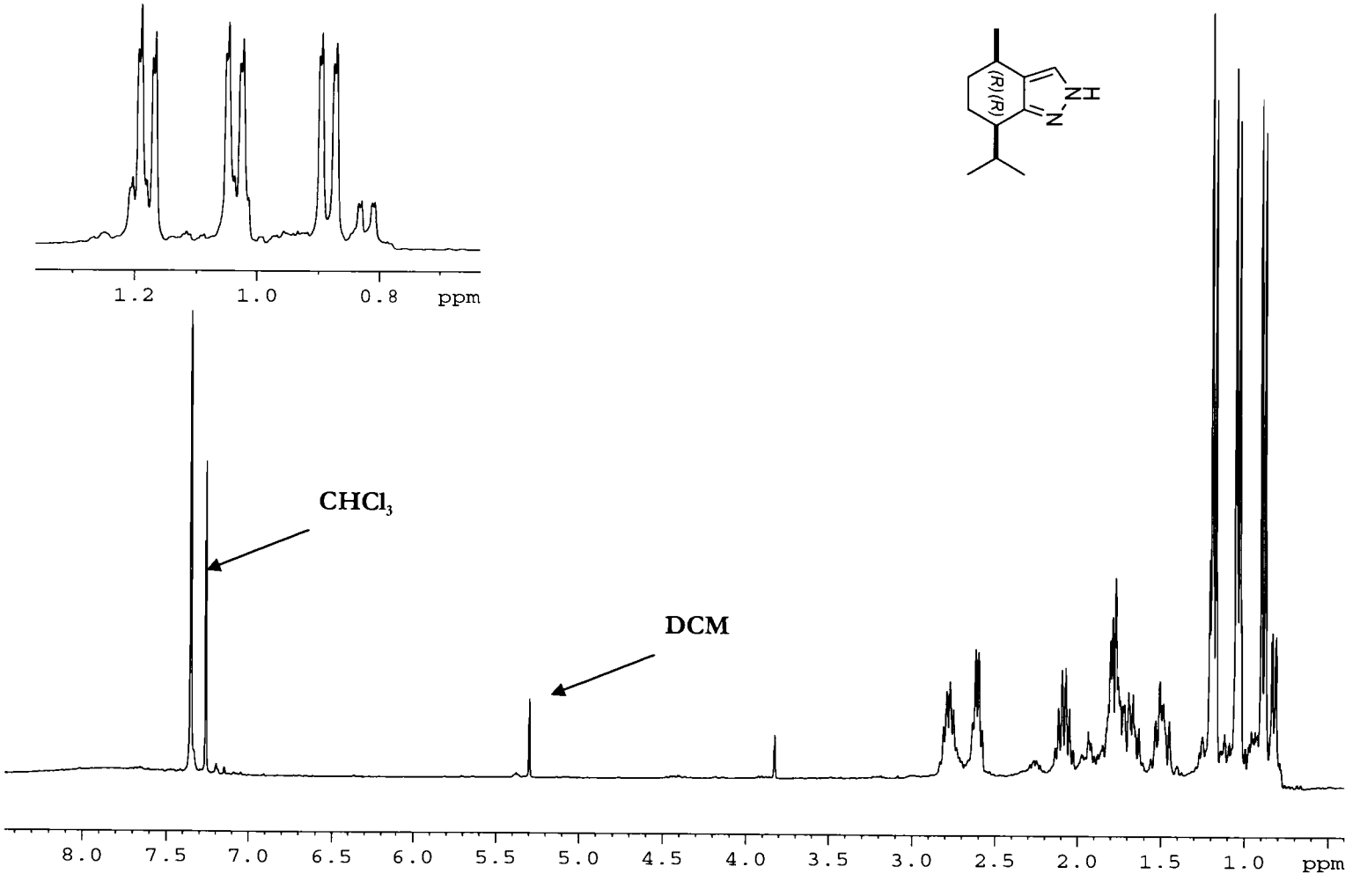
1.2
1.0
0.8
ppm
(R)(R)
NH
N
CHCl3
DCM
8.0
7.5
7.0
6.5
6.0
5.5
5.0
4.5
4.0
3.5
3.0
2.5
2.0
1.5
1.0
ppm

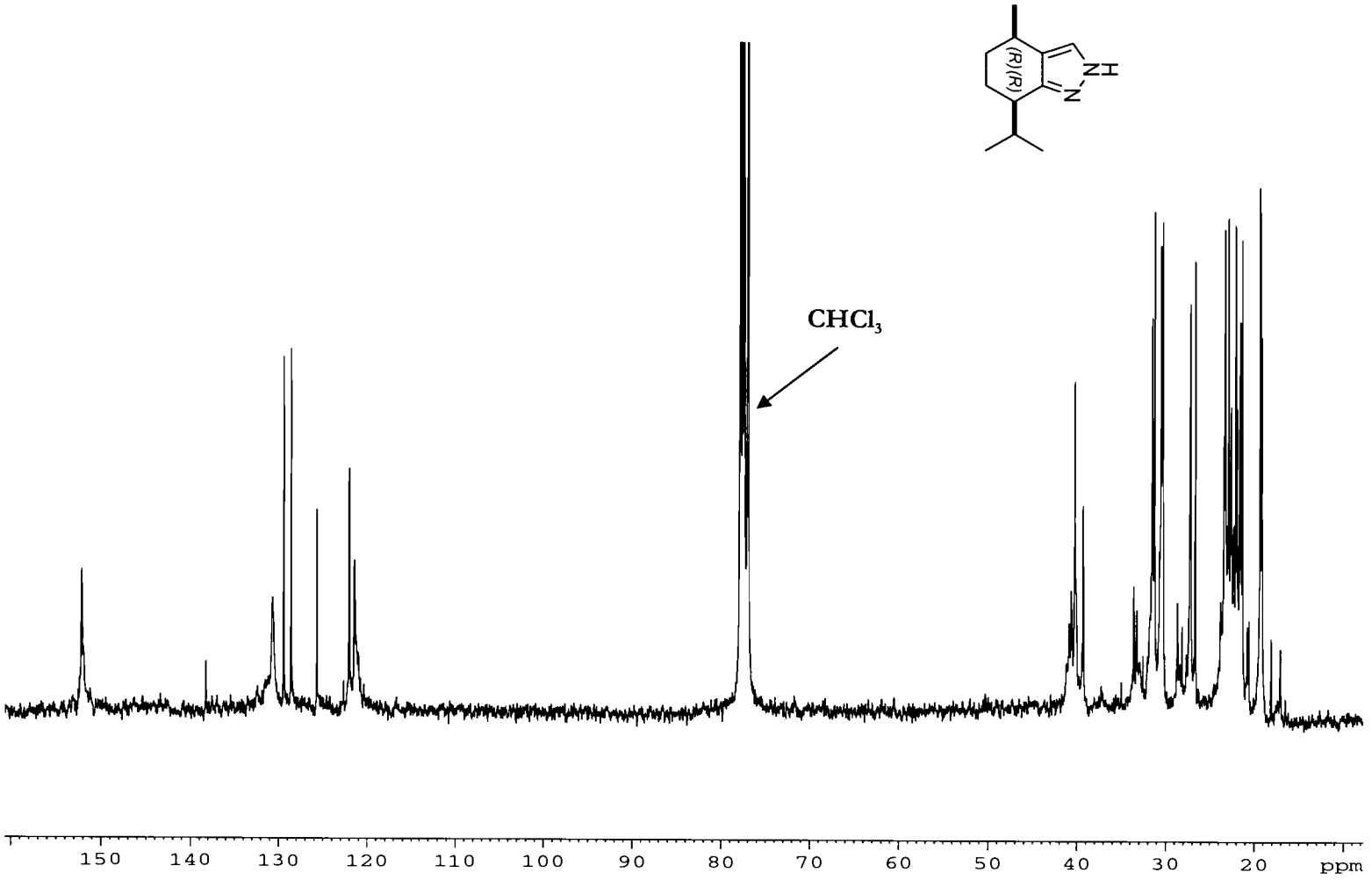
(R)(R)
NH
N
CHCl3
150
140
130
120
110
100
90
80
70
60
50
40
30
20
ppm

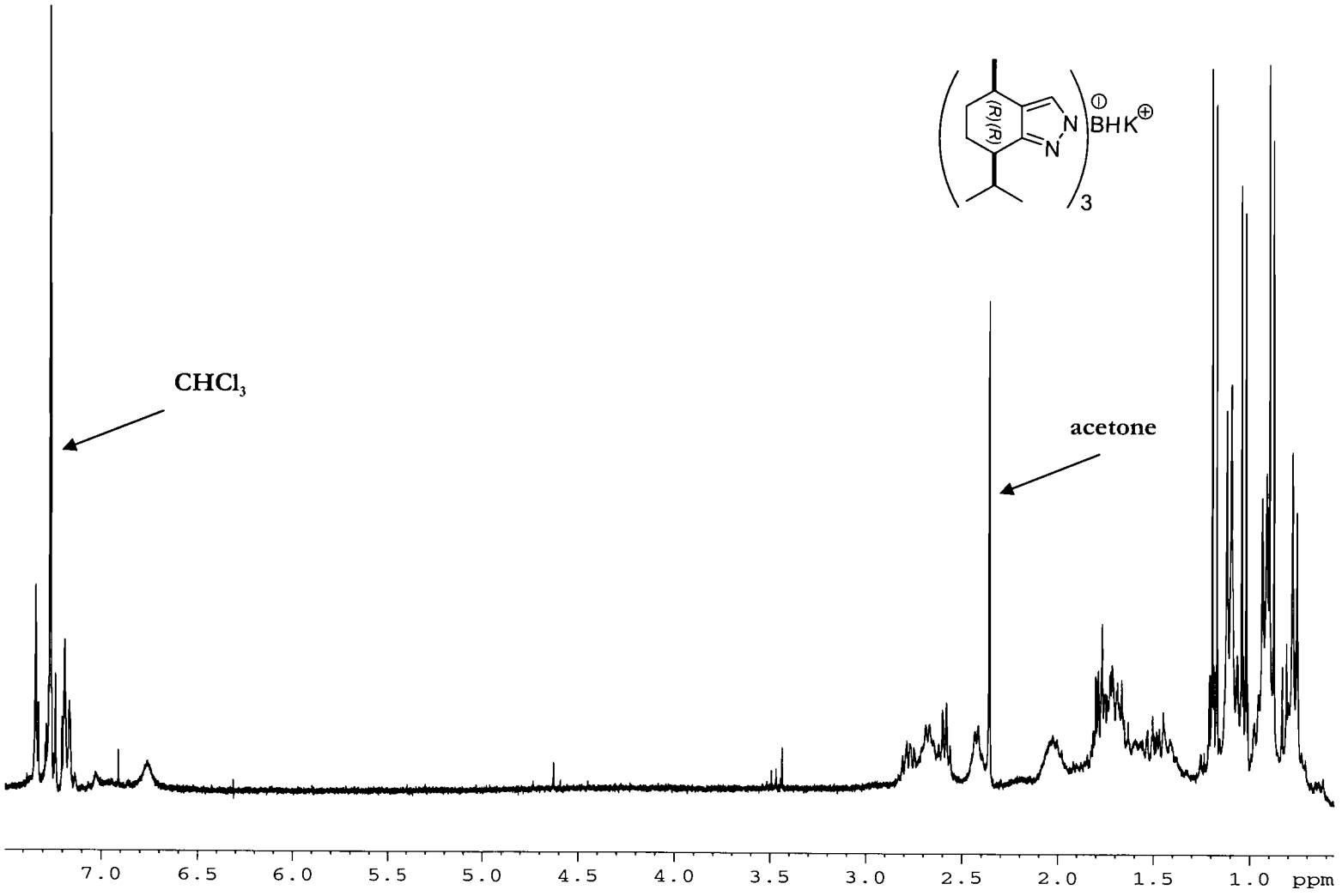
CHCl3
acetone
(R)(R)
N
N
BHK
3
7.0
6.5
6.0
5.5
5.0
4.5
4.0
3.5
3.0
2.5
2.0
1.5
1.0
ppm

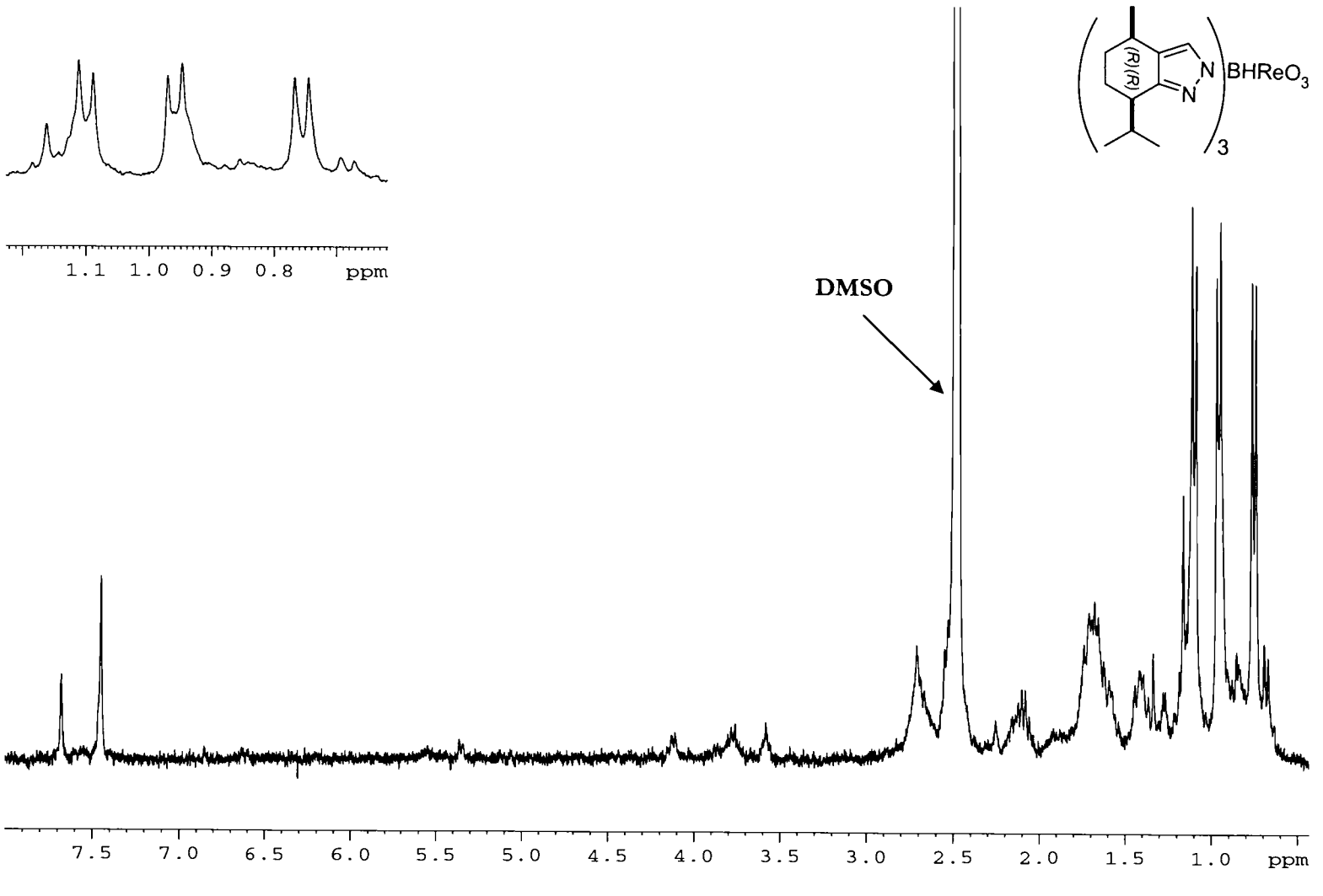
1.1 1.0 0.9 0.8 ppm
DMSO
(R)(R)
N
N
BHReO3
3
7.5 7.0 6.5 6.0 5.5 5.0 4.5 4.0 3.5 3.0 2.5 2.0 1.5 1.0 ppm

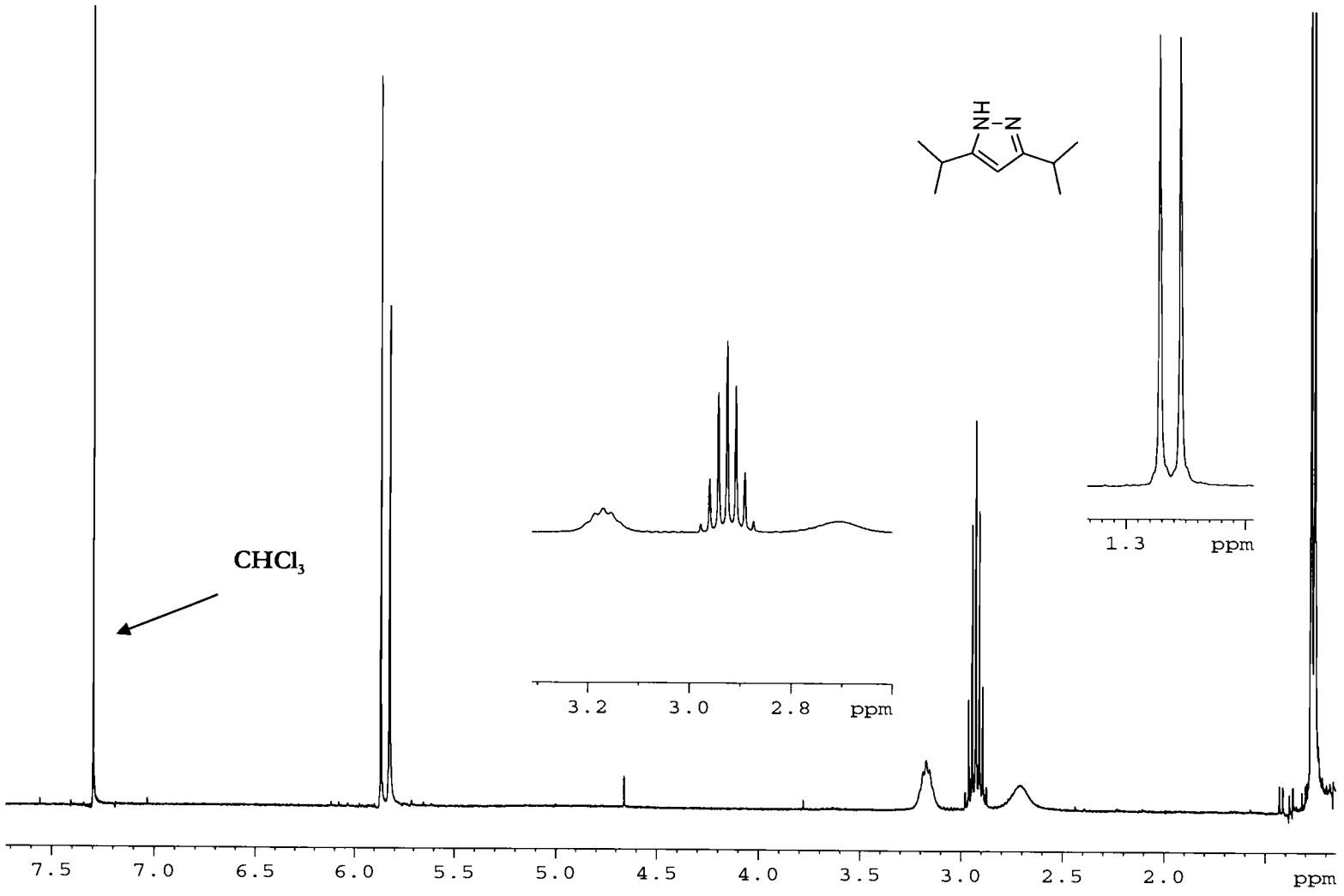
CHCl3
3.2
3.0
2.8
ppm
1.3
ppm
7.5
7.0
6.5
6.0
5.5
5.0
4.5
4.0
3.5
3.0
2.5
2.0
ppm

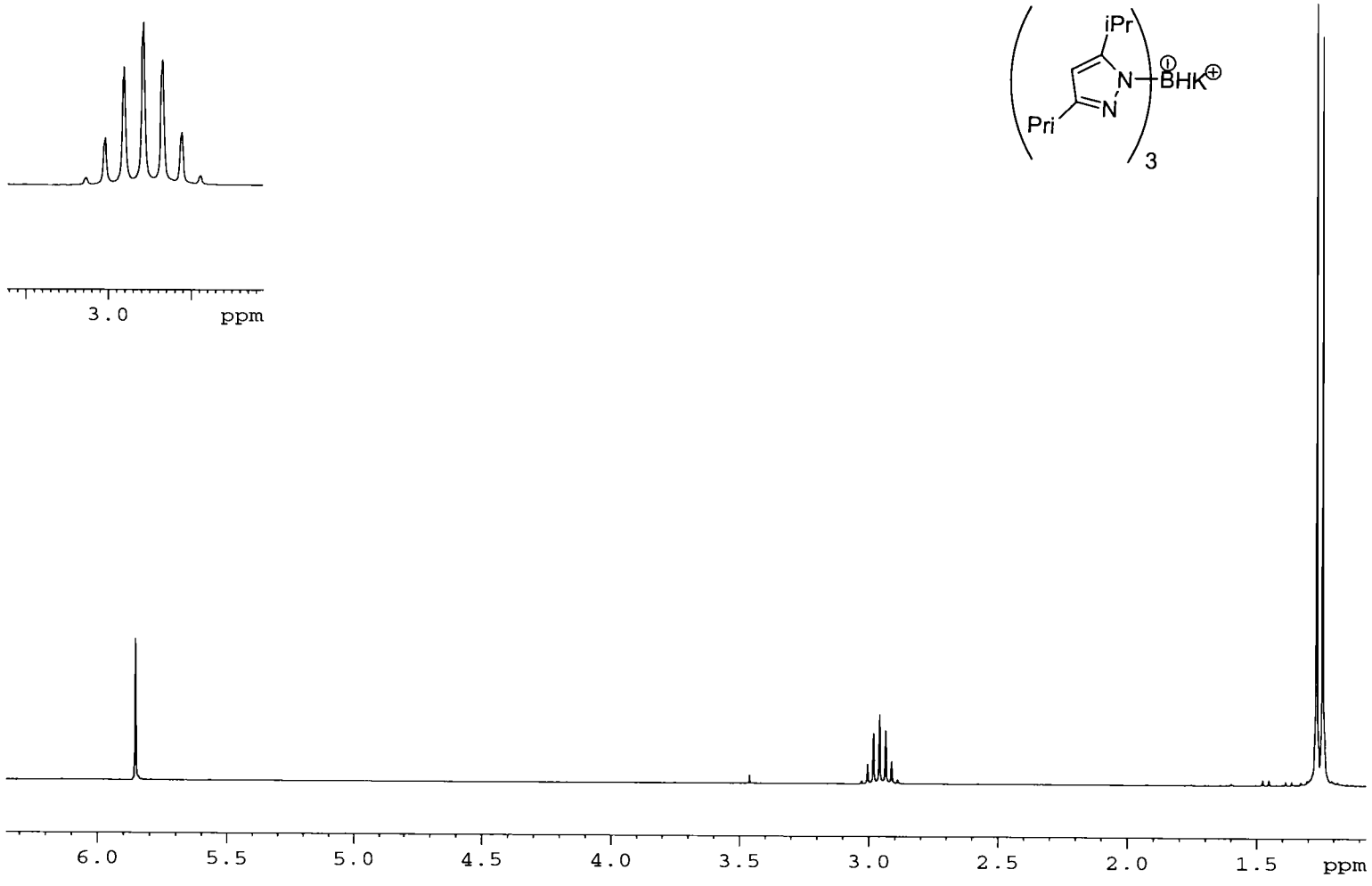
iPr
N
BHK
N
Pri
3
3.0
ppm
6.0
5.5
5.0
4.5
4.0
3.5
3.0
2.5
2.0
1.5
ppm

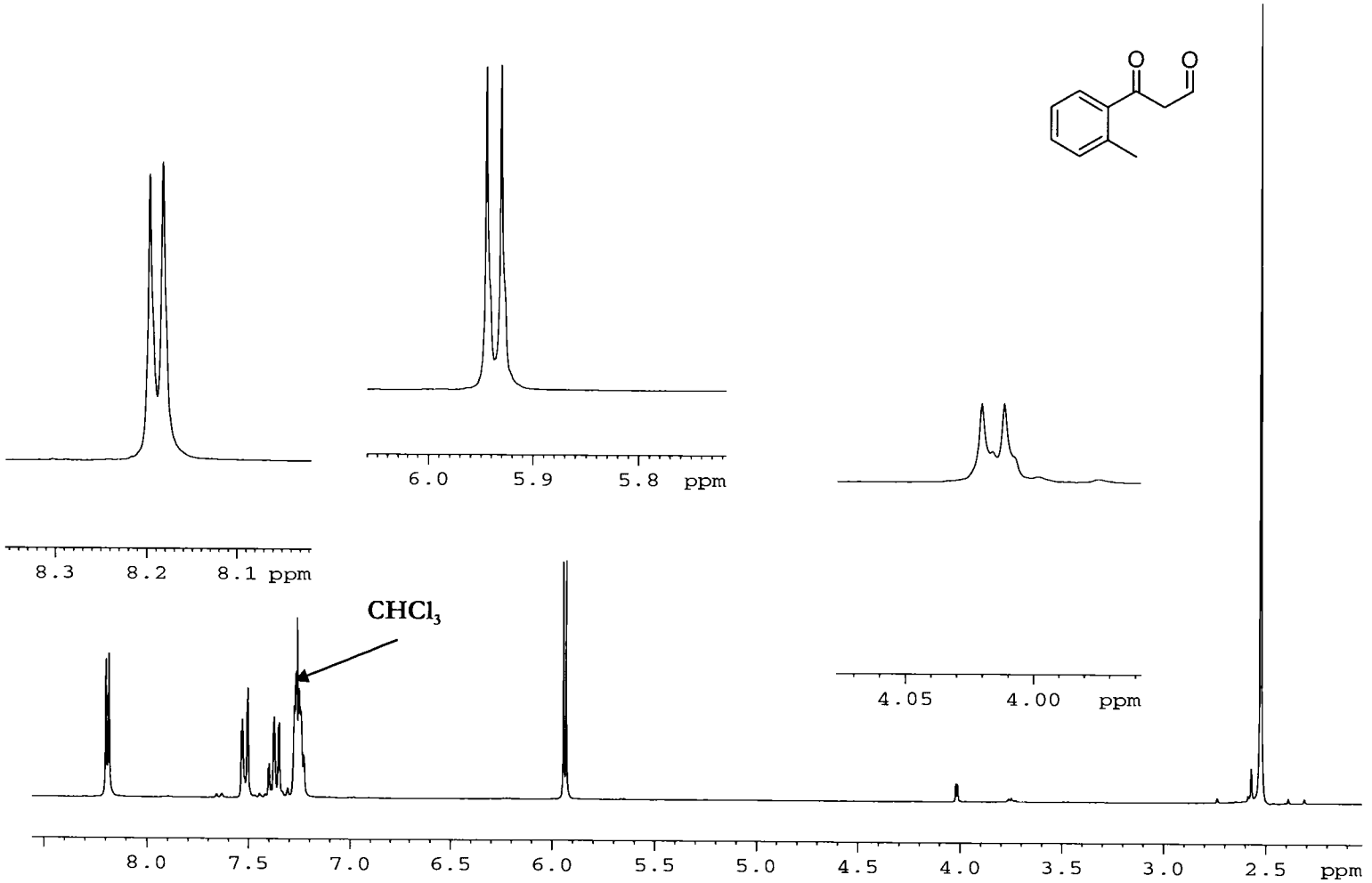
O
O
6.0
5.9
5.8 ppm
8.3
8.2
8.1 ppm
CHCl3
4.05
4.00 ppm
8.0
7.5
7.0
6.5
6.0
5.5
5.0
4.5
4.0
3.5
3.0
2.5 ppm

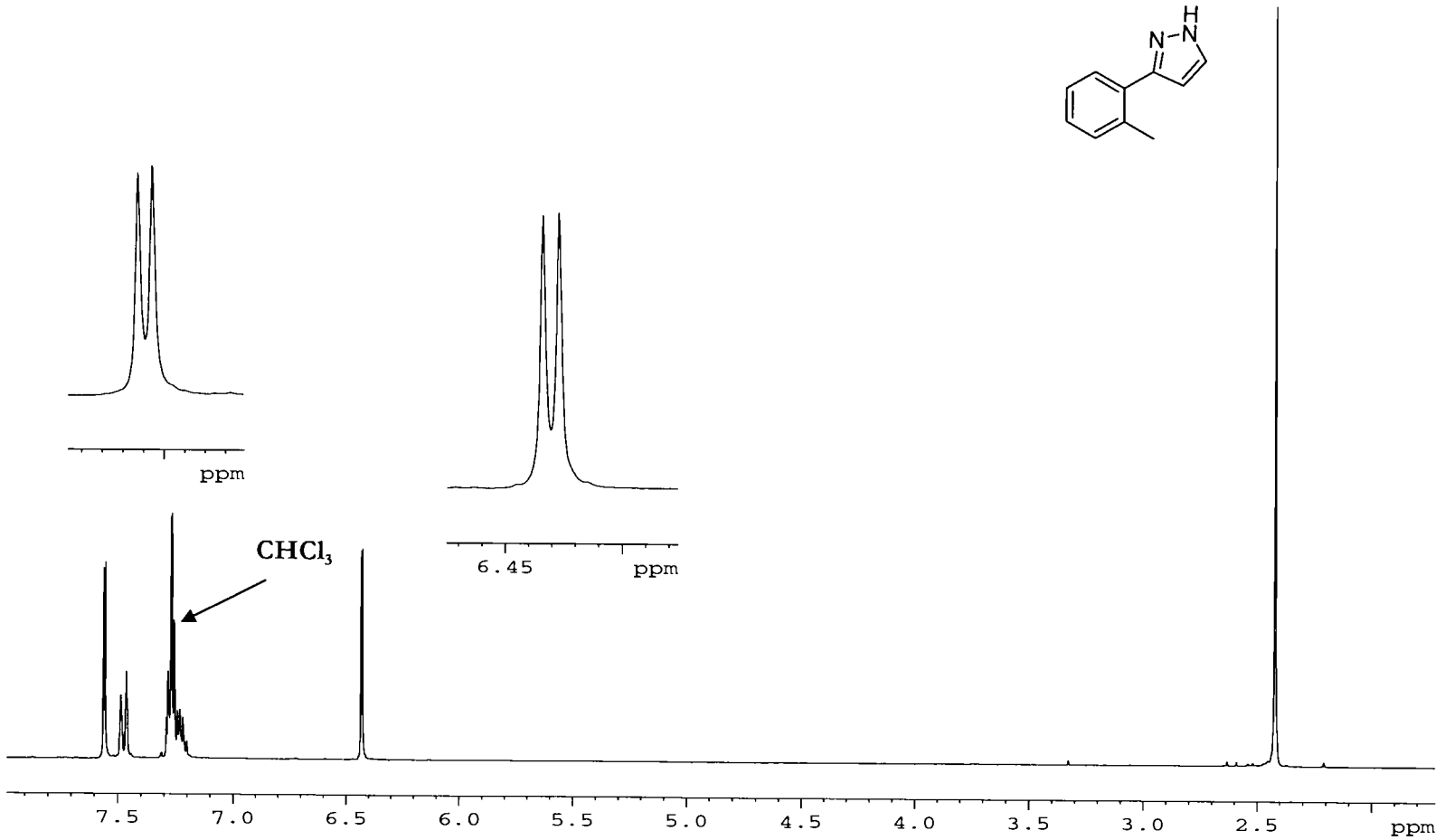
H
N
N
ppm
6.45
ppm
CHCl3
7.5
7.0
6.5
6.0
5.5
5.0
4.5
4.0
3.5
3.0
2.5
ppm

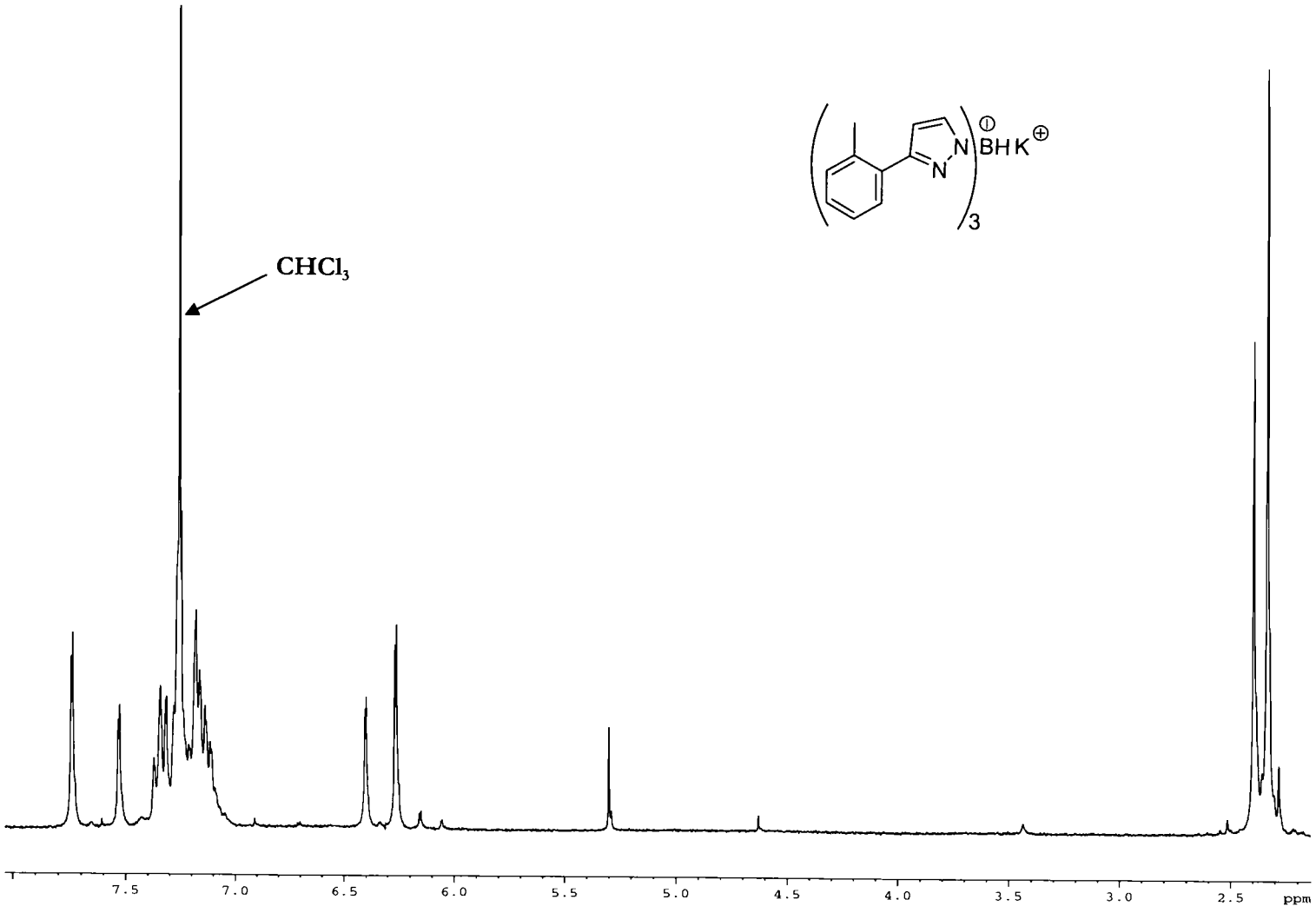
CHCl3
BHK
3
7.5
7.0
6.5
6.0
5.5
5.0
4.5
4.0
3.5
3.0
2.5
ppm

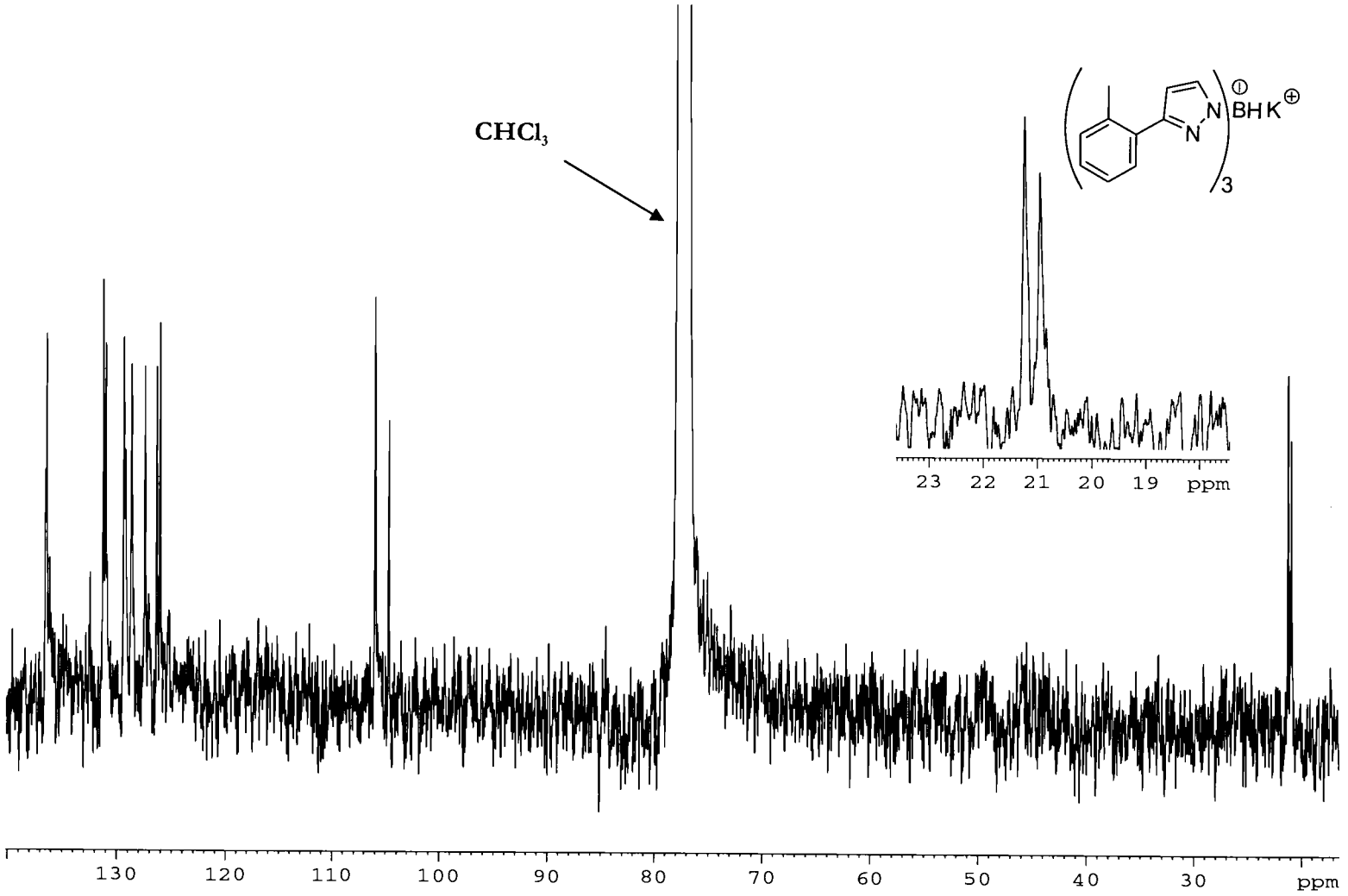
CHCl3
BHK
3
23 22 21 20 19 ppm
130 120 110 100 90 80 70 60 50 40 30 ppm

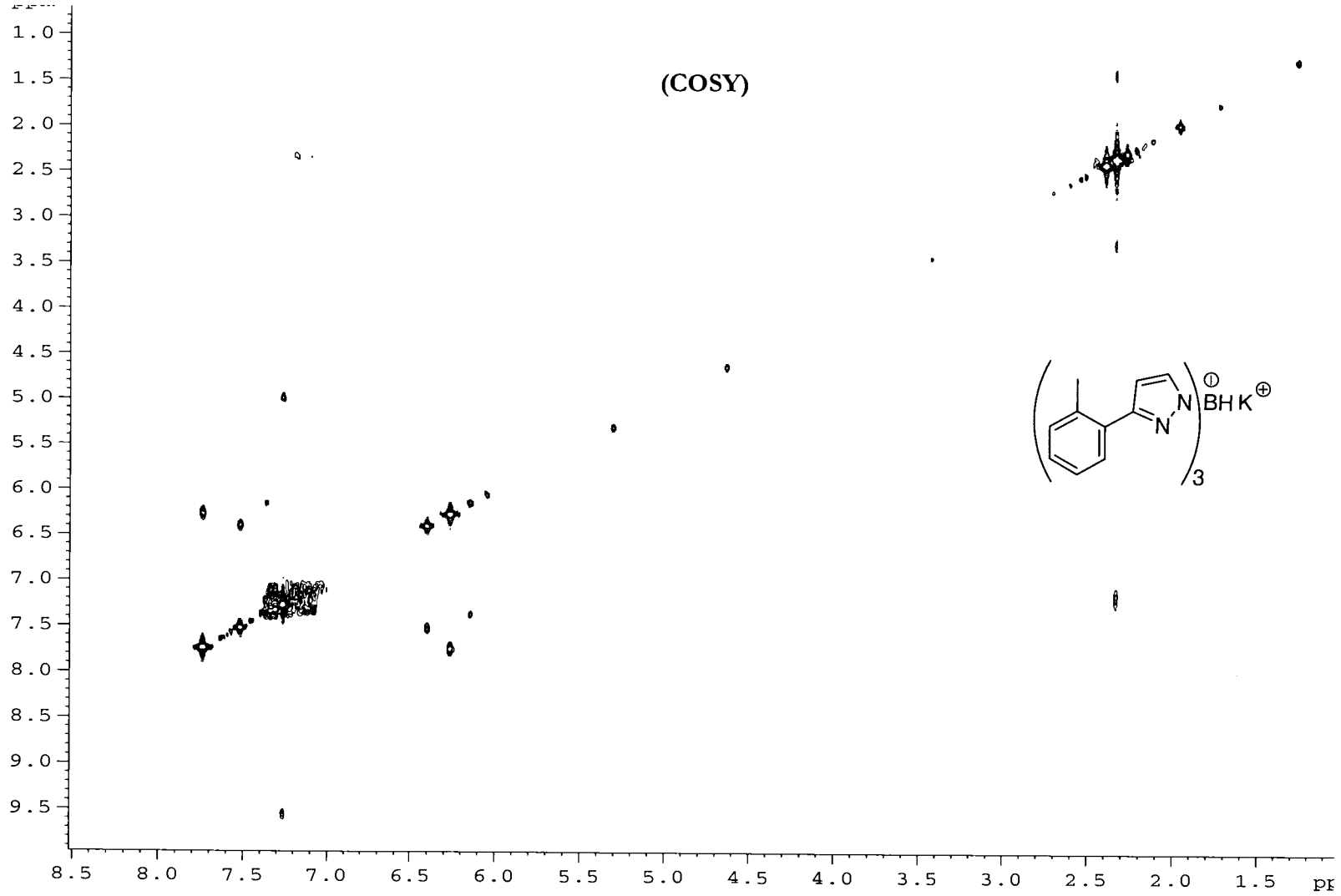
(COSY)
1.0
1.5
2.0
2.5
3.0
3.5
4.0
4.5
5.0
5.5
6.0
6.5
7.0
7.5
8.0
8.5
9.0
9.5
8.5
8.0
7.5
7.0
6.5
6.0
5.5
5.0
4.5
4.0
3.5
3.0
2.5
2.0
1.5
pp
N
N
BH
K
3

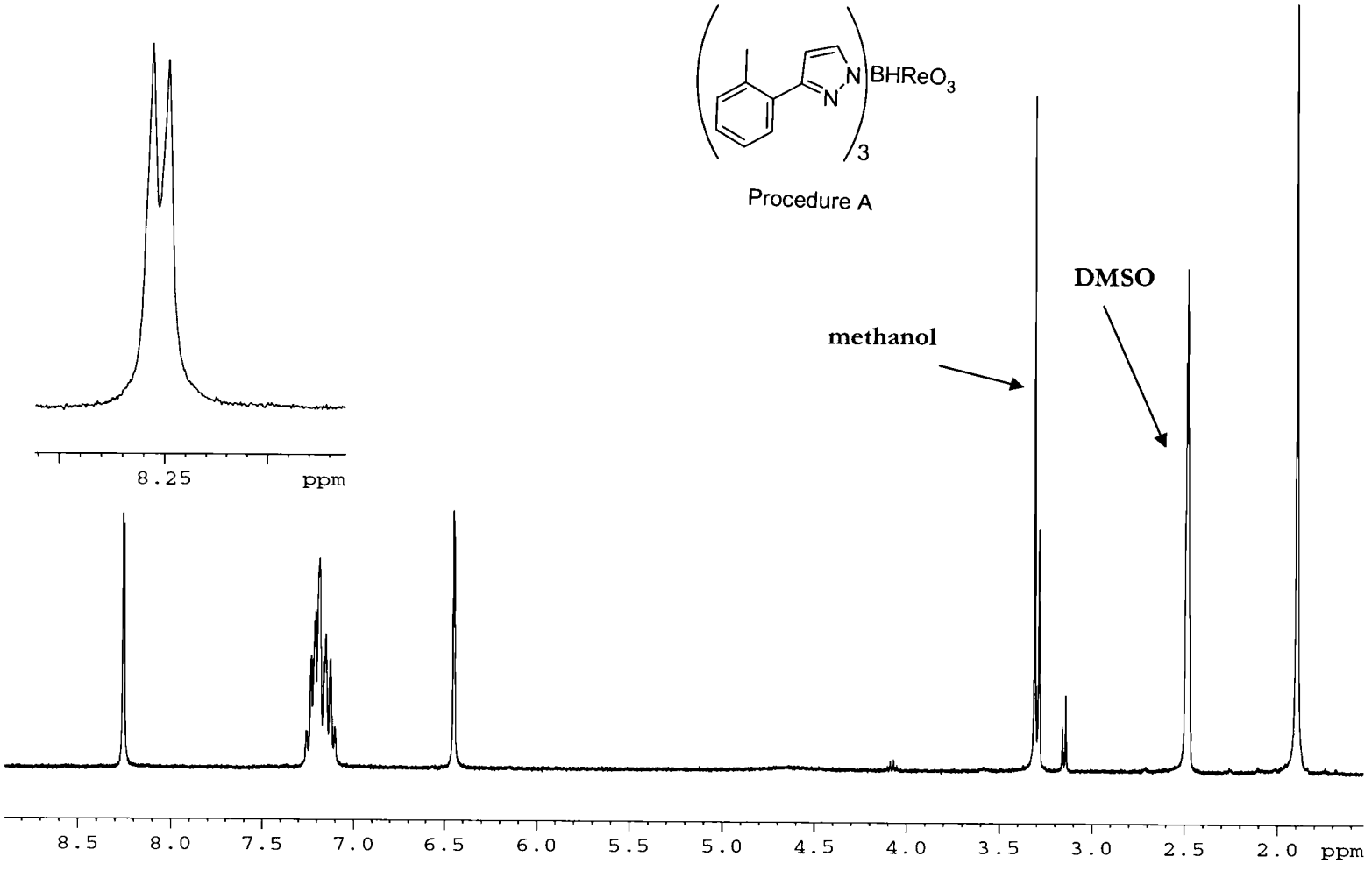
BHReO3
3
Procedure A
DMSO
methanol
8.25
ppm
8.5
8.0
7.5
7.0
6.5
6.0
5.5
5.0
4.5
4.0
3.5
3.0
2.5
2.0
ppm

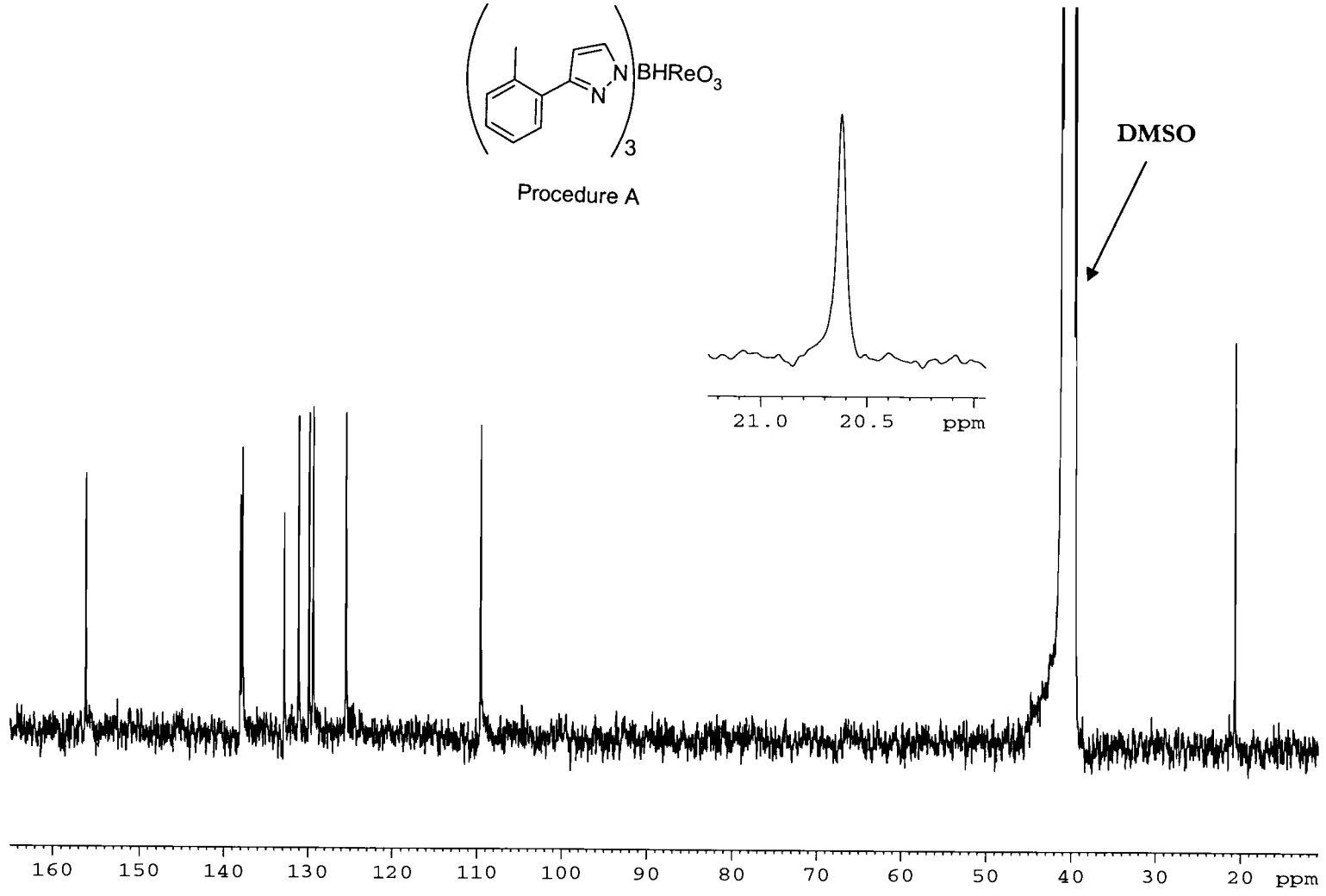
BHReO3
3
Procedure A
DMSO
21.0
20.5
ppm
160
150
140
130
120
110
100
90
80
70
60
50
40
30
20
ppm

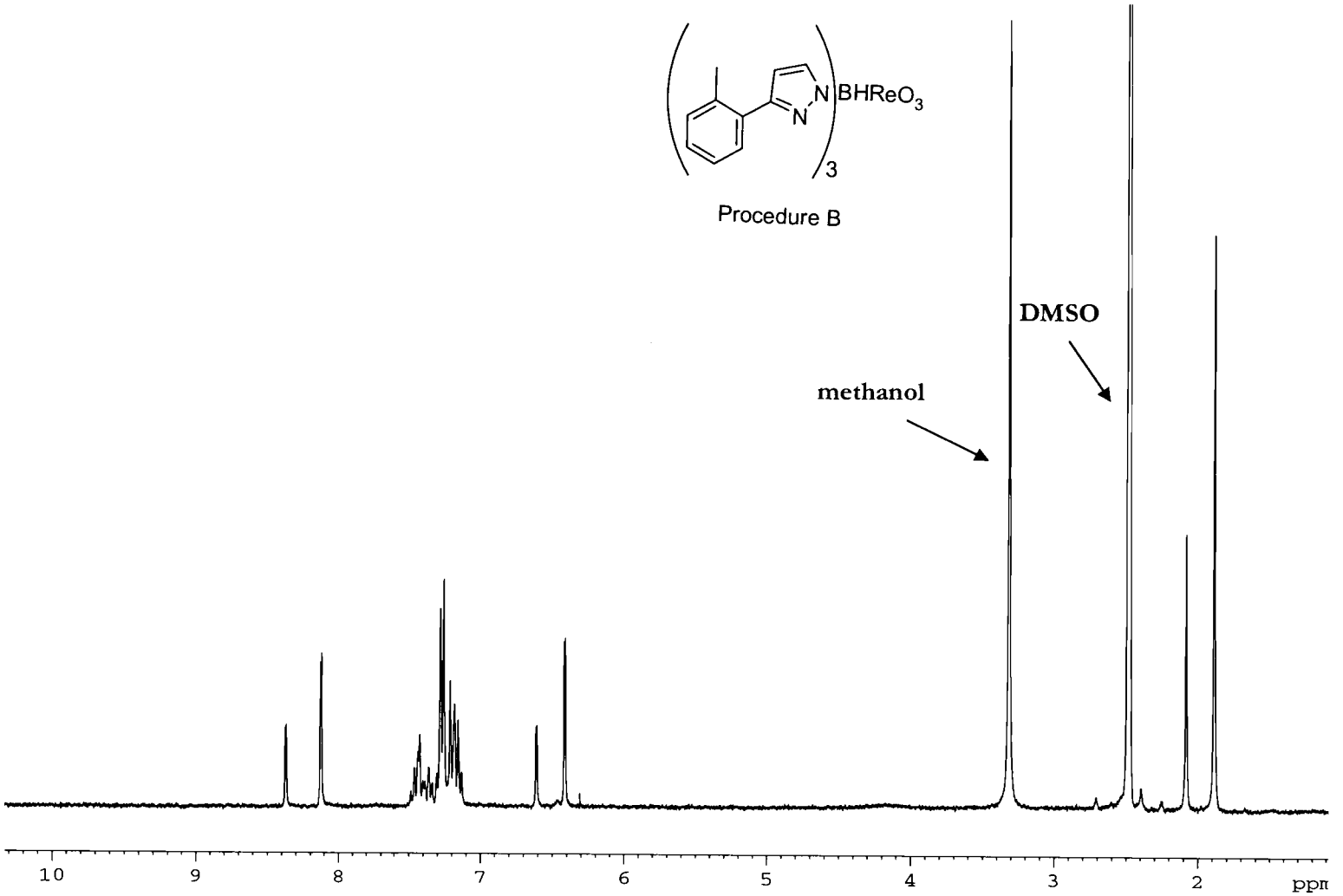
BHReO3
3
Procedure B
DMSO
methanol
10
9
8
7
6
5
4
3
2
ppm

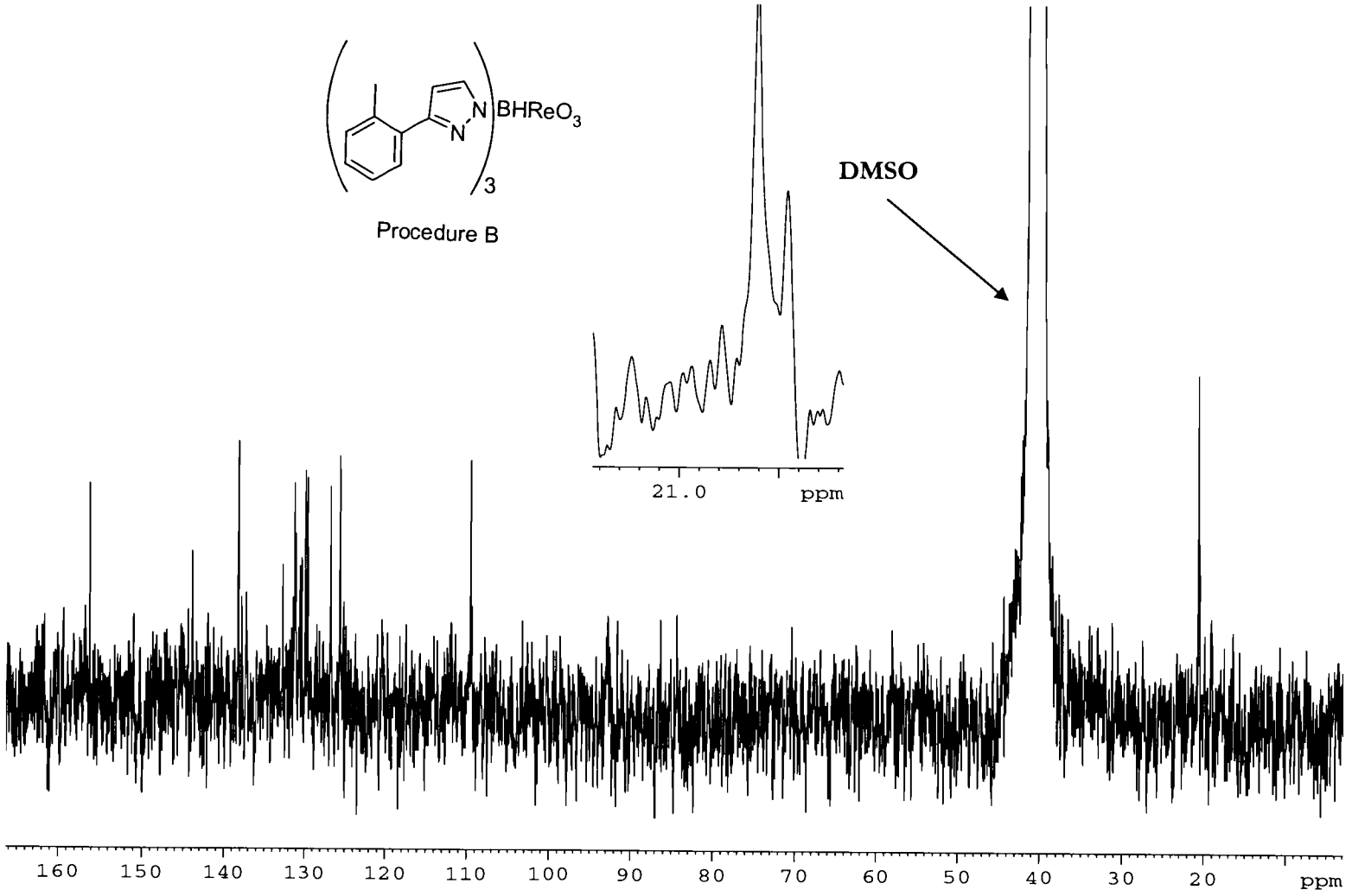
BHReO3
3
Procedure B
DMSO
21.0
ppm
160
150
140
130
120
110
100
90
80
70
60
50
40
30
20
ppm

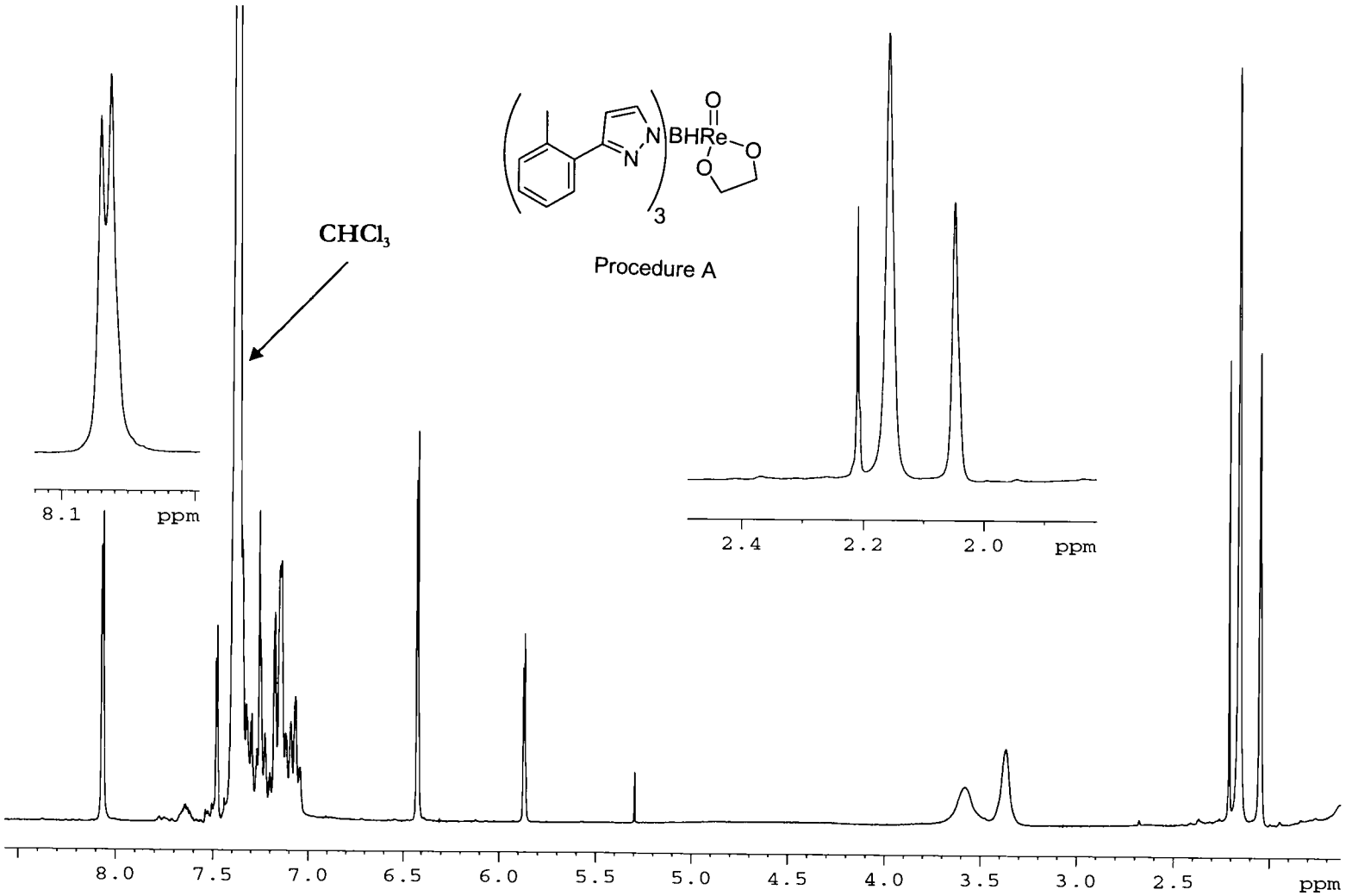
CHCl3
Procedure A
8.1
ppm
2.4
2.2
2.0
ppm
8.0
7.5
7.0
6.5
6.0
5.5
5.0
4.5
4.0
3.5
3.0
2.5
ppm

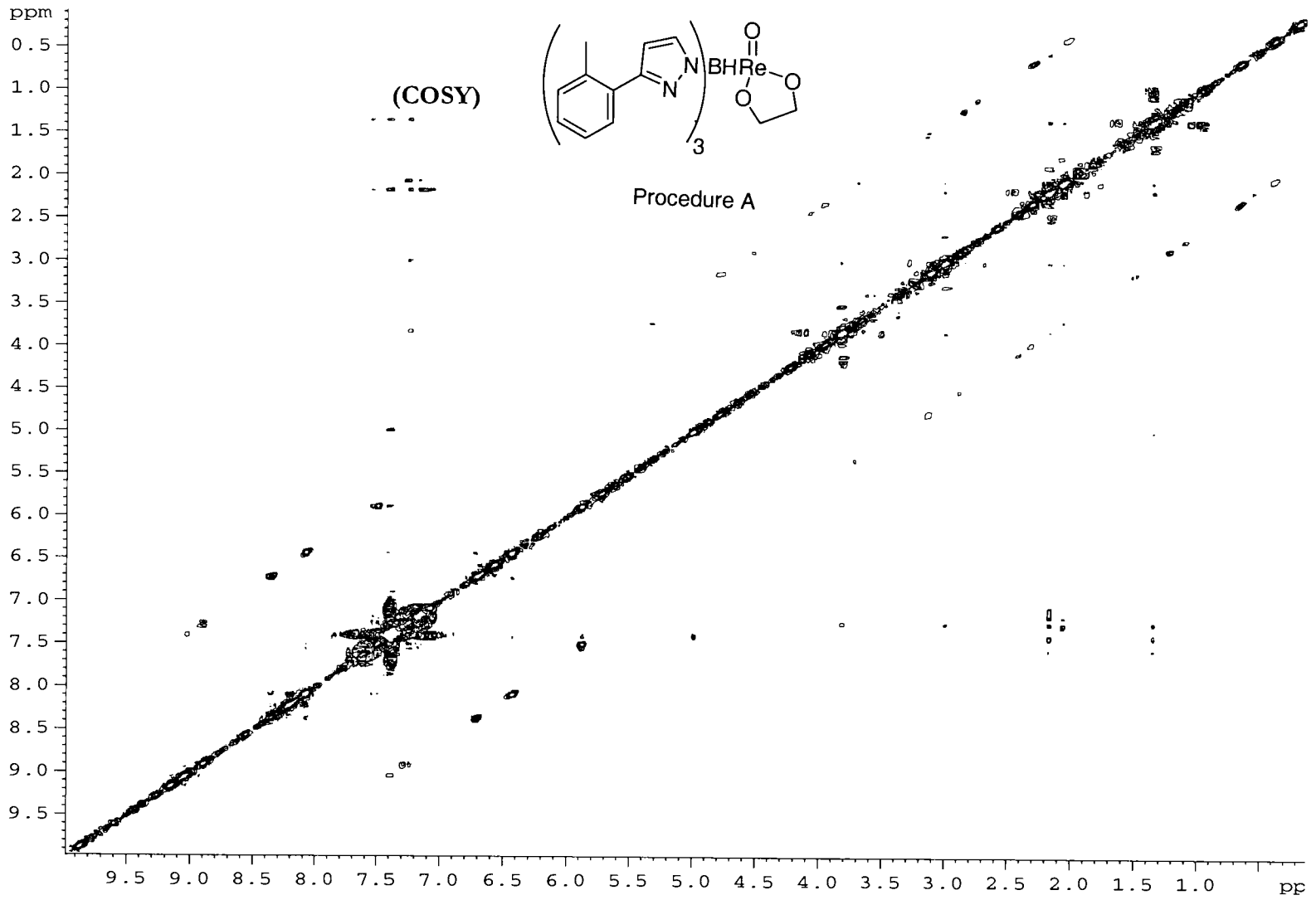
(COSY)
Procedure A
ppm
0.5
1.0
1.5
2.0
2.5
3.0
3.5
4.0
4.5
5.0
5.5
6.0
6.5
7.0
7.5
8.0
8.5
9.0
9.5
9.5 9.0 8.5 8.0 7.5 7.0 6.5 6.0 5.5 5.0 4.5 4.0 3.5 3.0 2.5 2.0 1.5 1.0
pp

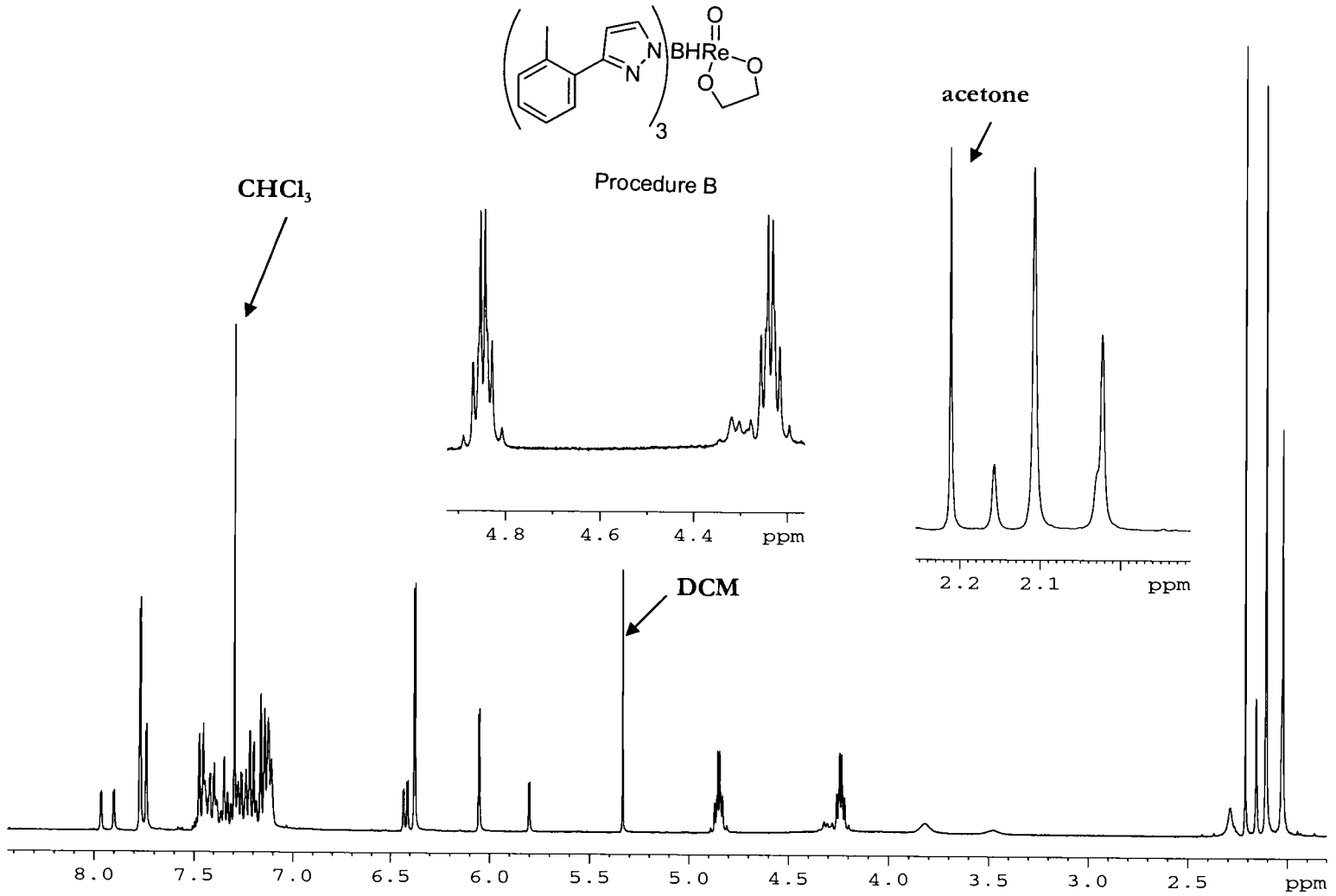
Procedure B
acetone
CHCl3
DCM
4.8
4.6
4.4
ppm
2.2
2.1
ppm
8.0
7.5
7.0
6.5
6.0
5.5
5.0
4.5
4.0
3.5
3.0
2.5
ppm

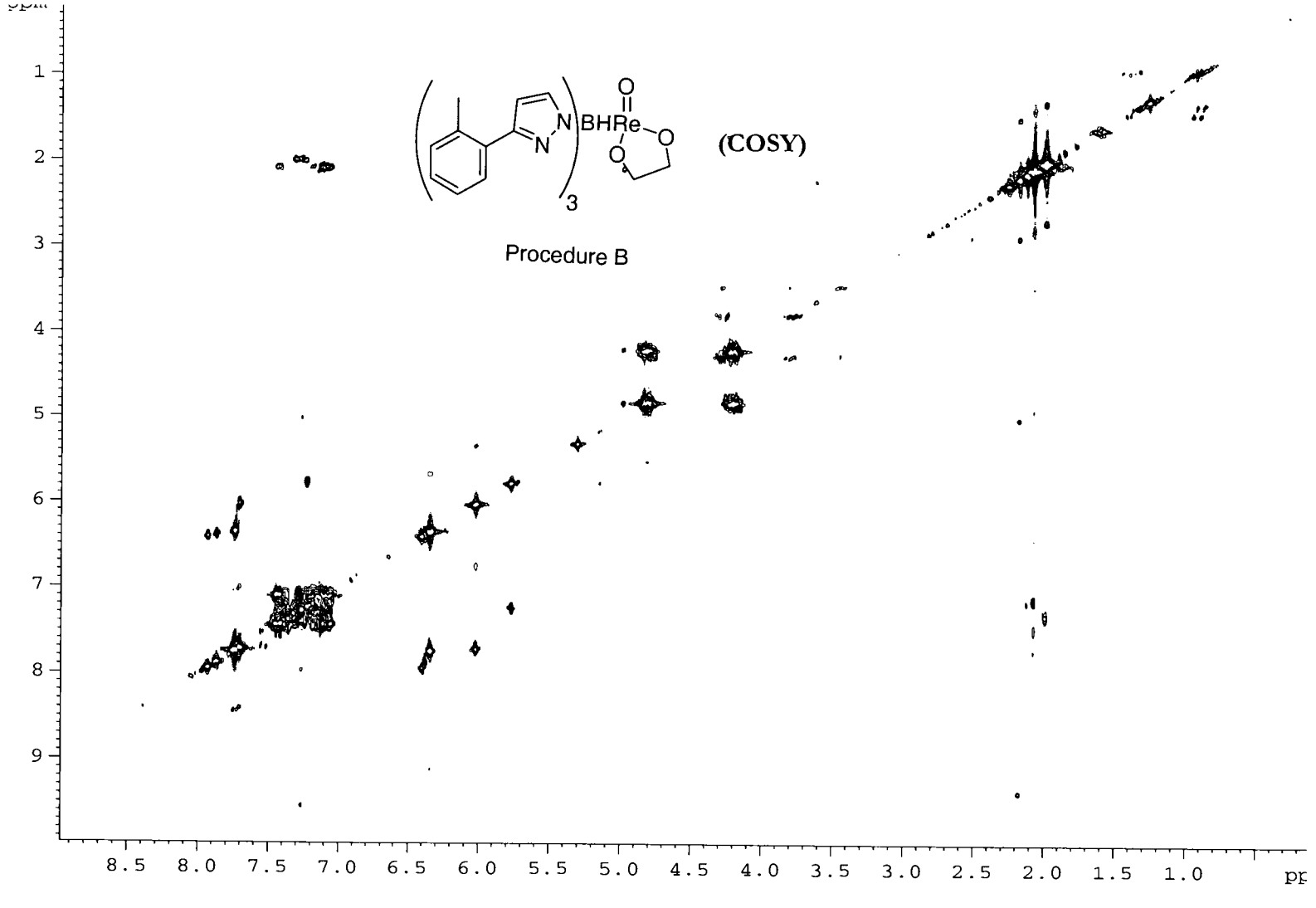
(COSY)
Procedure B
1
2
3
4
5
6
7
8
9
8.5
8.0
7.5
7.0
6.5
6.0
5.5
5.0
4.5
4.0
3.5
3.0
2.5
2.0
1.5
1.0

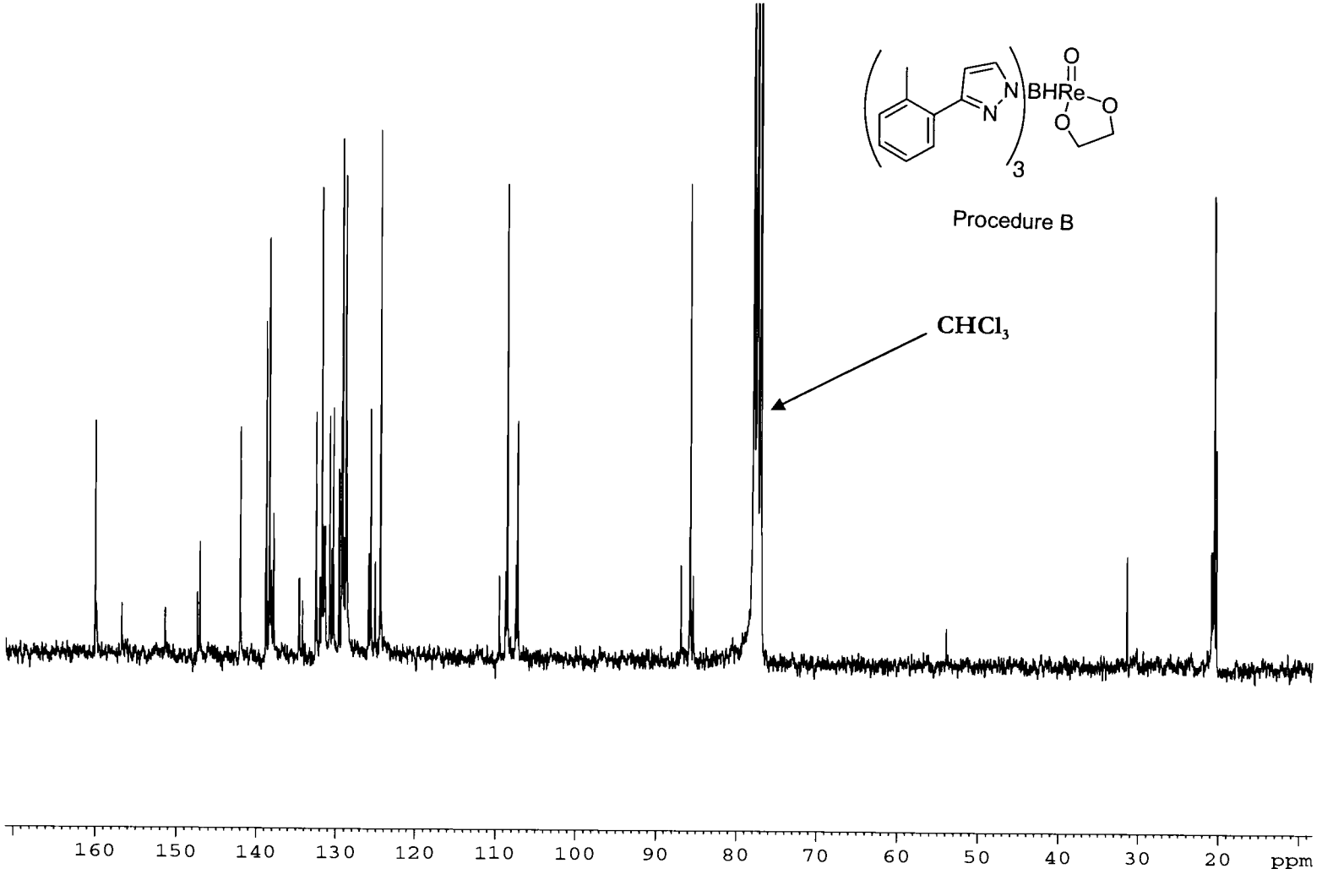
O
N
BHRe
N
O
O
3
Procedure B
CHCl3
160
150
140
130
120
110
100
90
80
70
60
50
40
30
20
ppm

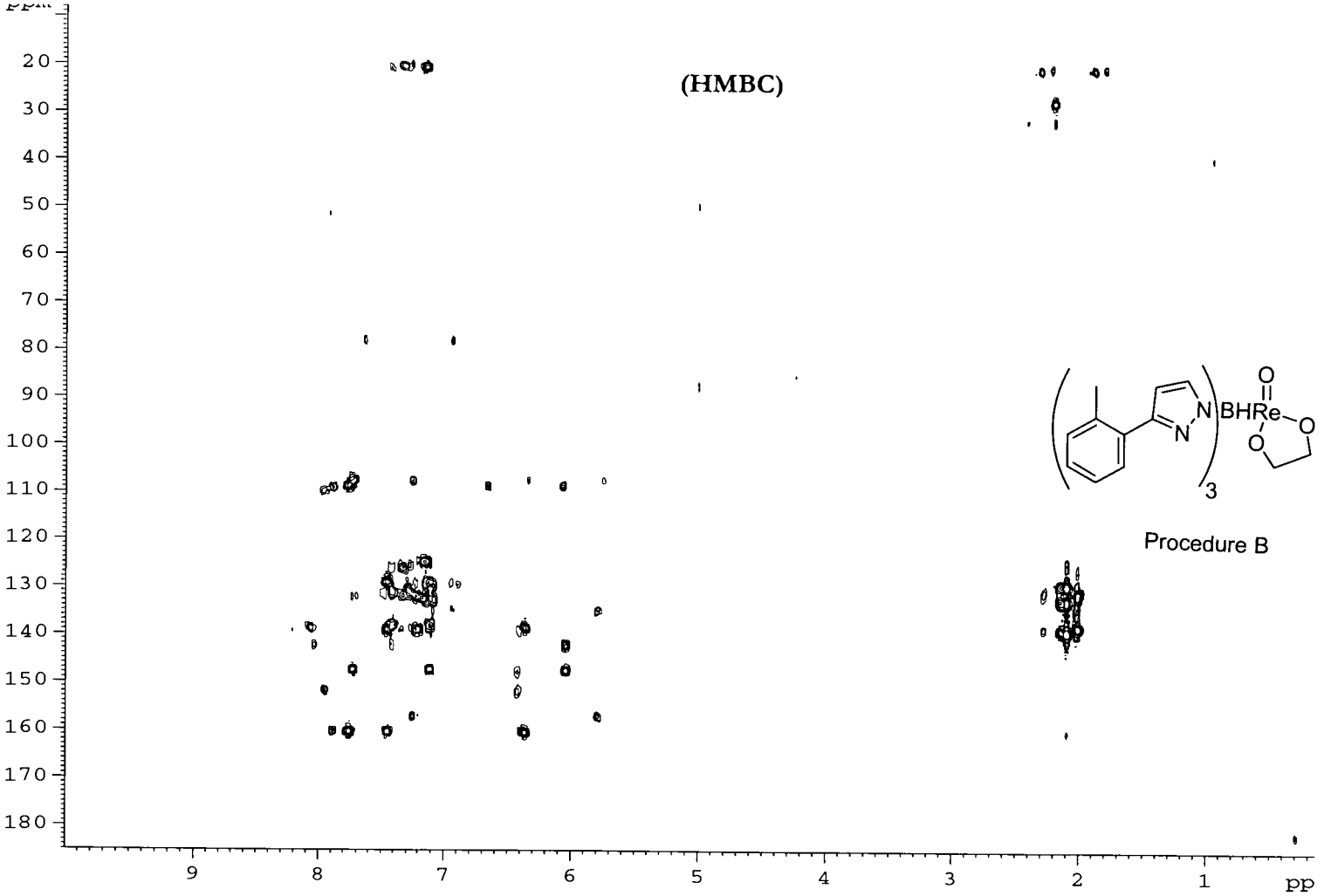
(HMBC)
20
30
40
50
60
70
80
90
100
110
120
130
140
150
160
170
180
9
8
7
6
5
4
3
2
1
pp
O
BHRe
O
O
N
N
3
Procedure B

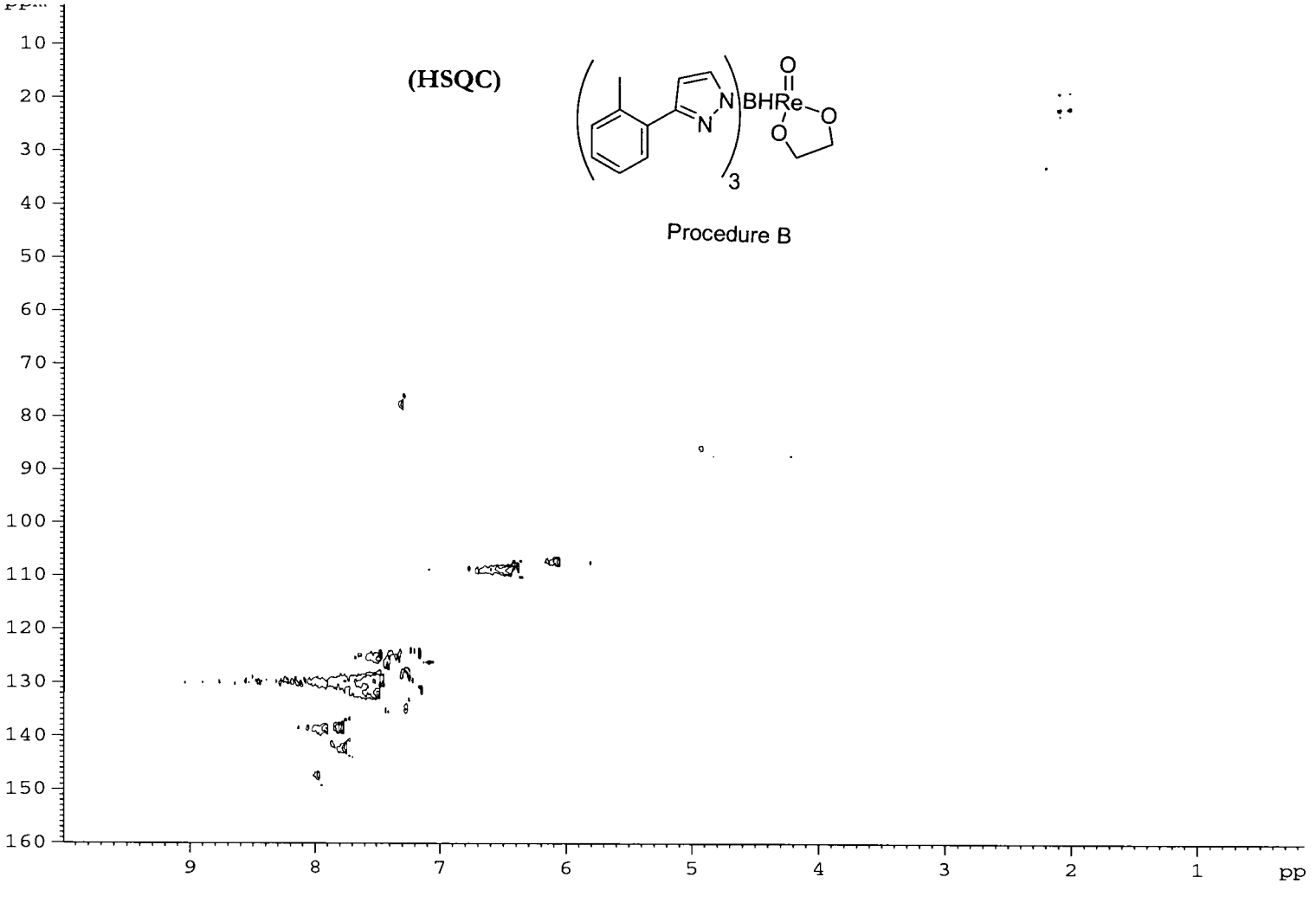
(HSQC)
BHRe
O
O
O
N
N
3
Procedure B
10
20
30
40
50
60
70
80
90
100
110
120
130
140
150
160
9
8
7
6
5
4
3
2
1
pp

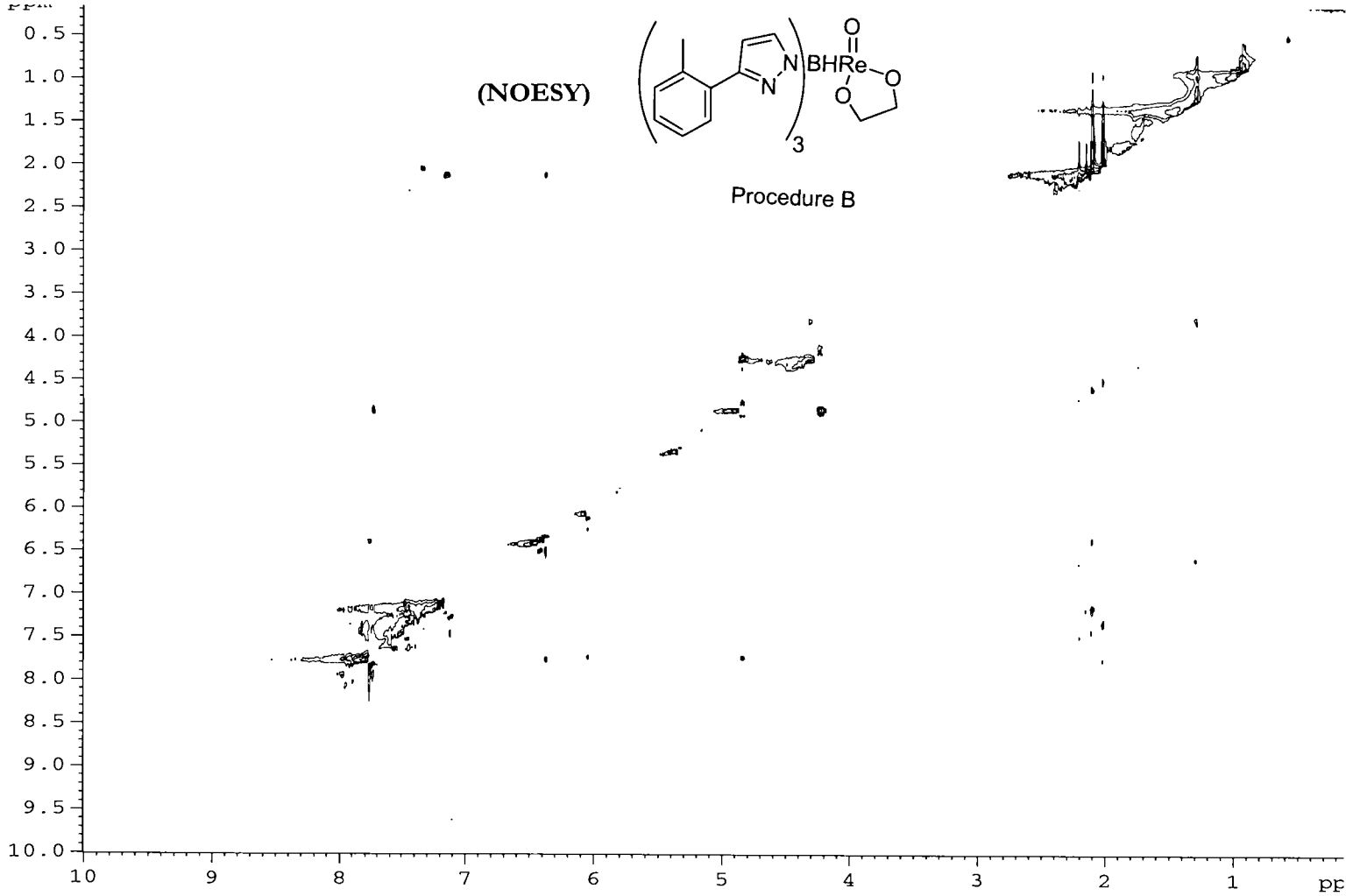
(NOESY)
N
N
BHRe
O
O
O
3
Procedure B
0.5
1.0
1.5
2.0
2.5
3.0
3.5
4.0
4.5
5.0
5.5
6.0
6.5
7.0
7.5
8.0
8.5
9.0
9.5
10.0
10
9
8
7
6
5
4
3
2
1
pp

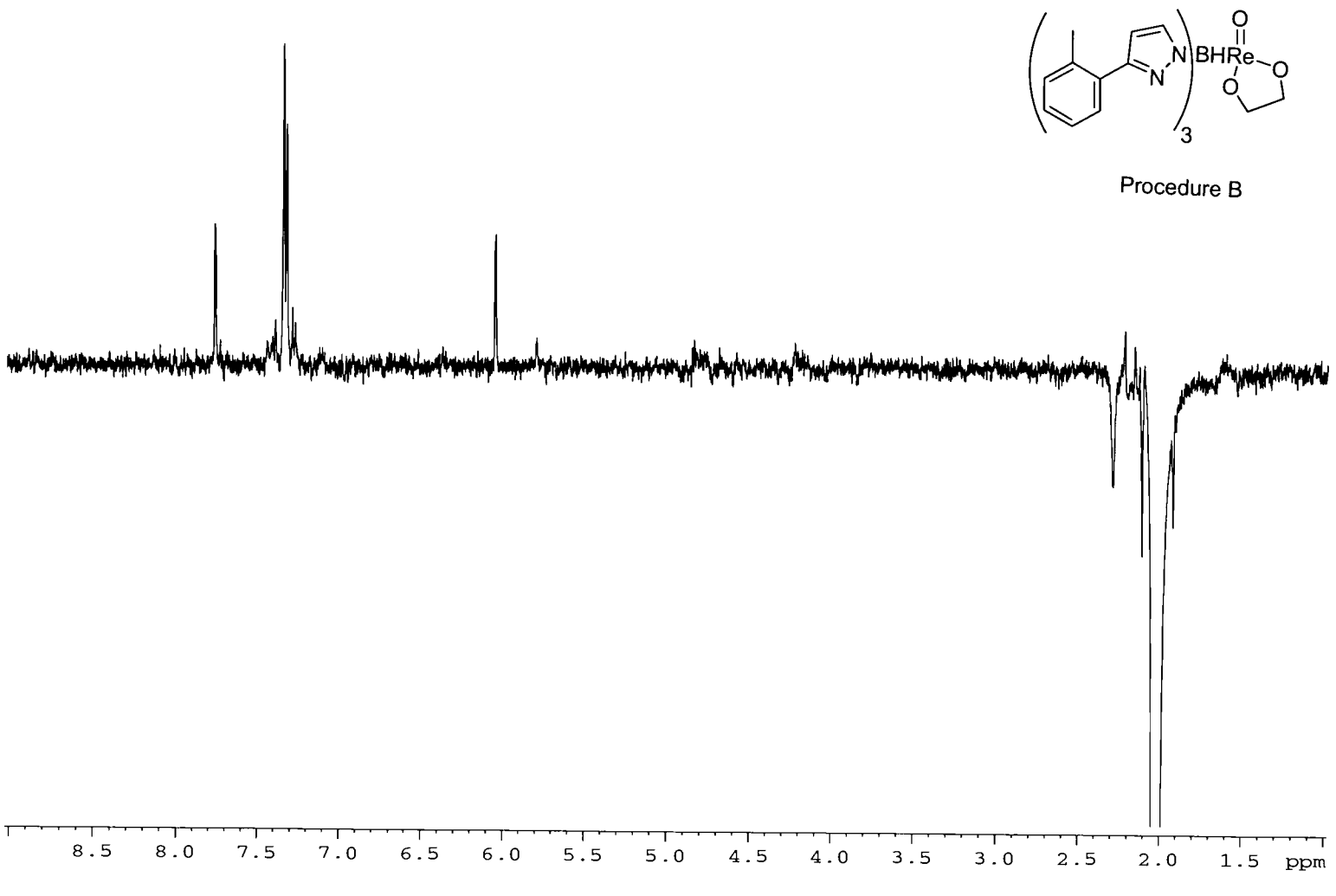

Procedure B

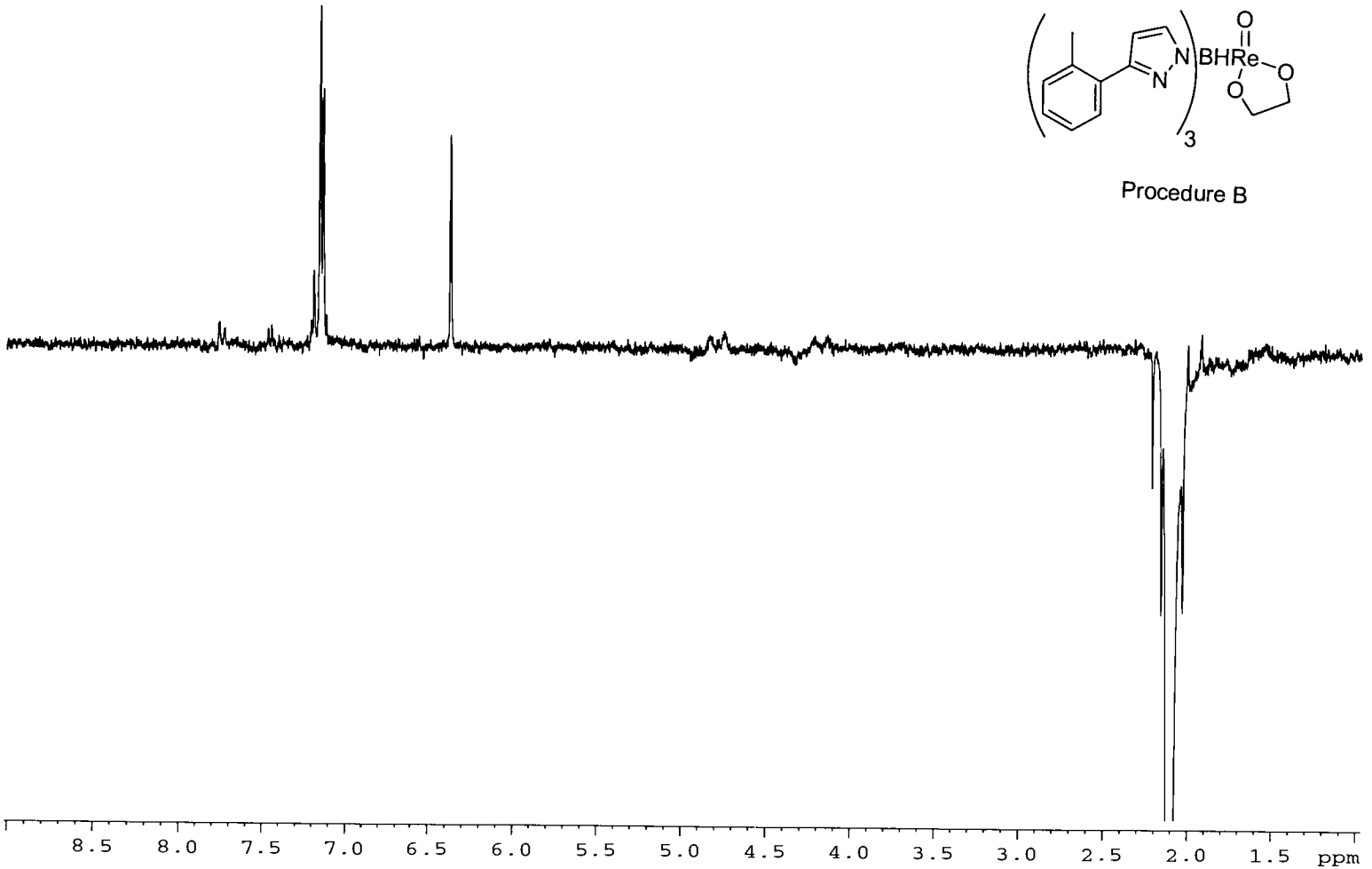

Procedure B

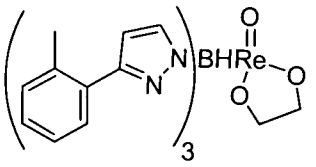

Procedure B

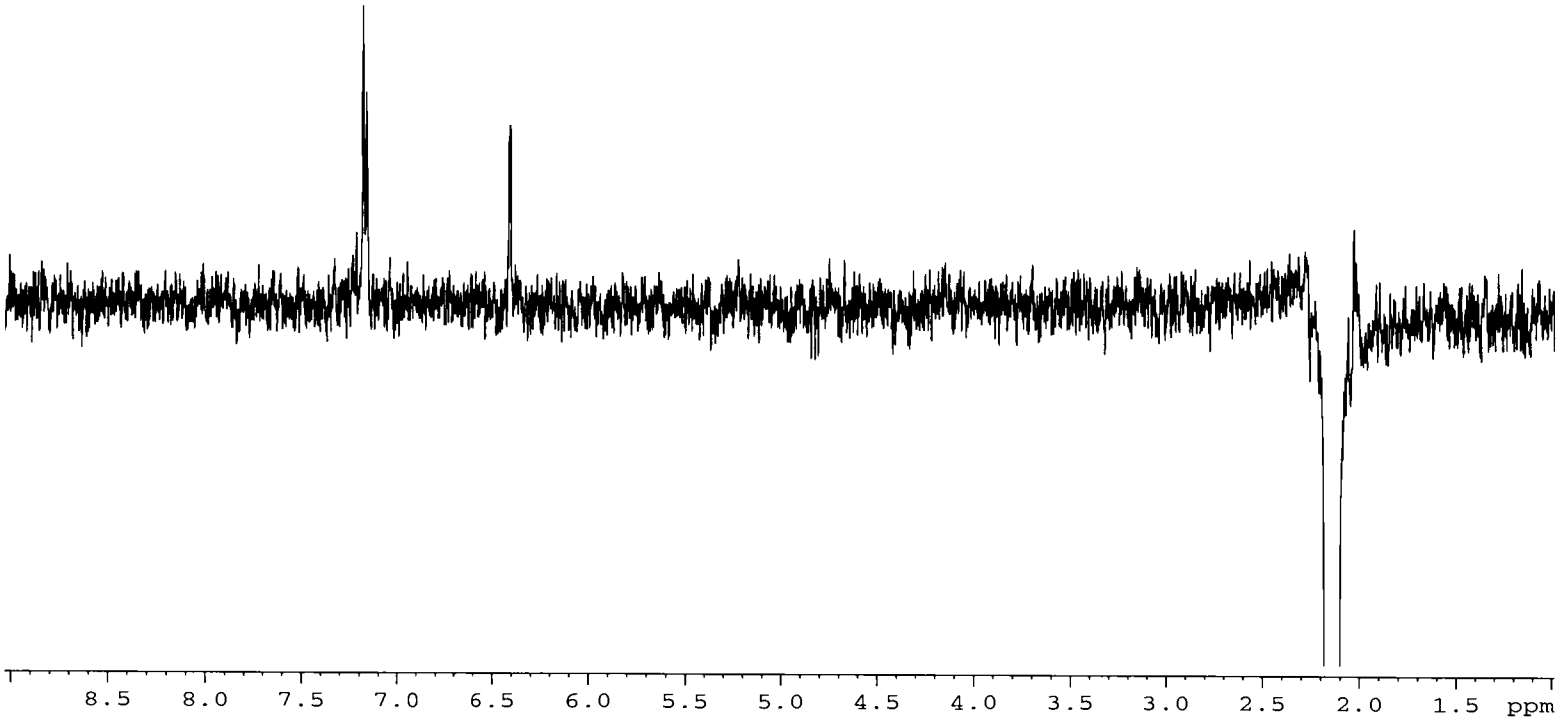

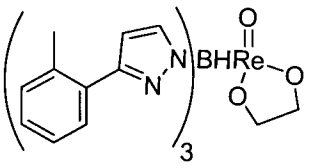

Procedure B

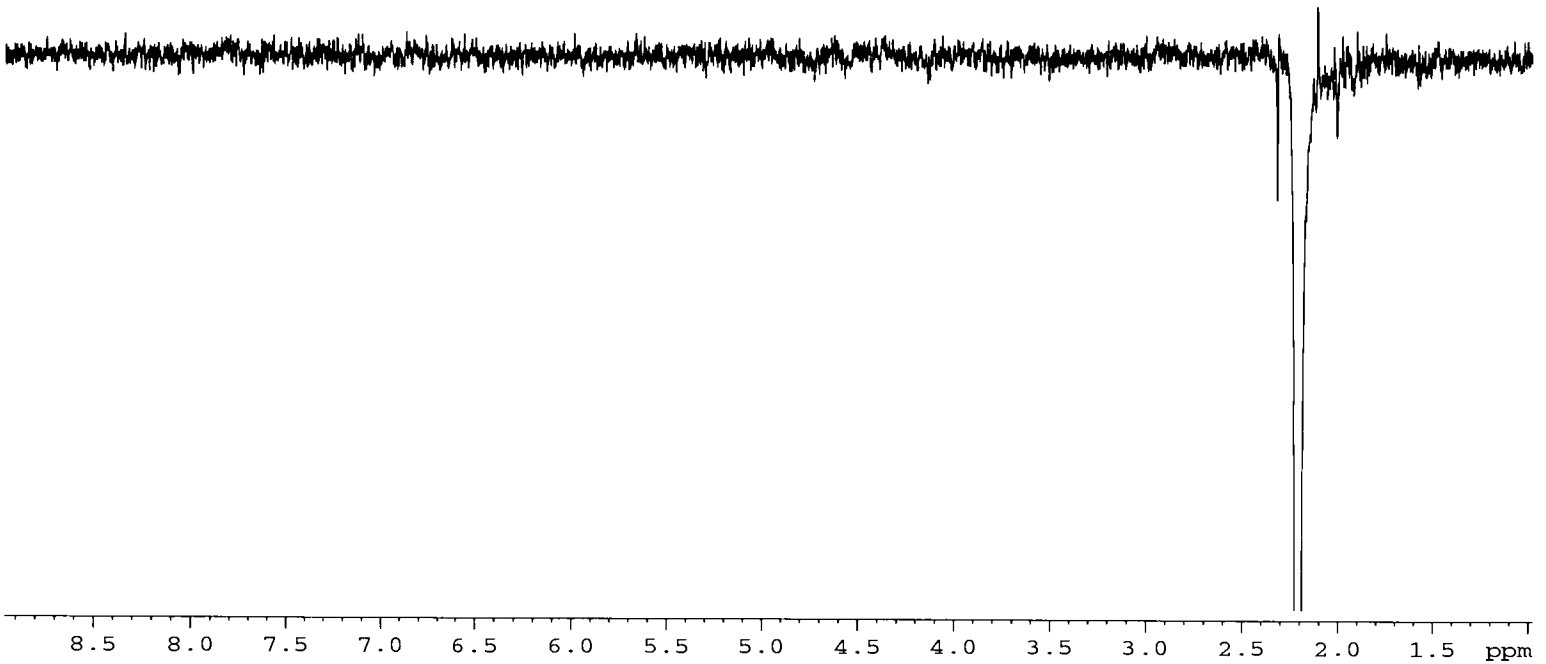

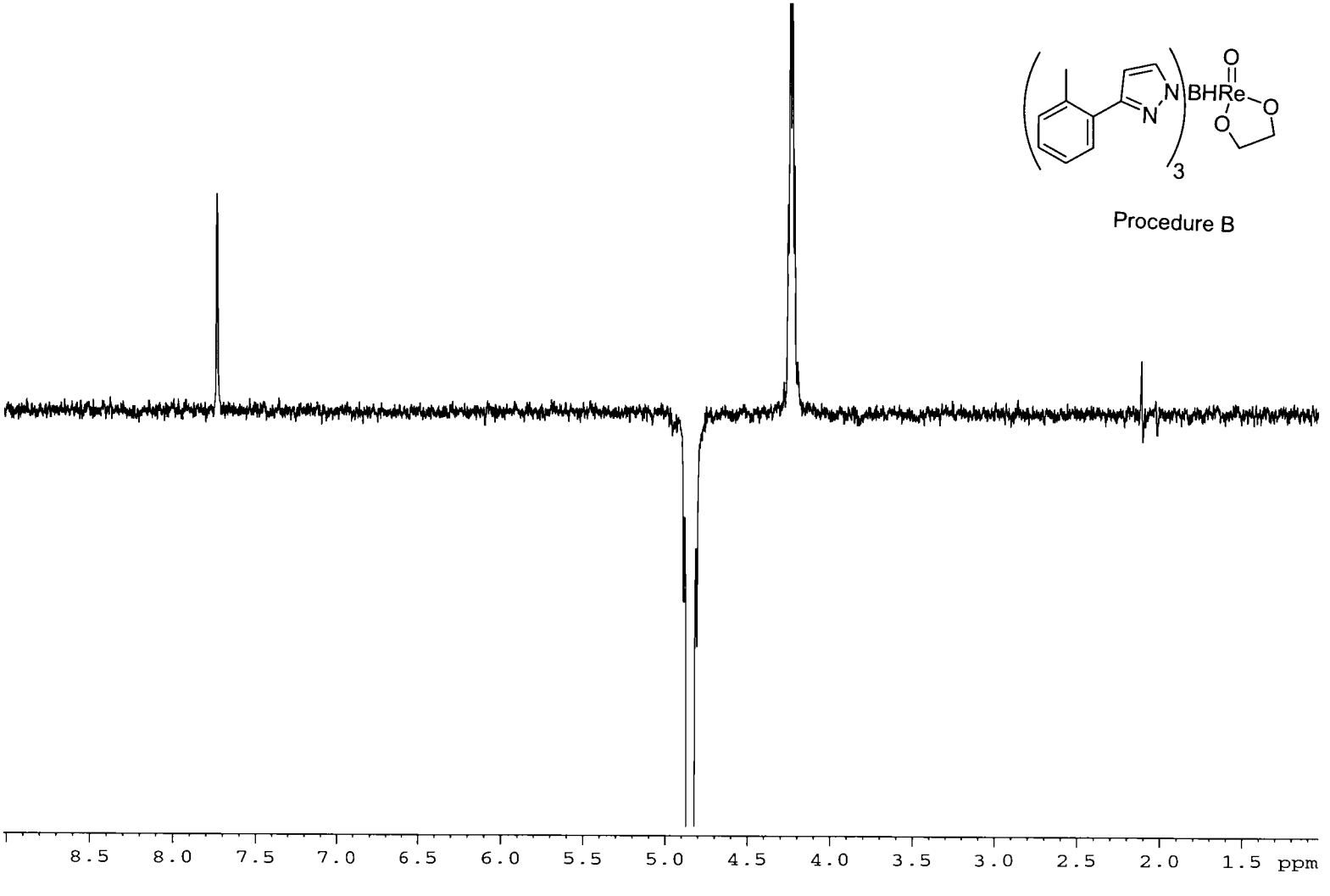
O
BHRe
N
N
O
O
3
Procedure B
8.5
8.0
7.5
7.0
6.5
6.0
5.5
5.0
4.5
4.0
3.5
3.0
2.5
2.0
1.5
ppm

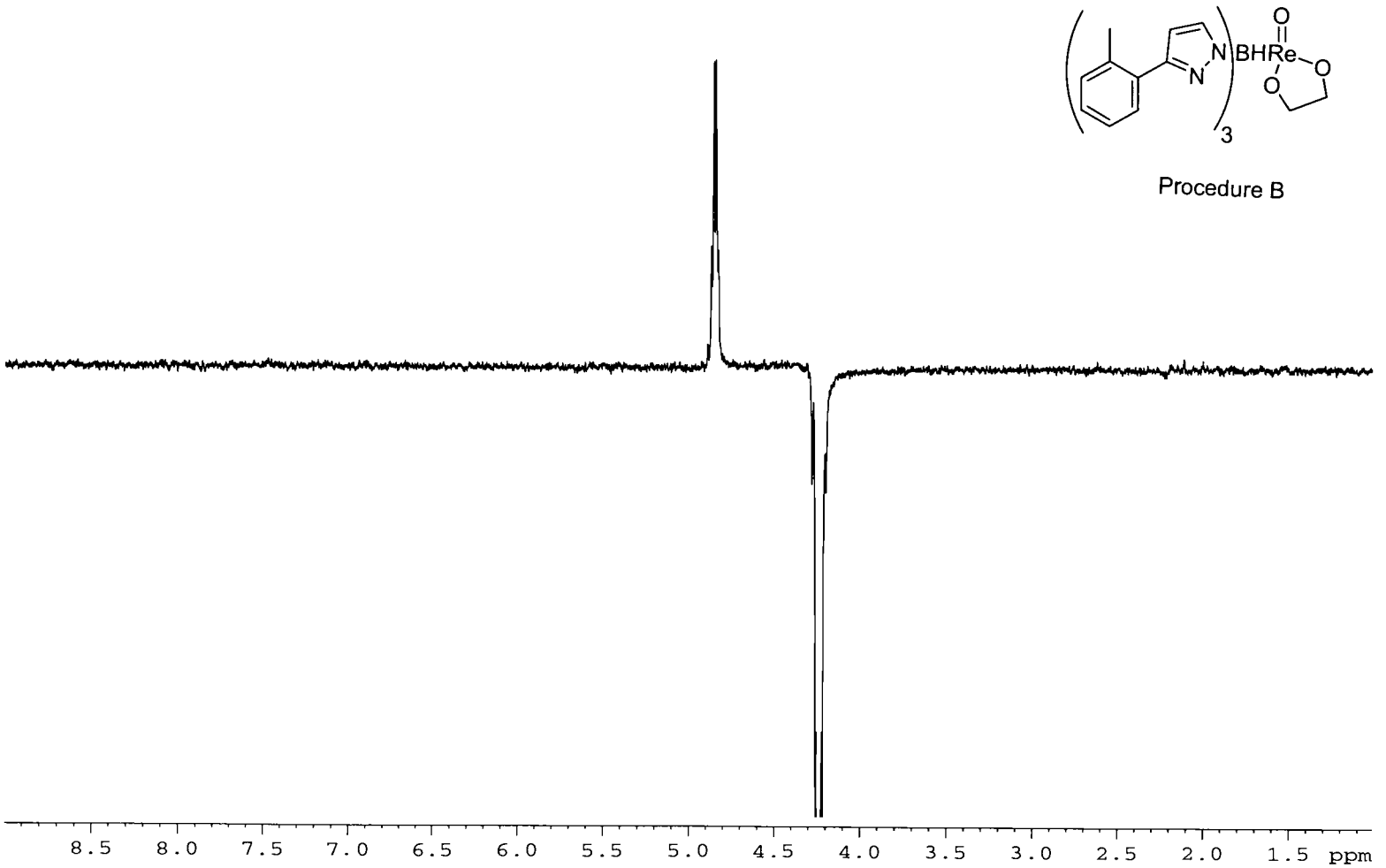

Procedure B

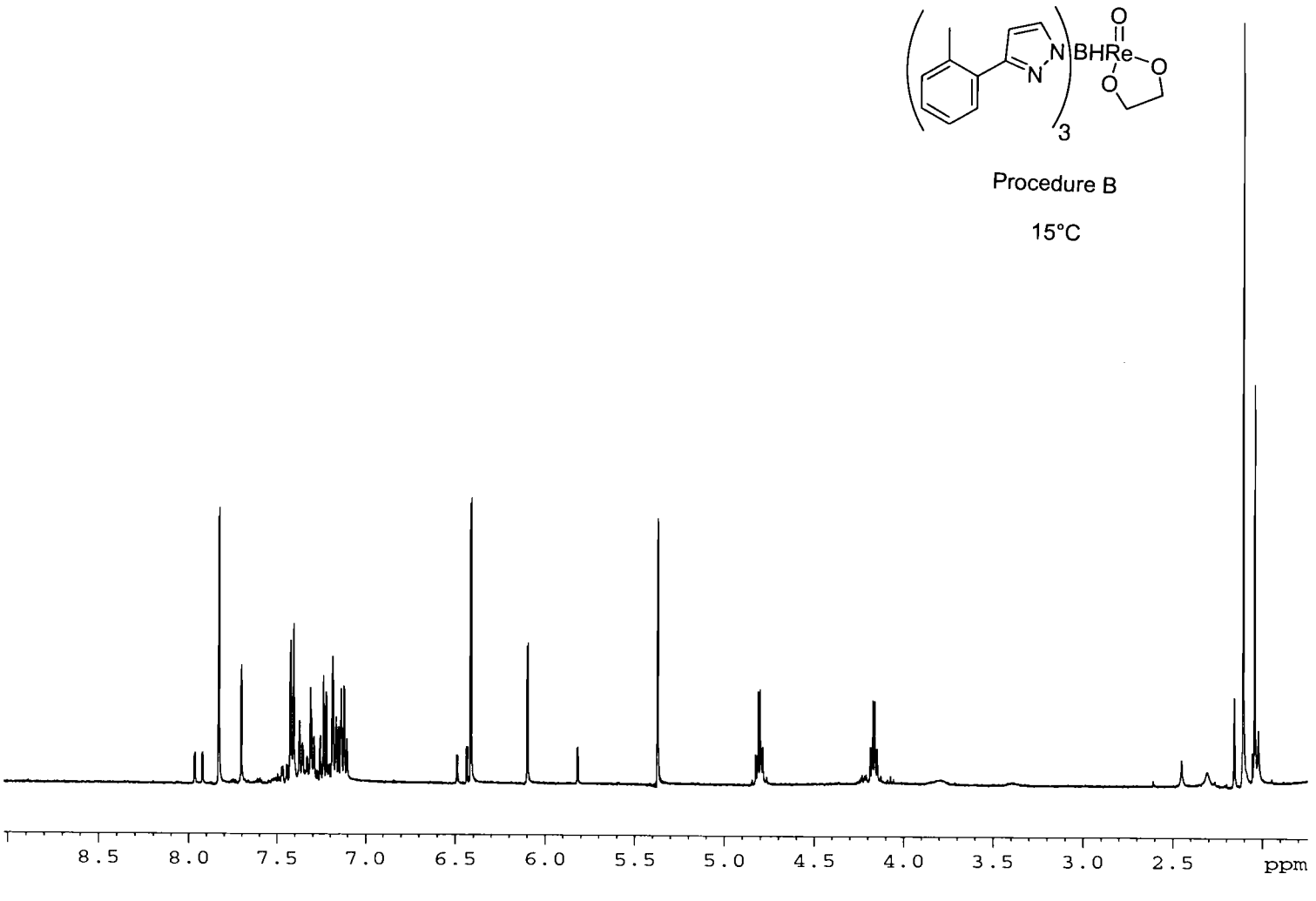
O
N
N
BHRe
O
O
3
Procedure B
15°C
8.5
8.0
7.5
7.0
6.5
6.0
5.5
5.0
4.5
4.0
3.5
3.0
2.5
ppm

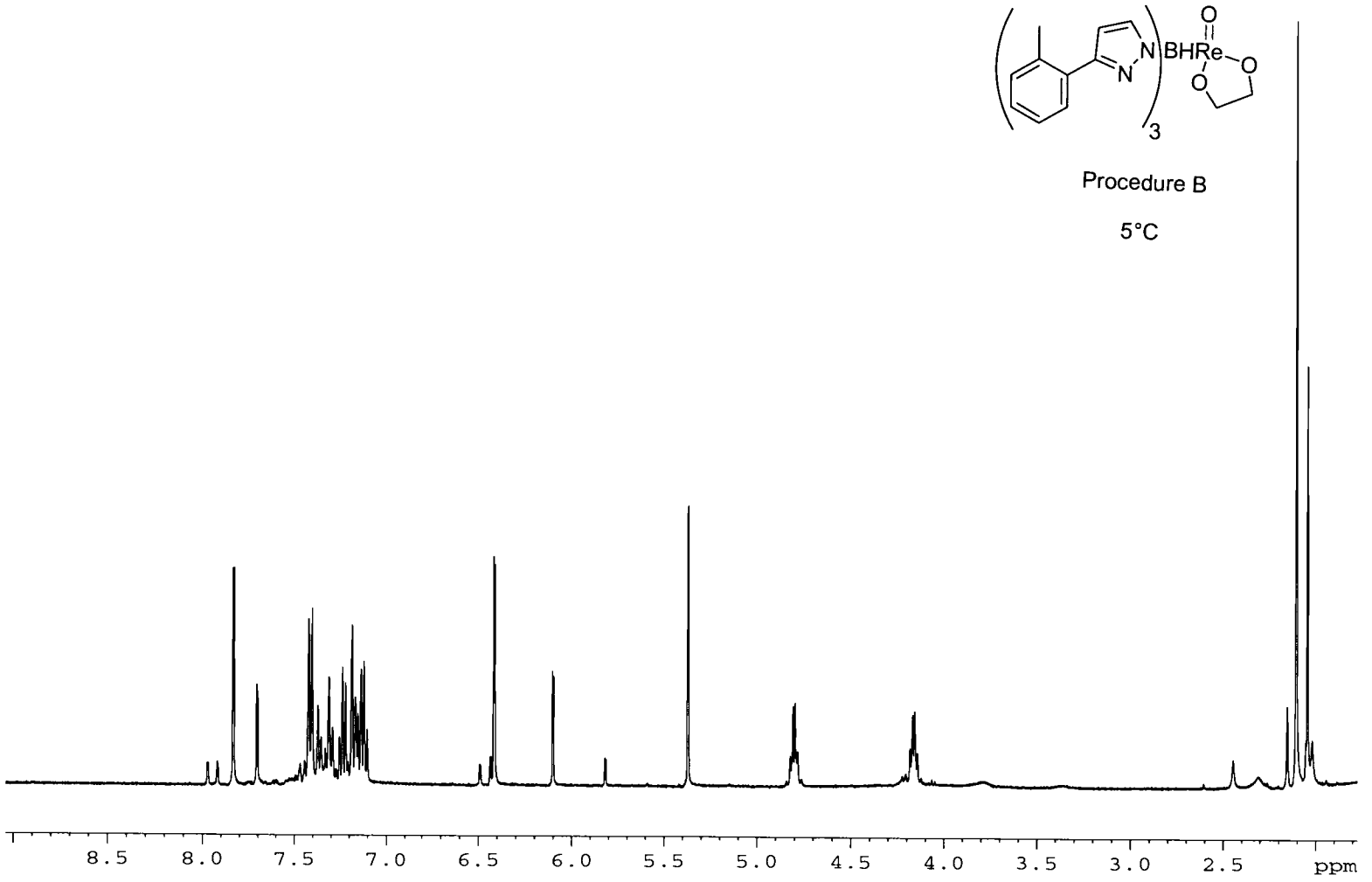
Procedure B
5°C
8.5
8.0
7.5
7.0
6.5
6.0
5.5
5.0
4.5
4.0
3.5
3.0
2.5
ppm

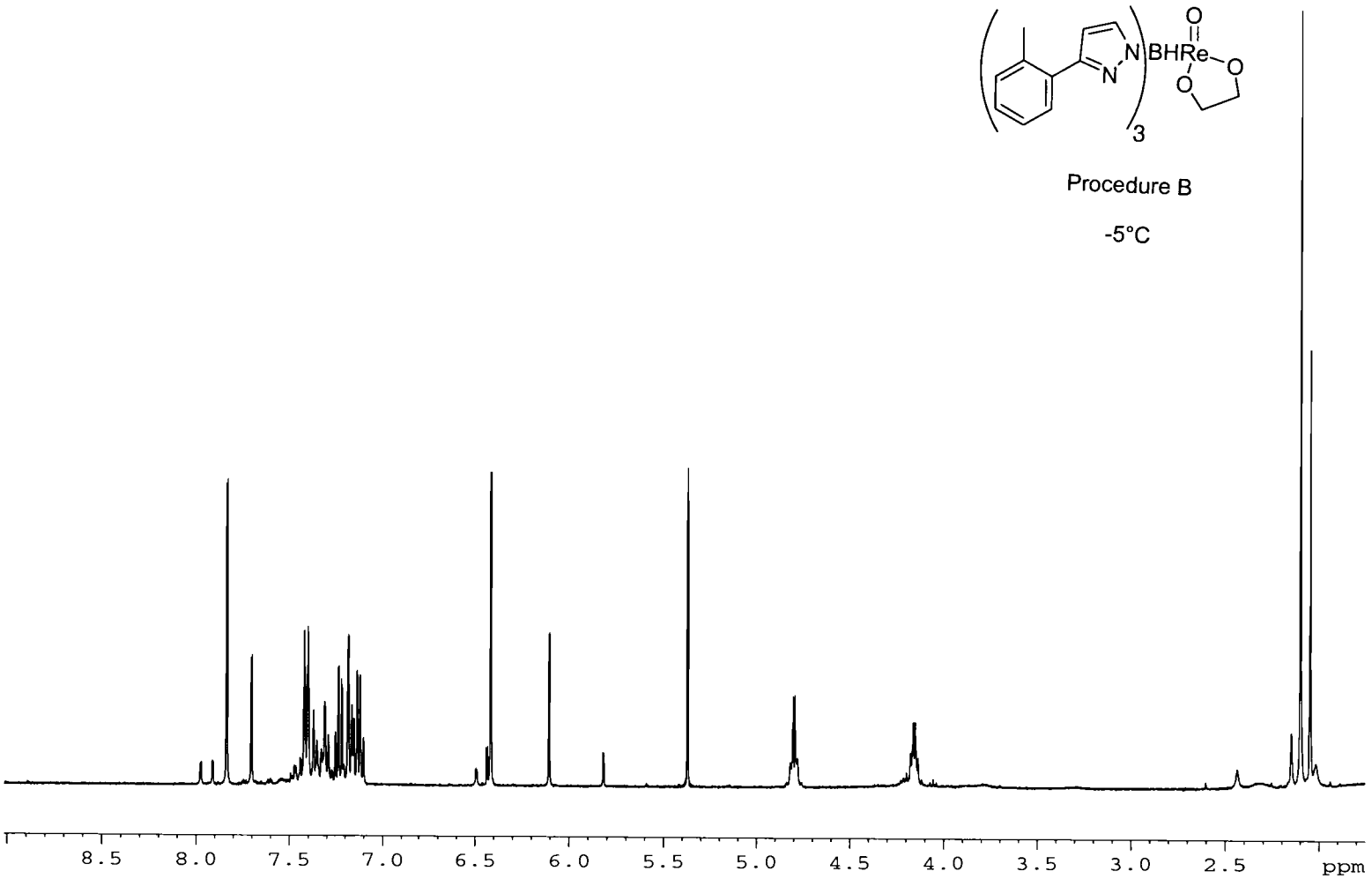
Procedure B
-5°C
8.5
8.0
7.5
7.0
6.5
6.0
5.5
5.0
4.5
4.0
3.5
3.0
2.5
ppm

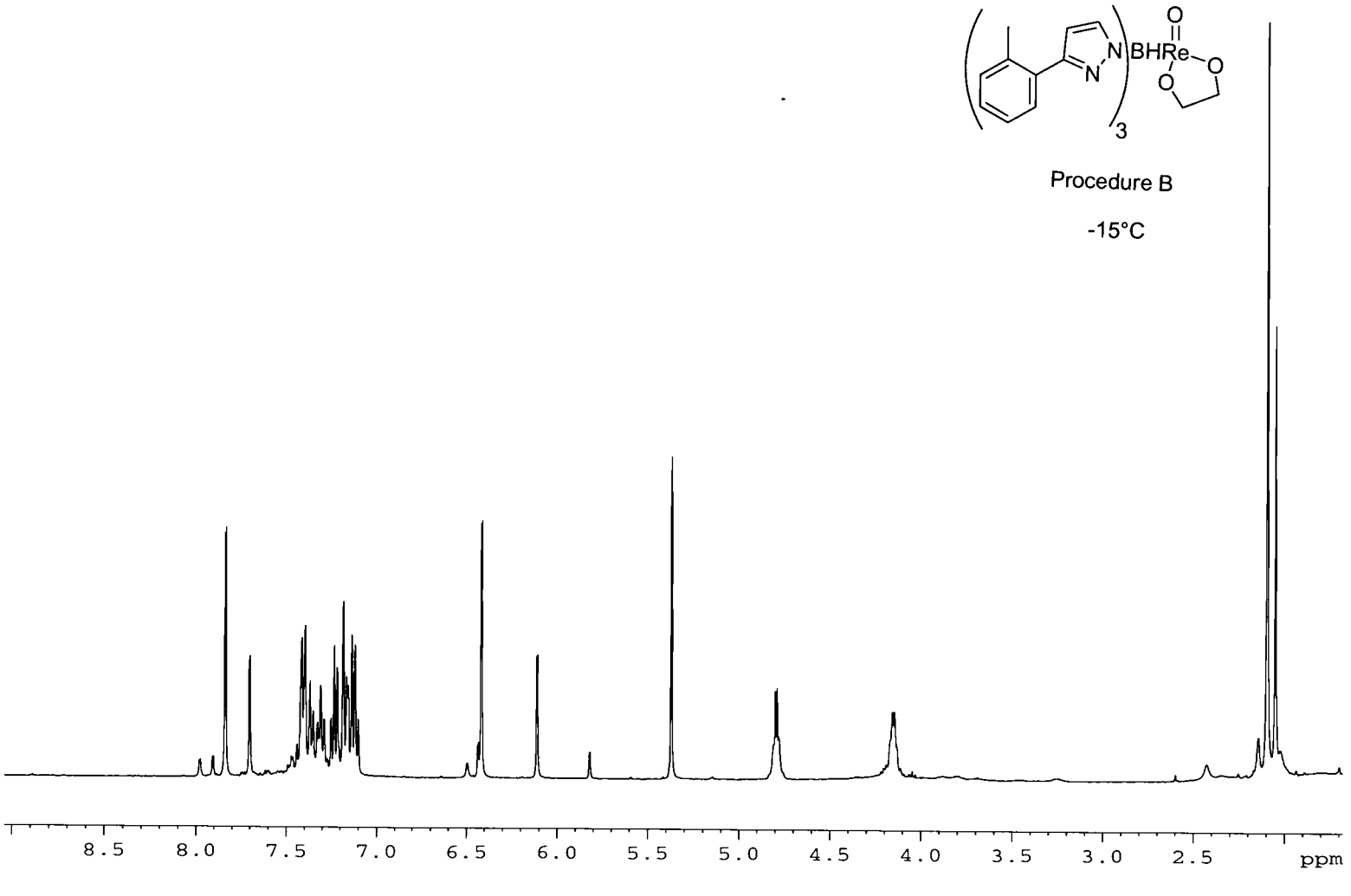
Procedure B
-15°C
8.5
8.0
7.5
7.0
6.5
6.0
5.5
5.0
4.5
4.0
3.5
3.0
2.5
ppm

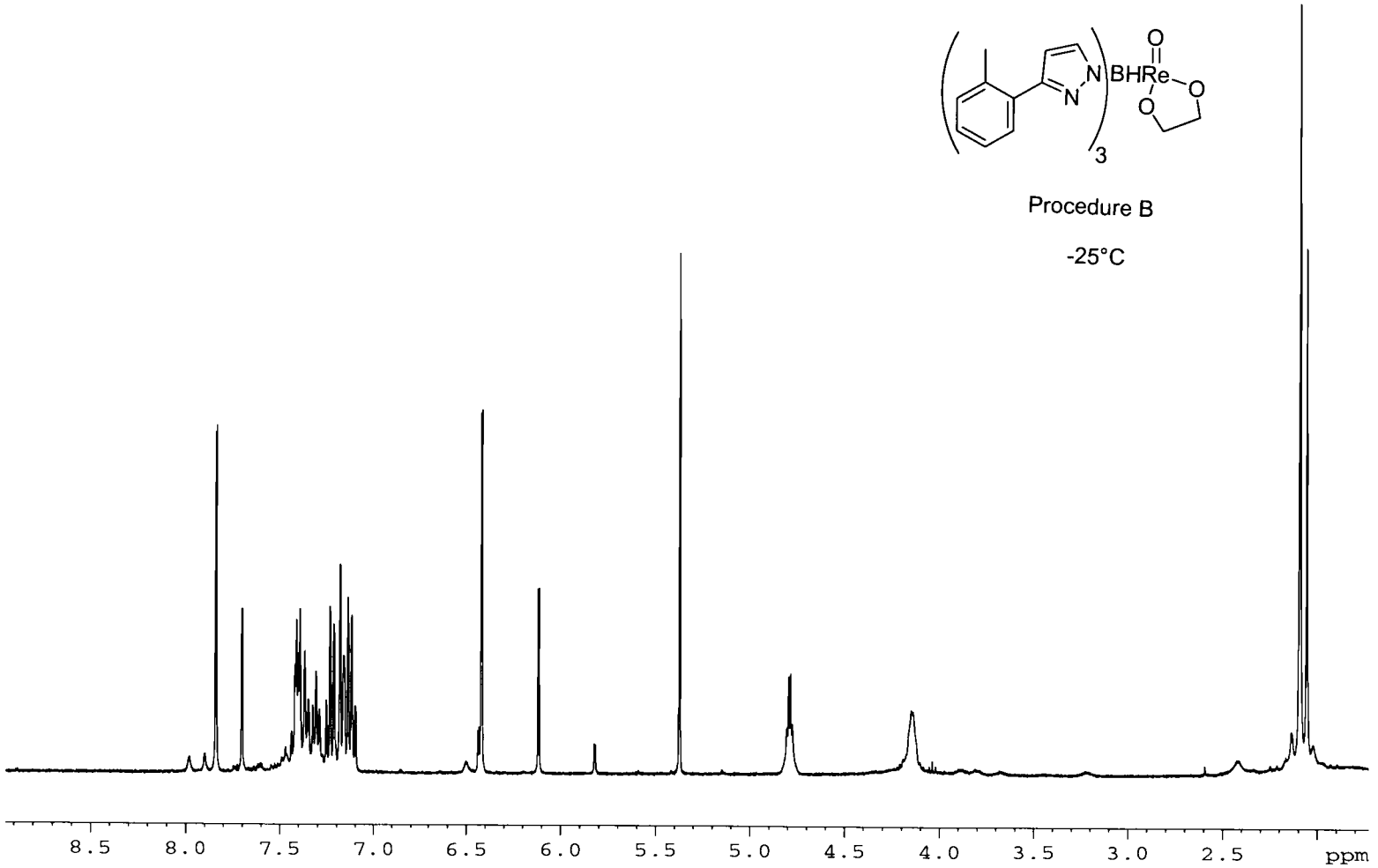
Procedure B
-25°C
8.5
8.0
7.5
7.0
6.5
6.0
5.5
5.0
4.5
4.0
3.5
3.0
2.5
ppm

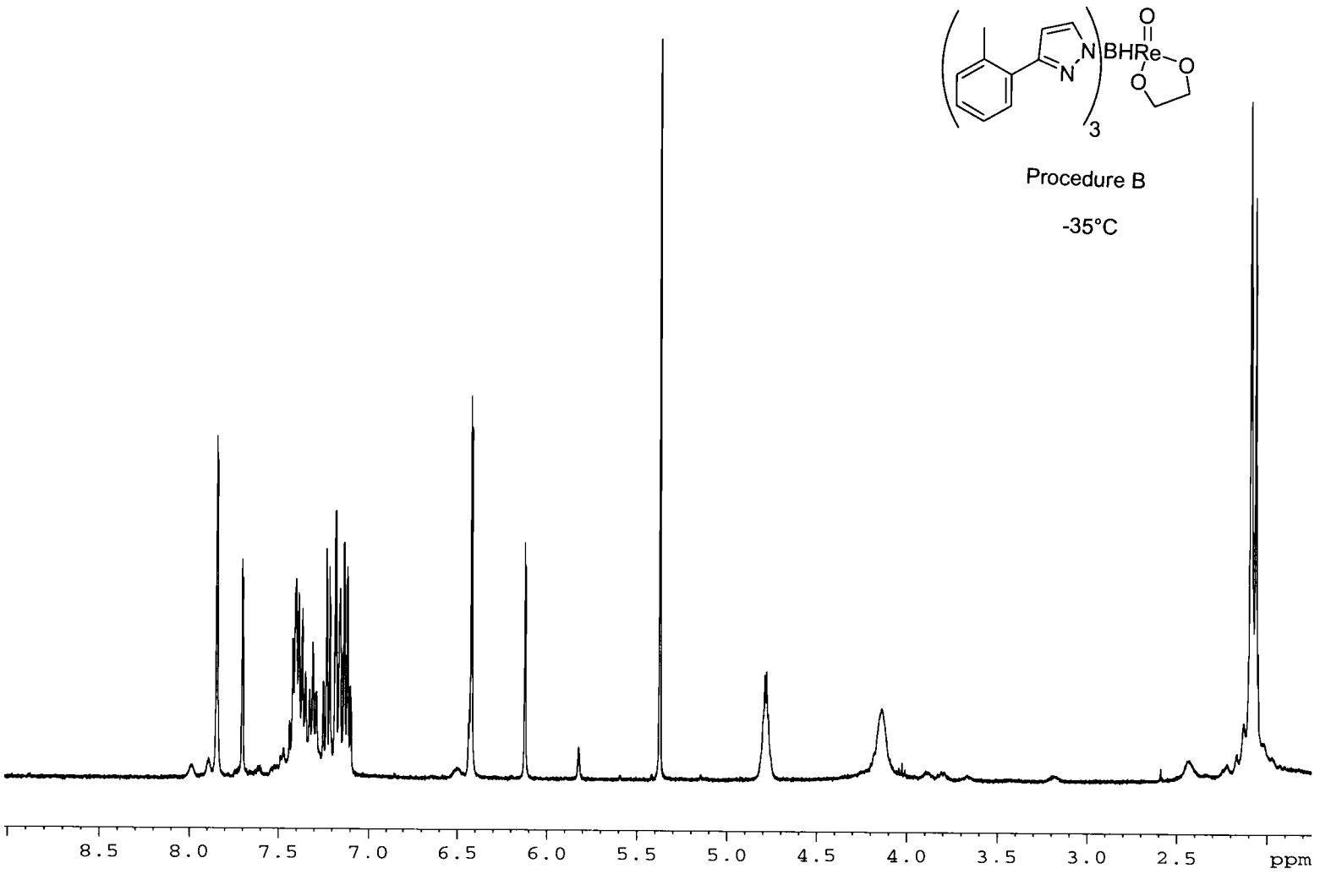
Procedure B
-35°C
8.5
8.0
7.5
7.0
6.5
6.0
5.5
5.0
4.5
4.0
3.5
3.0
2.5
ppm

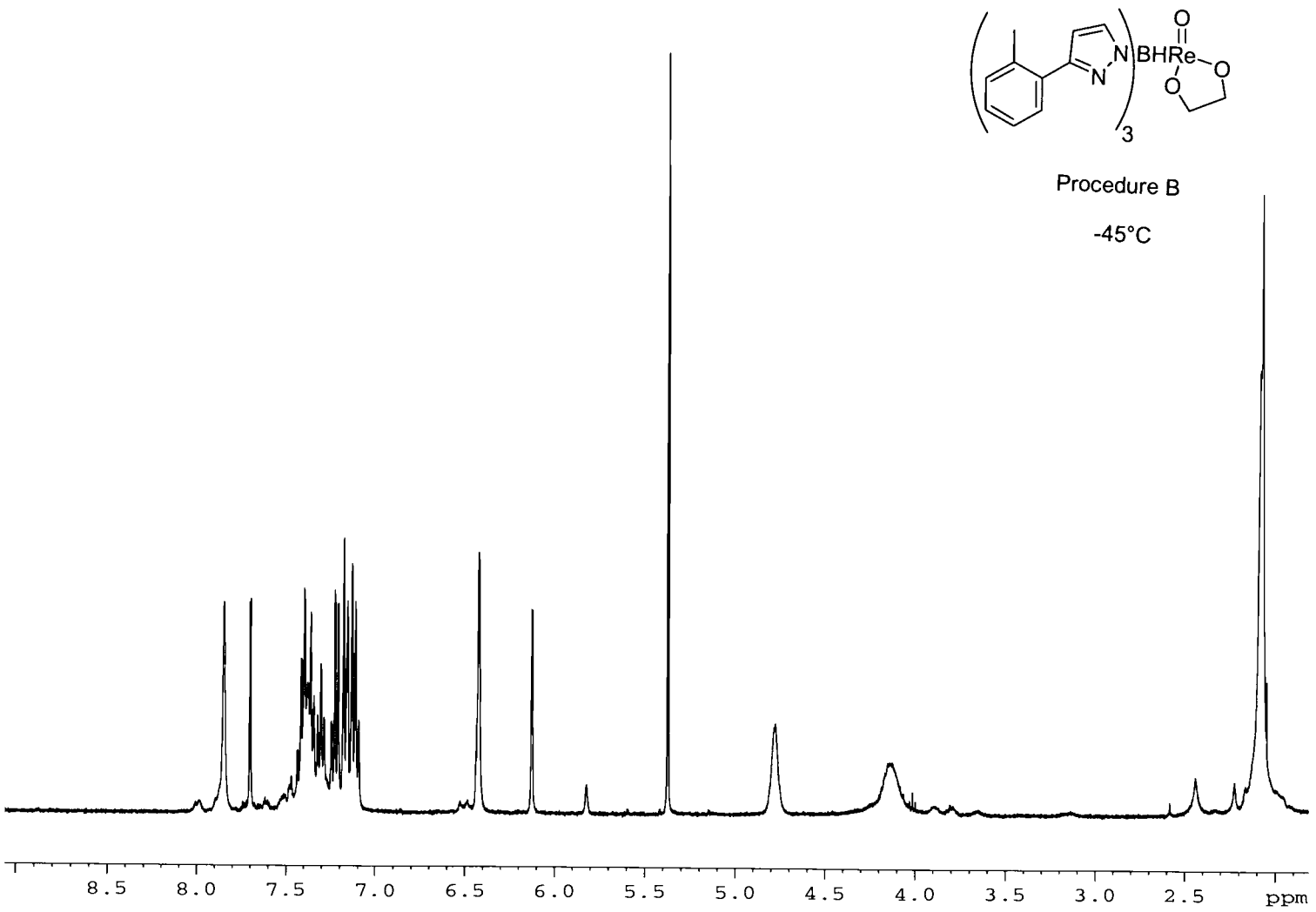
Procedure B
-45°C
8.5
8.0
7.5
7.0
6.5
6.0
5.5
5.0
4.5
4.0
3.5
3.0
2.5
ppm

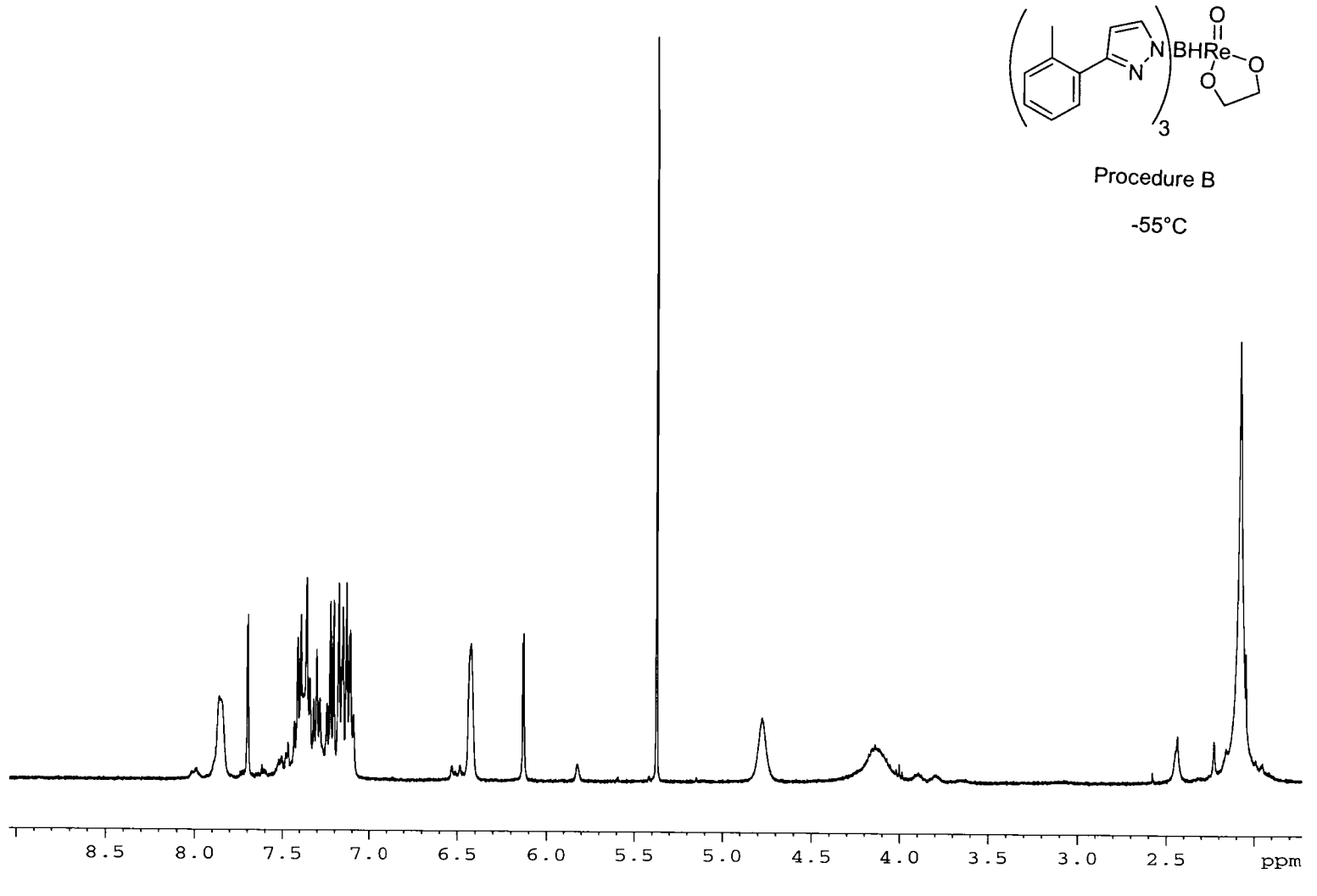
BHRe
O
O
O
N
N
3
Procedure B
-55°C
8.5
8.0
7.5
7.0
6.5
6.0
5.5
5.0
4.5
4.0
3.5
3.0
2.5
ppm

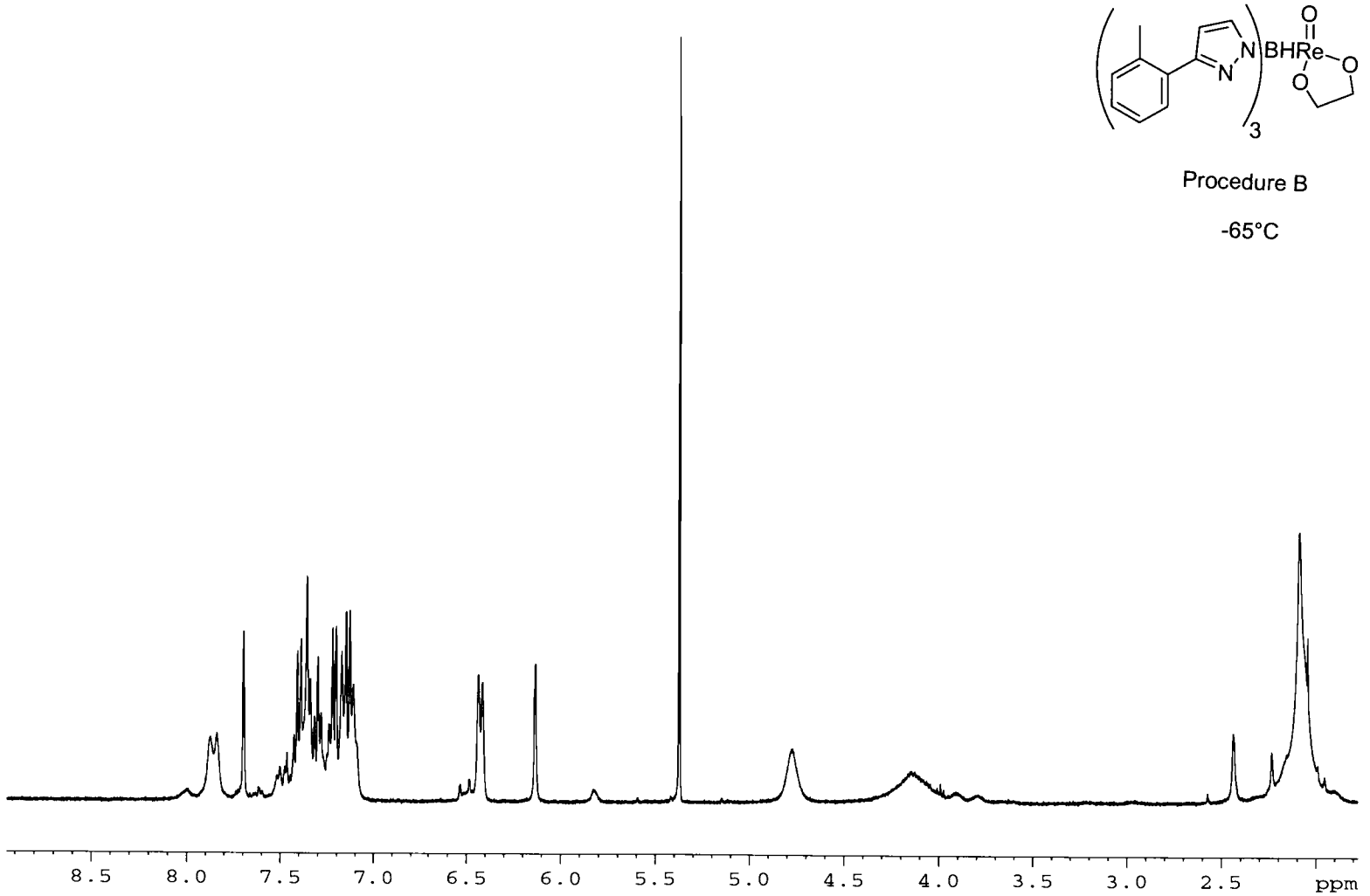
O
N
BHRe
O
N
O
3
Procedure B
-65°C
8.5
8.0
7.5
7.0
6.5
6.0
5.5
5.0
4.5
4.0
3.5
3.0
2.5
ppm

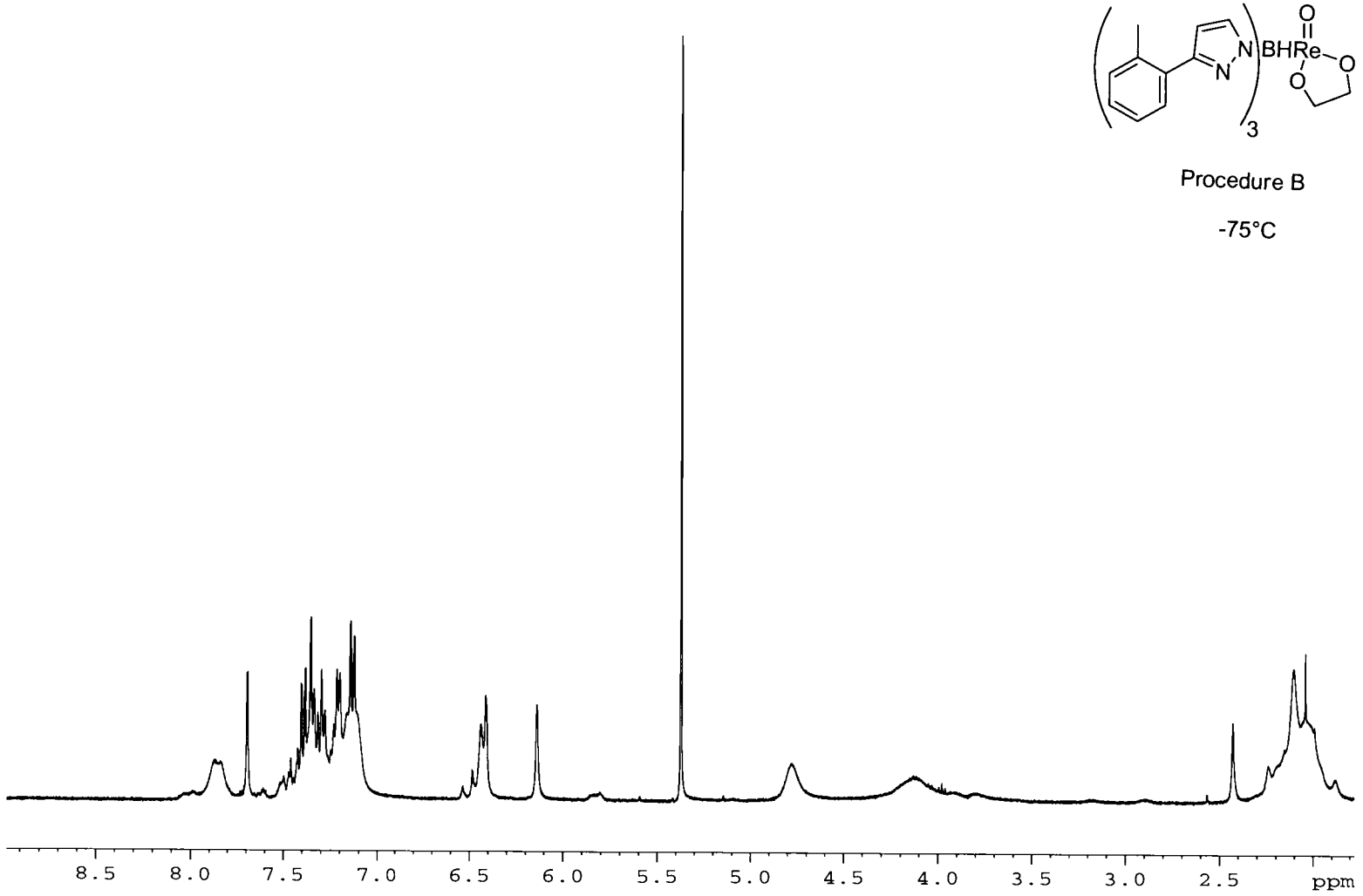
O
N
BHRe
O
N
O
3
Procedure B
-75°C
8.5
8.0
7.5
7.0
6.5
6.0
5.5
5.0
4.5
4.0
3.5
3.0
2.5
ppm

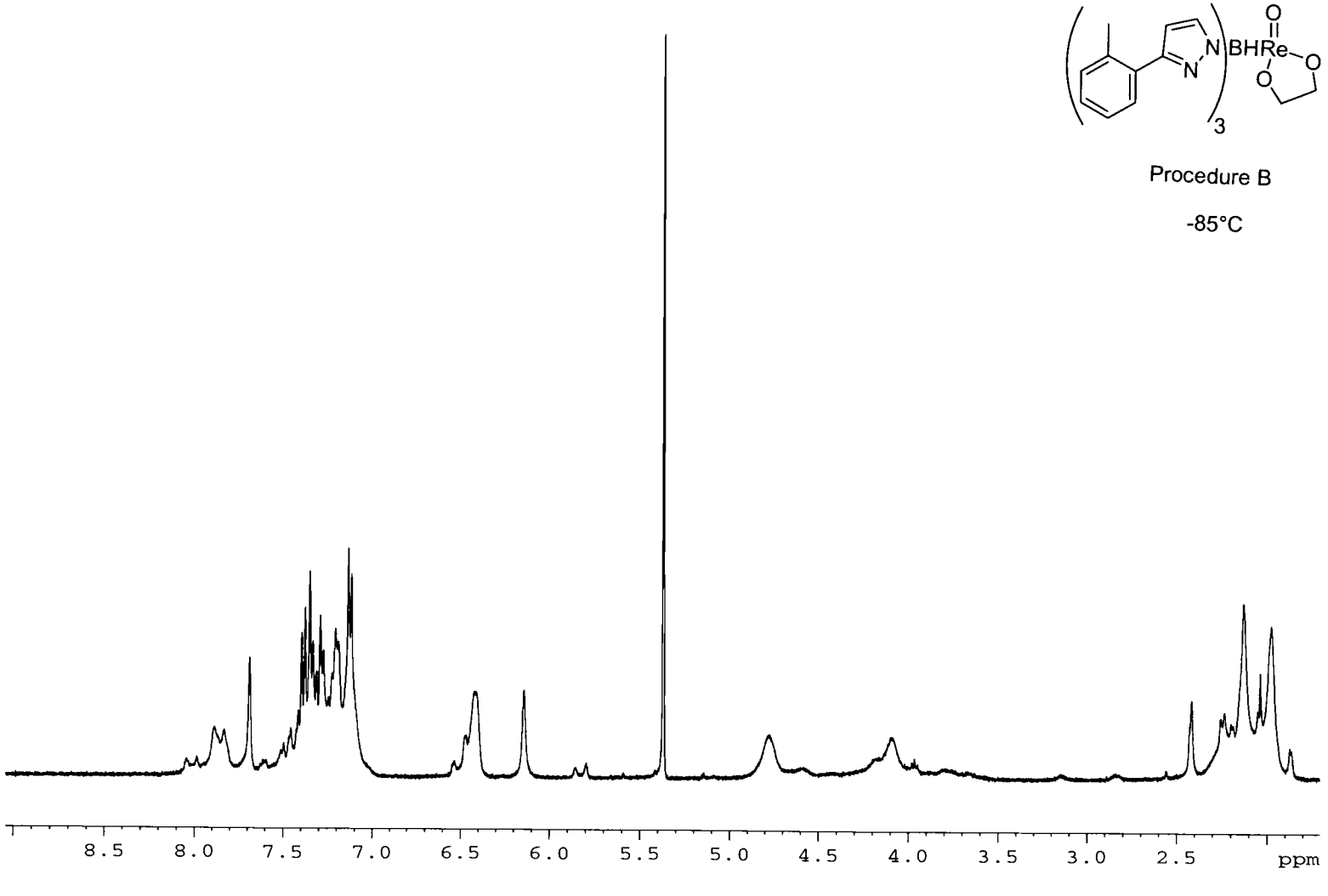
O
N
N
BHRe
O
O
3
Procedure B
-85°C
8.5
8.0
7.5
7.0
6.5
6.0
5.5
5.0
4.5
4.0
3.5
3.0
2.5
ppm

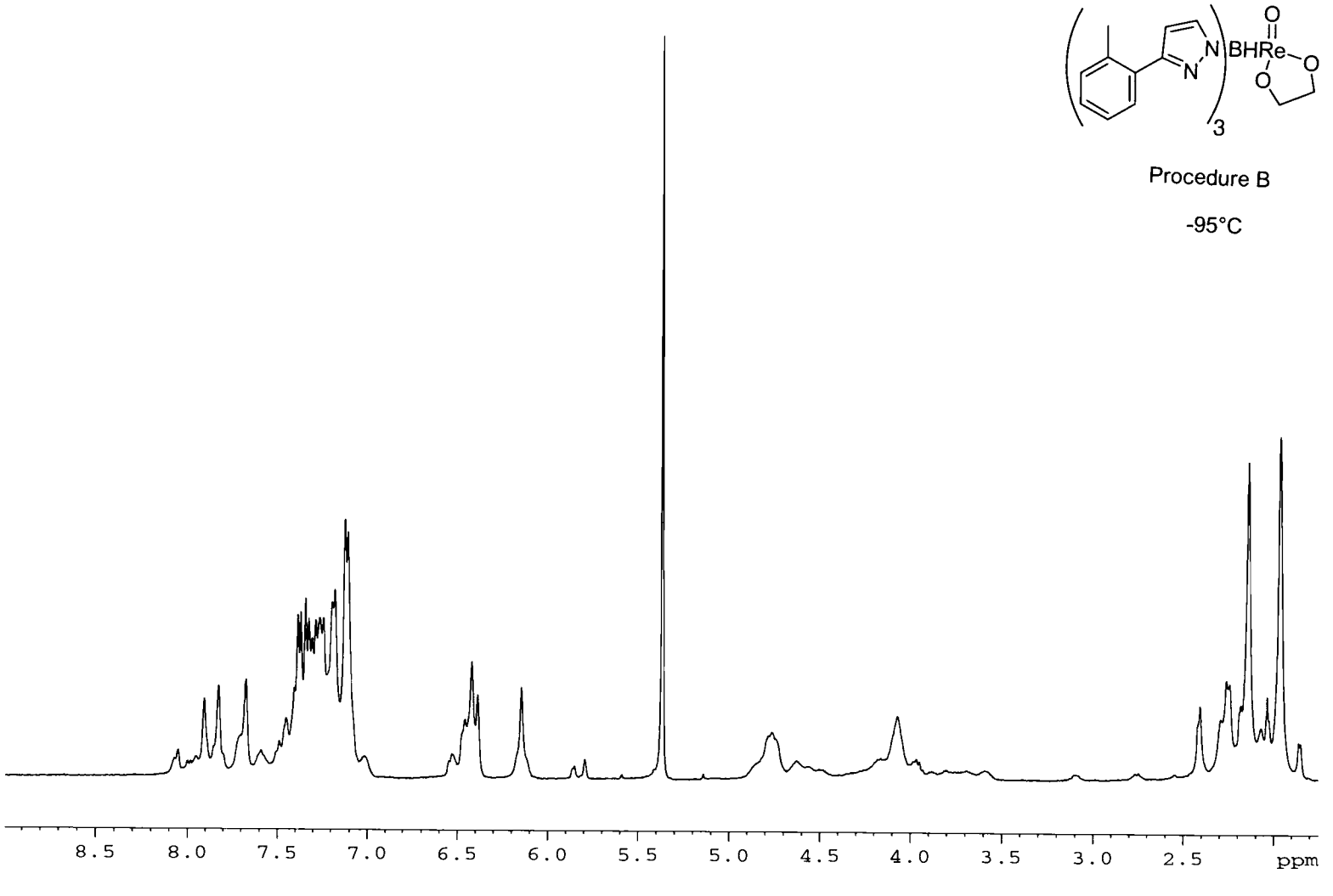
O
N
BHRe
O
N
O
3
Procedure B
-95°C
8.5
8.0
7.5
7.0
6.5
6.0
5.5
5.0
4.5
4.0
3.5
3.0
2.5
ppm

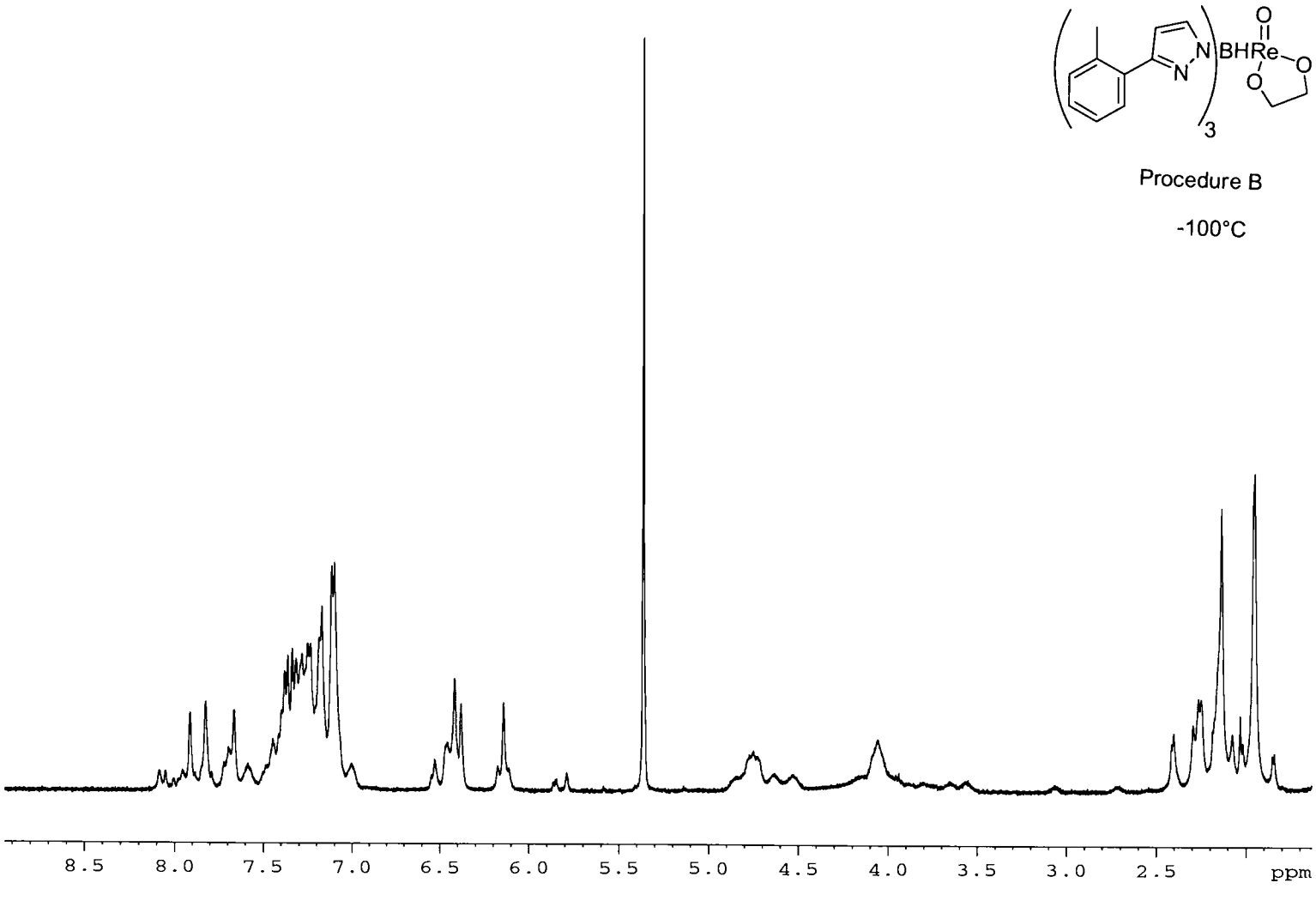
O
N
N
BHRe
O
O
3
Procedure B
-100°C
8.5
8.0
7.5
7.0
6.5
6.0
5.5
5.0
4.5
4.0
3.5
3.0
2.5
ppm

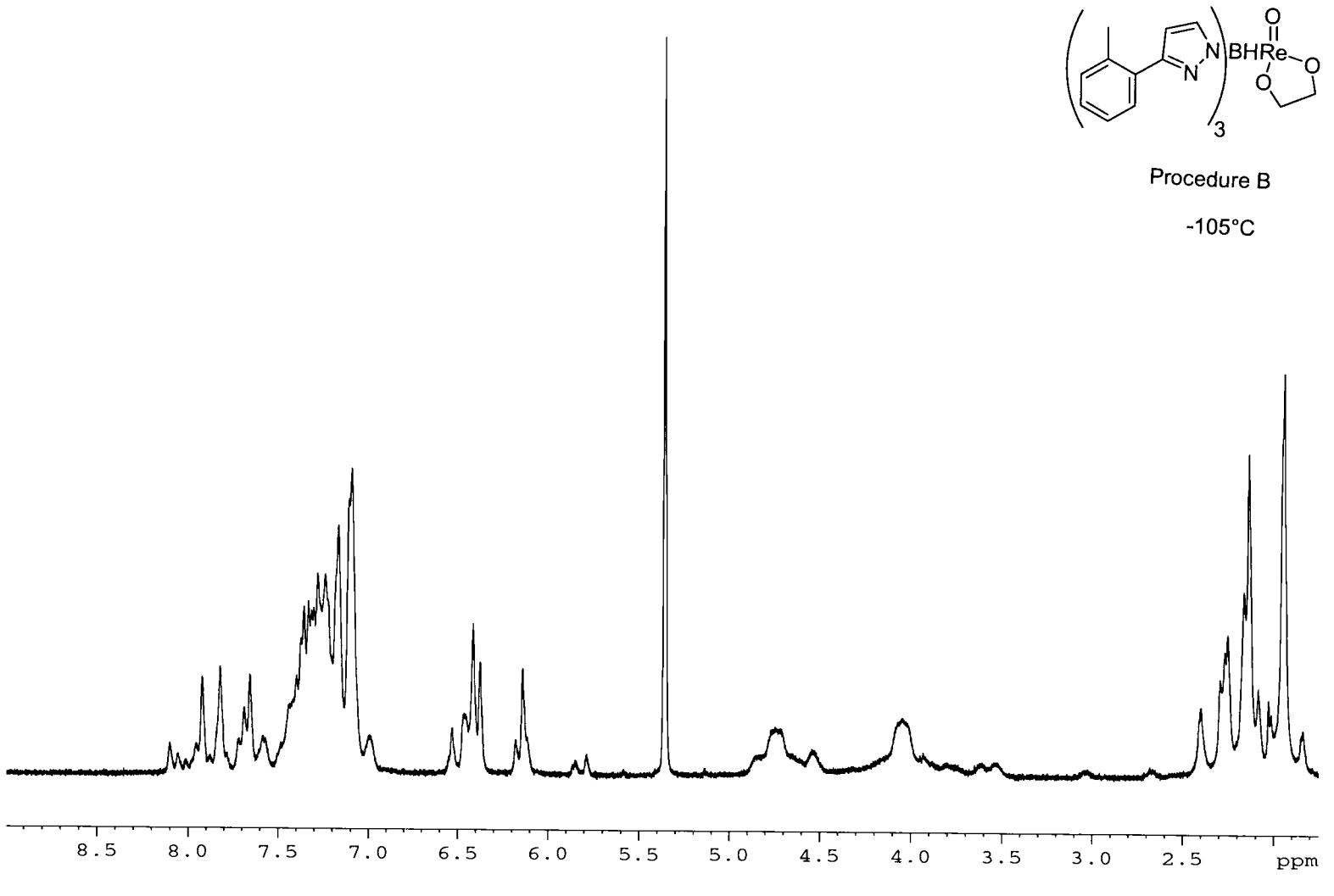
Procedure B
-105°C
8.5
8.0
7.5
7.0
6.5
6.0
5.5
5.0
4.5
4.0
3.5
3.0
2.5
ppm

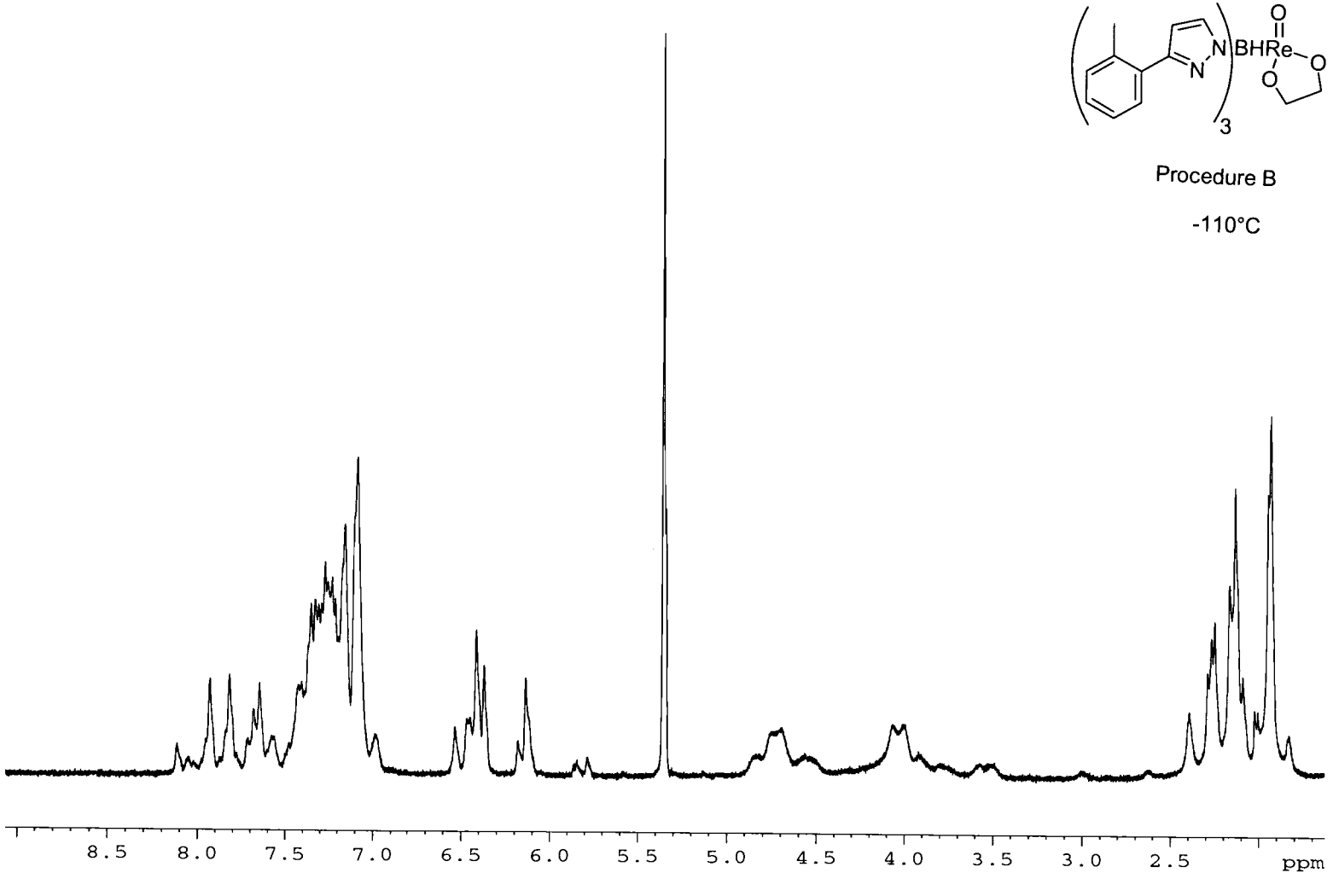
Procedure B
-110°C
8.5
8.0
7.5
7.0
6.5
6.0
5.5
5.0
4.5
4.0
3.5
3.0
2.5
ppm

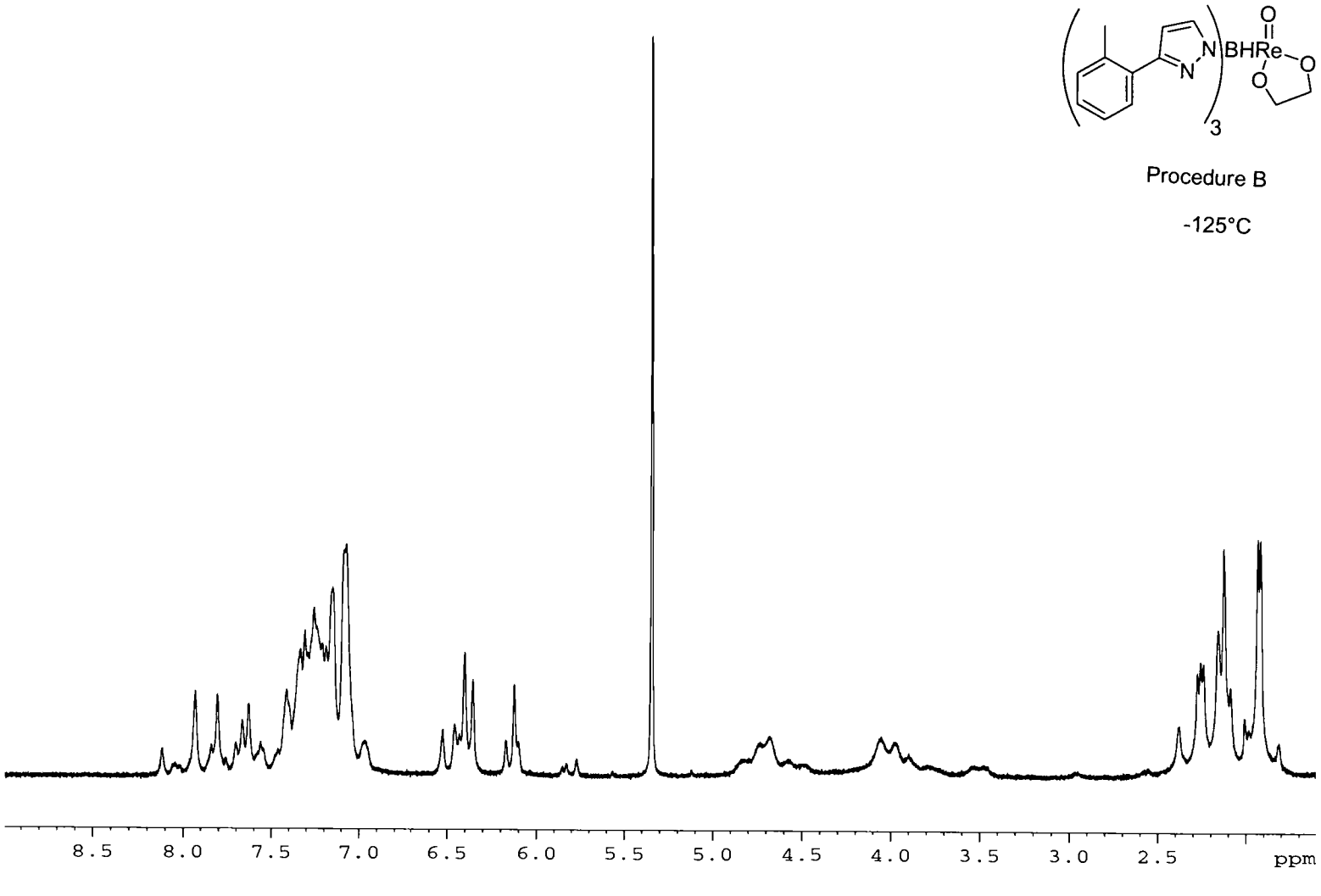
O
N
N
BHRe
O
O
3
Procedure B
-125°C
8.5
8.0
7.5
7.0
6.5
6.0
5.5
5.0
4.5
4.0
3.5
3.0
2.5
ppm

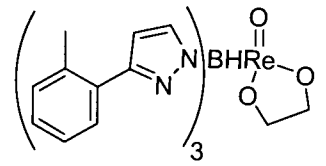

Procedure B

-130°C

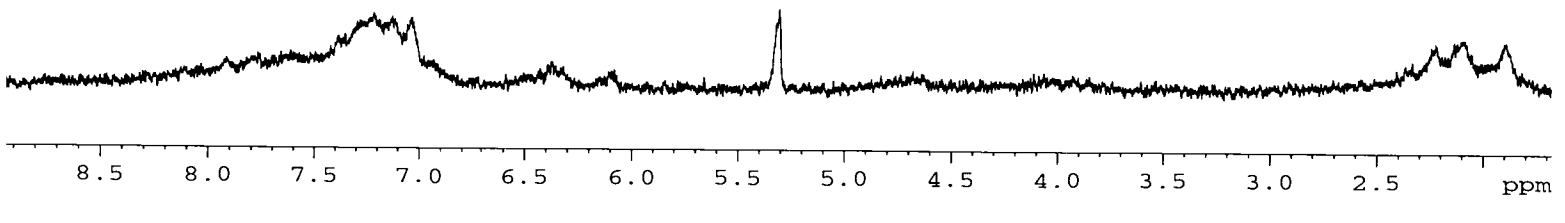

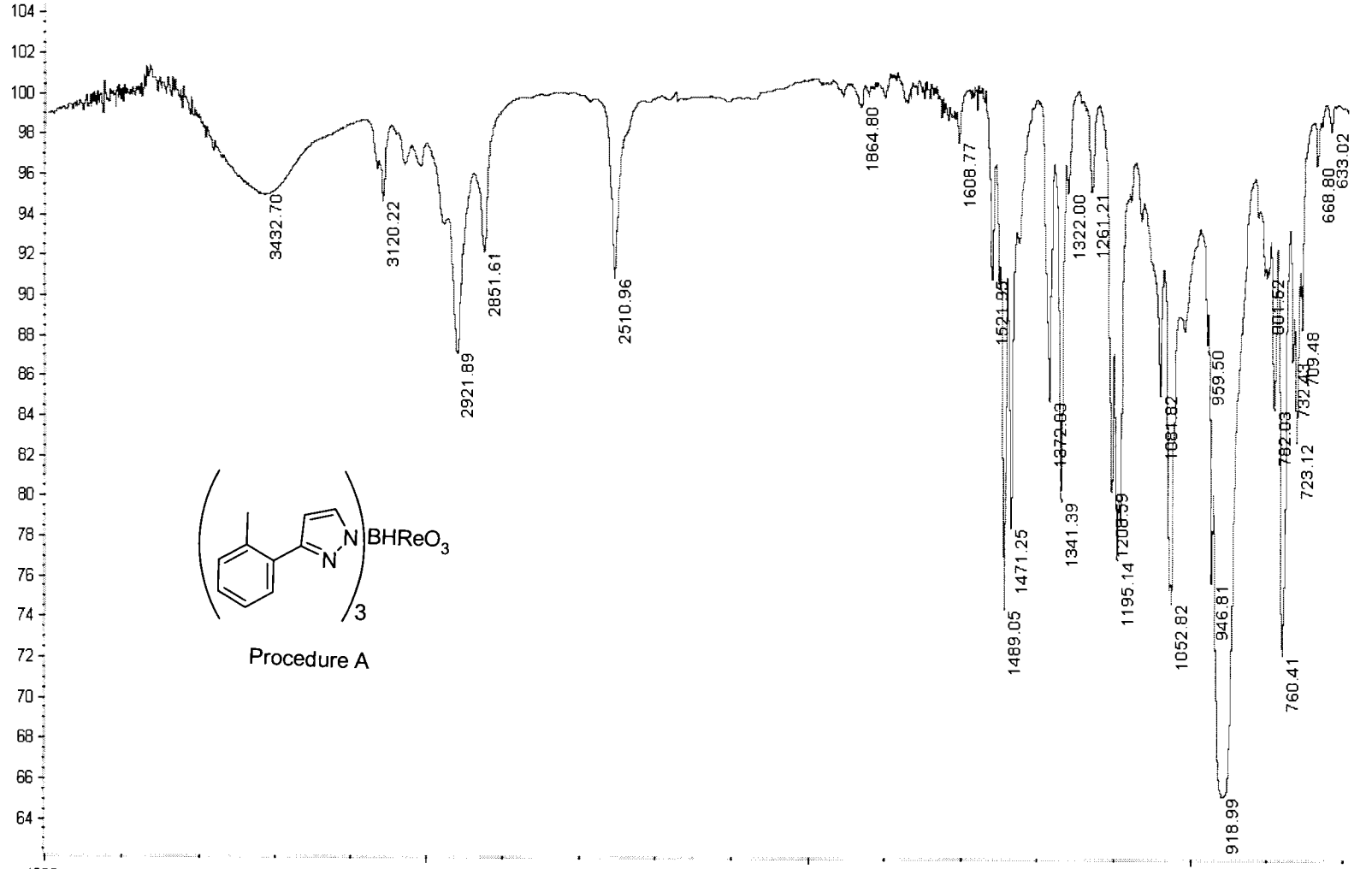
3432.70
3120.22
2921.89
2851.61
2510.96
1864.80
1608.77
1521.95
1489.05
1471.25
1372.03
1341.39
1322.00
1261.21
1208.59
1195.14
1081.82
1052.82
959.50
946.81
918.99
801.62
782.03
760.41
732.45
723.12
709.48
668.80
633.02
104
102
100
98
96
94
92
90
88
86
84
82
80
78
76
74
72
70
68
66
64
4000
3000
2000
1000
N
N
BHReO3
3
Procedure A

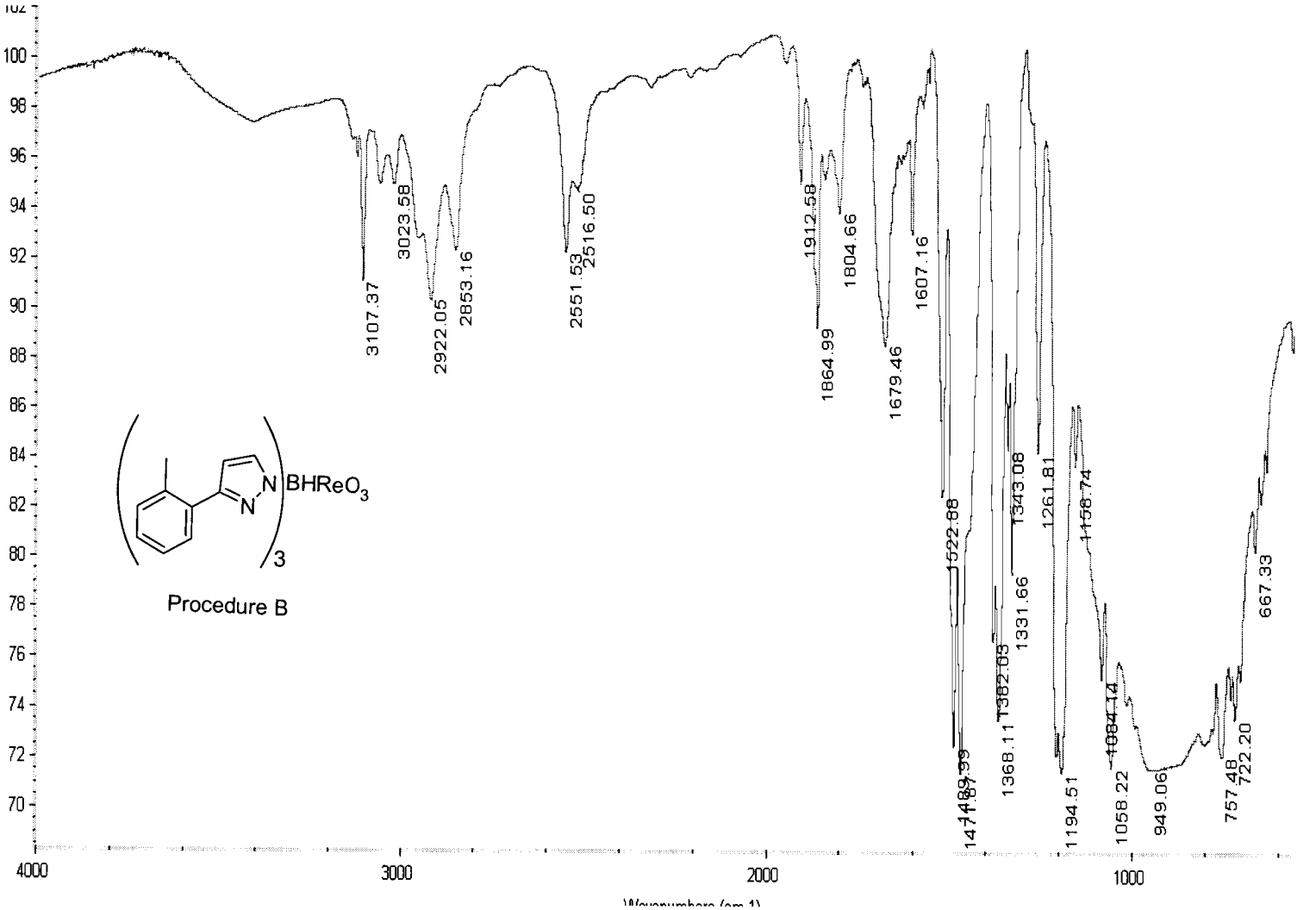
3107.37
3023.58
2922.05
2853.16
2551.53
2516.50
1912.58
1864.99
1804.66
1679.46
1607.16
1522.88
1489.39
1474.87
1368.11
1362.03
1343.08
1331.66
1261.81
1194.51
1158.74
1084.14
1058.22
949.06
757.48
722.20
667.33
4000
3000
2000
1000
BHReO3
3
Procedure B

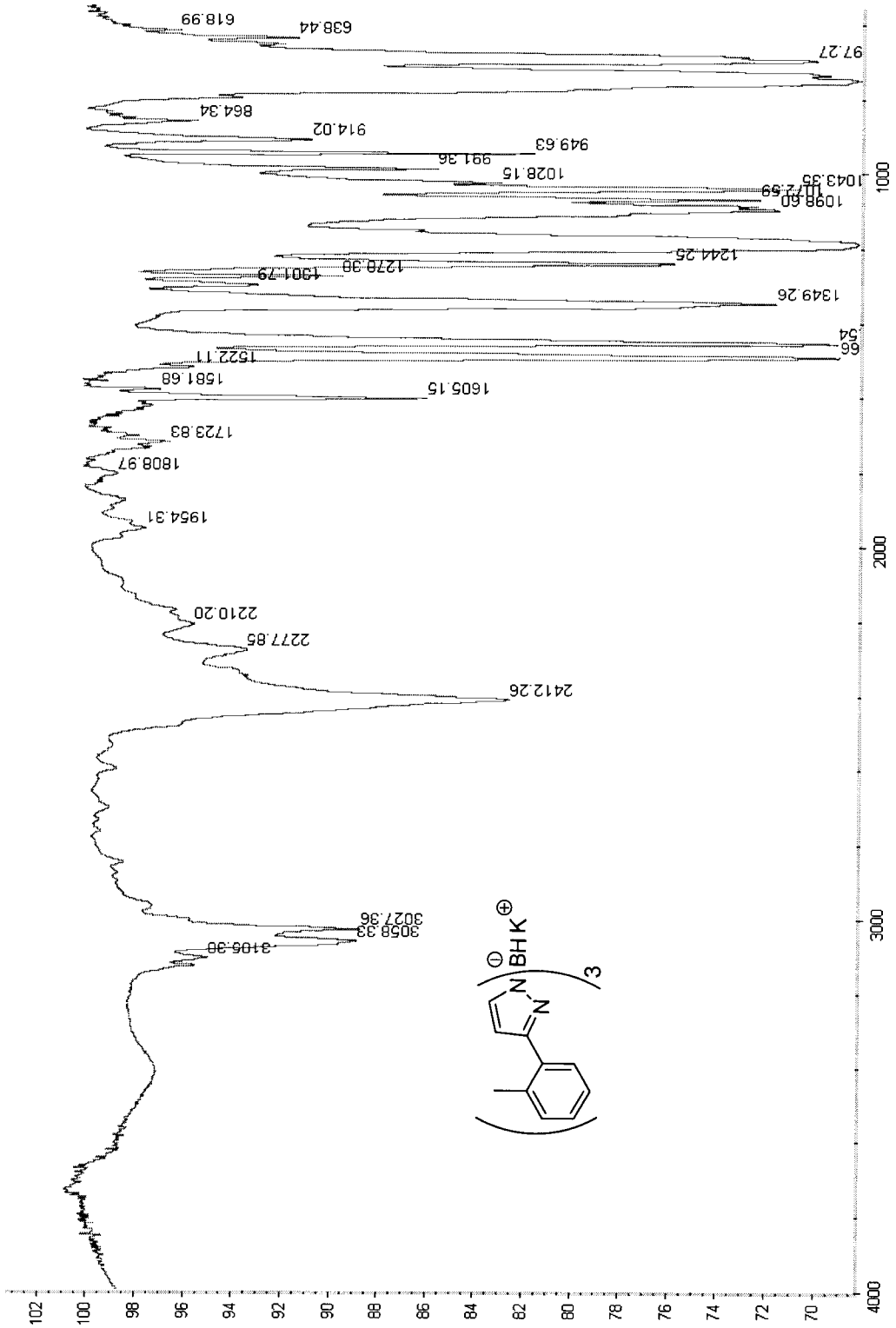
618.99
638.44
97.27
864.34
914.02
949.63
991.36
1028.15
1043.35
1098.60
1244.25
1278.38
1301.79
1349.26
54
66
1522.11
1581.68
1605.15
1723.83
1808.97
1954.31
2210.20
2277.85
2412.26
3027.36
3058.33
3106.30
BH K
3
N
N
102
100
98
96
94
92
90
88
86
84
82
80
78
76
74
72
70
4000
3000
2000
1000

3448.26
3022.10
2919.88
2850.01
2506.60
1735.66
1654.87
1607.93
1472.64
1365.72
1345.13
1260.67
1189.05
1055.82
1017.58
963.75
905.62
852.58
759.79
723.88
640.14
544.84
459.97
Procedure B
4000
3000
2000
1000

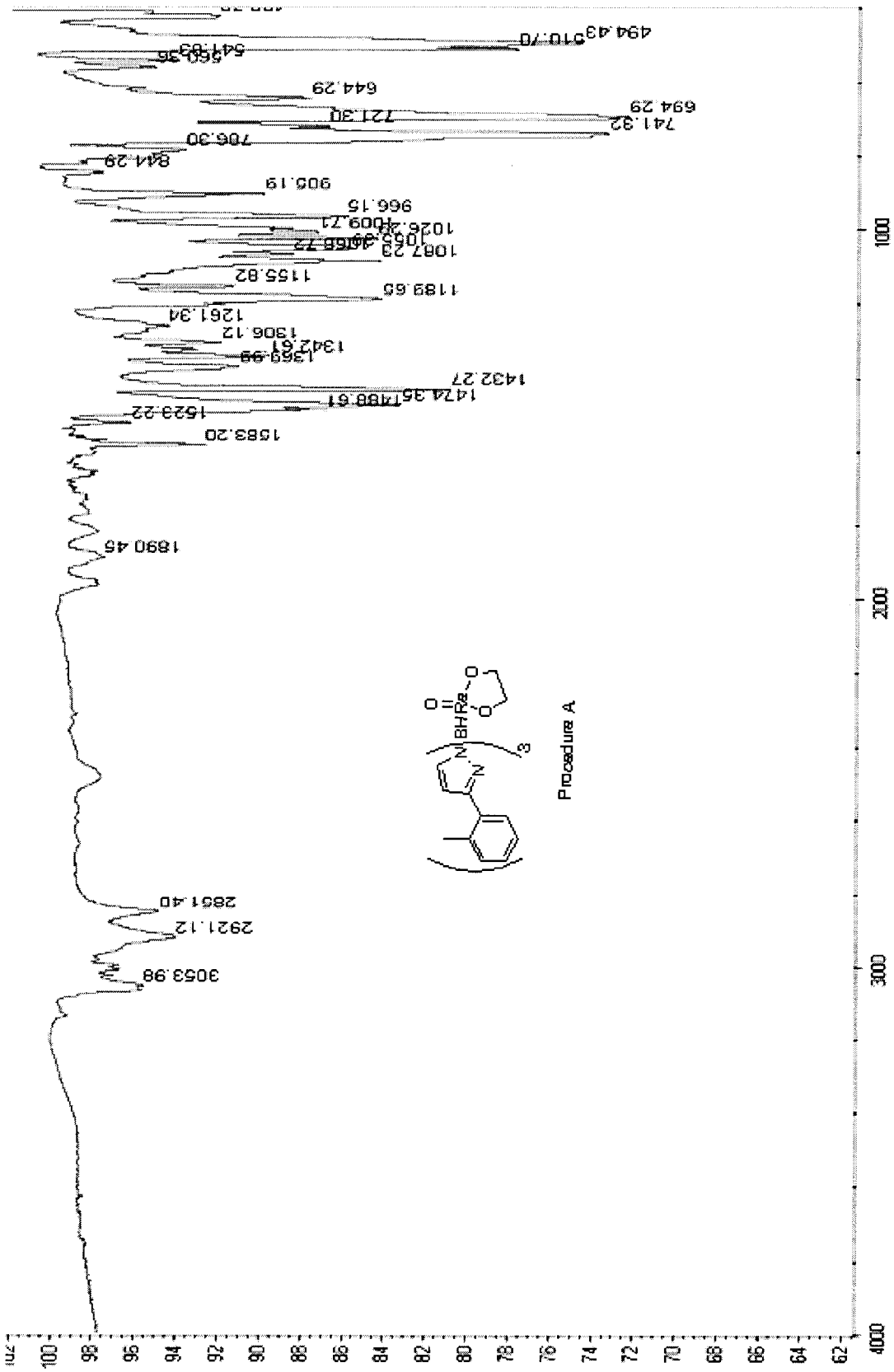
Procedure A